PROGRAM FOR THE EVALUATION OF STRUCTURAL REINFORCED PLASTIC MATERIALS AT CRYOGENIC TEMPERATURES

ANNUAL AND FOURTH QUARTERLY REPORT - PHASE II

29 JUNE 1964 THROUGH 30 JUNE 1965

CONTRACT NAS 8-11070

PROGRESS REPORT NO. 23

GER 11214 S/22

30 JUNE 1965

FOR:
GEORGE C. MARSHALL SPACE FLIGHT CENTER
NATIONAL AERONAUTICS AND SPACE ADMINISTRATION

GOODYEAR AEROSPACE
CORPORATION

GER 11214 S/22
CODE IDENT NO. 25500

GOODYEAR AEROSPACE CORPORATION

AKRON 15 OHIO

PROGRAM FOR THE EVALUATION OF STRUCTURAL REINFORCED PLASTIC MATERIALS AT CRYOGENIC TEMPERATURES

Annual and Fourth Quarterly Report - Phase II

29 June 1964 through 30 June 1965

Progress Report No. 23 30 June 1965

Contract No. NAS 8-11070
Control No. CPB-02-1151-64
DCN-1-4-50-01122-01

L. W. Toth
T. J. Boller
A. H. Kariotis
F. D. Yoder
G. Nagy
I. R. Butcher

For

George C. Marshall Space Flight Center
National Aeronautics and Space Administration

ABSTRACT

This annual summary report documents the second year's effort on a program of critical assessment and evaluation of procedures, test specimens, and test techniques for application to structural reinforced plastic materials at cryogenic temperatures.

The program covered by this reporting period includes a statistical evaluation of testing techniques and data, a determination of the possible effects of environment, and the testing of structural plastic models.

This report discusses the work performed by Goodyear Aerospace Corporation on National Aeronautics and Space Administration Contract NAS 8-11070 during the period from 29 June 1964 through 30 June 1965. This contract is under the direct supervision of Mr. John T. Schell of the Non-Metallic Materials Branch, Materials Division, Propulsion and Vehicle Engineering Laboratory, NASA-MSFC.

TABLE OF CONTENTS

LIST OF ILLUSTRATIONS

LIST OF TABLES

SECTION I. INTRODUCTION

The immediate goal of this program is the development of improved test techniques and methods to more realistically determine the engineering potential of reinforced plastics for structural applications at cryogenic temperatures. During the first year's effort on this program, four forms of reinforced plastic laminates were chosen as the most representative of the materials to be used in cryogenic applications. These laminates were reinforced with S/HTS glass in the form of Style 1543 and 1581 cloth and unidirectional and bidirectional 20-end roving, and used an epoxy prepreg resin system conforming to Specification WS-1028A. The basic physical and thermal properties to be determined for these laminates were tensile strength, elongation, modulus of elasticity, compressive strength, flexural strength, interlaminar shear strength, bearing strength, tensile hysteresis, tensile notched/unnotched ratio, density, thermal conductivity, and coefficient of expansion. Test temperatures were 298, 197, 77, and $20^{o}K$.

Test specimen design and testing techniques were of prime importance. Through a program using a literature survey and preliminary testing, test procedures were developed that yielded the desired data on physical and thermal properties for each material at all test temperatures. Using these test procedures, a limited amount of test data was developed for each of the laminates at the four test temperatures to complete the first year's effort.

The planned program for the second year's effort was a logical extension of the first year's effort and was divided into three tasks. The first task included a statistical evaluation of the first year's test effort to establish the reproducibility and general validity of this data. Simple mathematical expressions were derived that best characterize the test data, and the closeness of the fit of the test data to these mathematical expressions indicated the general validity of the test results. However, the need for additional test data or variations in test methods was also indicated in a few instances, and additional testing was performed in these areas. The second task of this year's program was a series of experiments conducted to determine the effects of environmental parameters upon physical properties. Panels of all four materials were exposed to a light and water exposure cycle prior to the testing of specimens in flexure and compression. Tests indicated no detrimental effects from this exposure. The final task was the validation of the previously developed data through the testing of structural models.

SECTION II. TASK I - EVALUATION OF TESTING TECHNIQUES

A. GENERAL

The purpose of Task I of this year's program was to further evaluate the testing techniques and methods developed during the first year's effort through a statistical analysis of the test data generated during the first year. If further data was needed or if an alternate test method was to be evaluated, supplemental testing was to be performed. The results of the Task I effort are discussed in this section.

B. STATISTICAL ANALYSIS

The objectives of the statistical analysis of the test data were as follows:

(1) To derive simple mathematical expressions that best characterize the test data.

(2) To evaluate the accuracy with which these equations represent the test data.

(3) To determine the lower tolerance limit, based on the standard deviation of the test data, which 95 percent or more of future specimens will exceed with a confidence level of 95 percent that the estimate is correct.

The first objective was met by fitting to the test data, through least squares principles, the following equation in which y is the dependent response variable, i. e., tensile strength, flexural modulus, etc:

$$y = a_0 + a_1x_1 + a_2x_2 + a_3x_3 + a_{11}x_1^2 + a_{22}x_2^2 + a_{33}x_3^2 + a_{111}x_1^3 + a_{222}x_2^3 + a_{12}x_1x_2 + a_{13}x_1x_3 + a_{333}x_3^3 \quad (1)$$

where

x_1 = test temperature (^oK),

x_2 = direction of loading on the test specimen,

x_3 = resin content (used only with unidirectional filament-wound interlaminar shear).

The multiple regression coefficients, a_{ijk}, in Equation 1 are obtained by least squares minimization in order to best fit the test data. These coefficients are listed in Tables 1 through 4 for the following laminates:

(1) Bidirectional Filament-Wound (BFW)

(2) Unidirectional Filament-Wound (UFW)

(3) 1543 Cloth

(4) 1581 Cloth

The second objective of the analysis is satisfied by the multiple correlation coefficient, R. The value of R is always between zero and unity. Zero means that there is no correlation between the y data and the independent x variables included in the form of equation used. Unity means that the fitted equation fits the data perfectly. However, the linear value, R, is difficult to quantitatively relate to the data; a more easily interpretable value is R^2. The number R, when squared and multiplied by 100 (R^2 x 100), represents statistically the percentage of random variation in the y variable that has been accounted for by the independent variables (x's) included in the analysis and/or the form of the equation fitted to the data. The value of R may be computed by using the simple correlation coefficient between the observed y values, designated y_o, and the y values computed from the equation, y_c, fitted to the data. Then,

$$R = \frac{n \sum y_o y_c - \left(\sum y_o\right)\left(\sum y_c\right)}{n \sum {y_o}^2 - \left(\sum y_o\right)^2 \sqrt{n \sum {y_c}^2 - \left(\sum y_c\right)^2}} ,$$

where n is the sample size and Σ represents summation.

Table 1. Multiple Regression Coefficients - Statistical Analysis (BFW Laminates)

Regression Coefficients	Bearing Strength (y)	Ult Comp Strength (y)	Flexural Mod (y)	Ult Flexural Strength (y)	Interlaminar Shear Strength (y)	Tensile Mod (y)	Ult Tensile Elong 20 - 197°K (y)	Ult Tensile Elong 298°K (y)	Ult Tensile Strength (y)
a_0	8.4924×10^4	1.2368×10^5	6.5166×10^6	2.2208×10^5	6.7371×10^3	6.0944×10^6	3.7642	3.6183	1.8361×10^5
a_1	-1.1075×10^2	2.3379×10^2	-9.6401×10^3	3.6817×10^2	2.1924×10	4.8244×10^3	2.1578×10^{-2}	--	-9.5356×10
a_2	-2.1540×10^2	-3.1809×10^3	-7.5789×10^{-4}	-6.6591×10^3	-8.8704×10	1.1493×10^5	-5.4256×10^4	1.4348×10^{-1}	-3.3533×10^3
a_3	--	--	--	--	--	--	--	--	--
a_{11}	-9.6570×10^{-3}	-1.0723	2.1575×10	-1.7394	-7.1832×10^{-2}	-2.7328×10	-7.2072×10^{-5}	--	--
a_{22}	2.8374	3.1781×10	6.7698×10^2	6.3852×10	8.8503×10^{-1}	-3.2525×10^3	1.2057×10^3	--	--
a_{12}	-1.8695×10^{-1}	3.0151×10^{-1}	-1.7655×10	1.9535	-2.2988×10^{-2}	-4.9679×10	-4.0540×10^{-5}	--	1.2218
a_{13}	--	--	--	--	--	--	--	--	--
Temp Range (°K)	20 - 298	20 - 298	20 - 298	20 - 298	20 - 298	20 - 298	20 - 197	298	20 - 298
Loading Direction Range (°)	0 - 90	0 - 90	0 - 90	0 - 90	0 - 90	0 - 45	0 - 45	0 - 45	0 - 45
$R^2 \times 100$(%)	81.82	87.05	92.26	95.57	50.75	94.62	83.17	99.25	97.46
Remarks	HVD	HVD			EVD		HVD		

HVD - Highly variable data EVD - Excessively variable data

Table 2. Multiple Regression Coefficients - Statistical Analysis (UFW Laminates)

Regression Coefficients	Bearing Strength (y)	Ult Comp Strength (y)	Flexural Modulus (y)	Ult Flexural Strength (y)	Ult Tensile Strength (y)	Interlaminar Shear Strength (y)	Tensile Modulus (y)
a_0	7.85255×10^4	2.3954×10^5	8.9724×10^6	5.1443×10^5	2.82496×10^5	-1.52560×10^7	1.00735×10^7
a_1	-4.02552×10^2	-2.2674×10^2	-6.0116×10^3	-9.4019×10^2	8.34574×10^2	3.70108×10^2	-3.03902×10^4
a_2	--	-5.2908×10^3	-1.5319×10^5	-1.3336×10^4	--	--	--
a_3	--	--	--	--	--	1.161128×10^6	--
a_{11}	2.99155	-2.5809×10^{-1}	1.2726×10	-2.5247×10^{-2}	-2.80203	-1.84633×10^{-1}	2.21997×10^2
a_{22}	--	3.5415×10	1.0834×10^3	8.3029×10	--	--	--
a_{33}	--	--	--	--	--	-4.25080×10^4	--
a_{12}	--	2.5203	-1.8854×10	1.2548×10	--	--	--
a_{111}	-6.15712×10^{-3}	--	--	--	--	--	-4.73501×10^{-1}
a_{13}	--	--	--	--	--	-1.71987×10	--
Temp Range (°K)	20 - 298	20 - 298	20 - 298	20 - 298	20 - 298	20 - 298	20 - 298
Loading Direction Range (°)	0	0 - 90	0 - 90	0 - 90	0	0	0
Resin Content Range (%)	--	--	--	--	--	18.68 - 19.03	--
$R^2 \times 100$ (%)	8.03	93.08	98.96	97.33	39.40	68.0	79.9
Remarks	HVD - SSS				HVD - SSS	HVD - SSS	SSS

HVD - Highly variable data SSS - Small sample size

Table 3. Multiple Regression Coefficients - Statistical Analysis (1543 Cloth Laminate)

Regression Coefficients	Tensile Notch Strength (y)	Tensile Mod (y)	Flexural Mod (y)	Ult Comp Strength (y)	Ult Tensile Strength (y)	Ult Flexural Strength (y)	Ult Tensile Elong (y)	Bearing Strength (y)	Interlaminar Shear Strength (y)
a_0	2.2098×10^{5}	5.99271×10^{6}	5.7378×10^{6}	1.2984×10^{5}	2.2693×10^{5}	2.2220×10^{5}	3.6119	8.0296×10^{4}	1.41917×10^{4}
a_1	-1.9910×10^{2}	-1.16431×10^{3}	-5.2262×10^{3}	-7.6047×10	-1.0192×10^{2}	-2.2200×10^{-2}	4.4558×10^{-3}	-1.0079×10^{2}	16.18501
a_2	-5.5305×10^{3}	-1.05632×10^{5}	-8.9160×10^{4}	-2.0123×10^{3}	-6.3454×10^{3}	-4.1549×10^{3}	-4.9196×10^{-2}	-2.6900×10^{2}	
a_{11}	-1.6600×10^{-1}	-2.68495	1.0539×10	-2.0602×10^{-1}	-3.0207×10^{-1}	-2.3144×10^{-1}	-1.3020×10^{-5}	3.1779×10^{-2}	-1.06253×10^{-1}
a_{22}	3.7849×10	8.42179×10^{2}	6.9446×10^{2}	1.4985×10	4.6529×10	2.7734×10	6.8142×10^{-4}	1.1096	
a_{12}	2.7632	-2.40059×10	-2.9308×10	2.1472×10^{-1}	2.1497	2.2649	9.7918×10^{-6}	-1.5431×10^{-1}	
Temp Range (°K)	20 - 298	20 - 298	20 - 298	20 - 298	20 - 298	20 - 298	20 - 298	20 - 298	20 - 298
Loading Direction Range (°)	0 - 90	0 - 90	0 - 90	0 - 90	0 - 90	0 - 90	0 - 90	0 - 90	0
$R^2 \times 100$(%)	97.87	95.19	97.73	95.59	98.09	97.63	29.86	73.86	66.4
Remarks							Contorted surface	EVD	SSS

EVD - Excessively variable data SSS - Small sample size

Table 4. Multiple Regression Coefficients - Statistical Analysis (1581 Cloth Laminate)

Regression Coefficients	Bearing Strength (y)	Ult Comp Strength (y)	Flexural Mod (y)	Ult Flexural Strength (y)	Tensile Mod (y)	Tensile Notch Strength (y)	Interlaminar Shear Strength (y)	Ult Tensile Strength (y)	Ult Tensile Elong (y)
a_0	7.2386×10^{4}	1.1395×10^{5}	3.9802×10^{6}	1.8371×10^{5}	4.3526×10^{6}	1.1933×10^{5}	1.2044×10^{4}	1.3915×10^{5}	4.1265
a_1	1.5317×10^{2}	-1.6368×10^{2}	-4.0087×10^{3}	-1.8539×10^{2}	-4.8399×10^{3}	-1.0206×10^{2}	7.4269	6.9711	2.9287×10^{-2}
a_2	-4.6551×10	-1.4047×10^{3}	-5.0530×10^{4}	-2.8266×10^{3}	-6.2960×10^{4}	-2.0407×10^{3}	-1.2714×10^{2}	-3.4149×10^{3}	4.6419×10^{2}
a_{11}	2.0818×10^{-1}	-3.2453×10^{-2}	5.1410	-2.6333×10^{-1}	3.4882	-1.8759×10^{-1}	-6.9378×10^{-2}	-5.2557×10^{-1}	-2.3048×10^{-4}
a_{22}	1.3000	1.4500×10	5.6436×10^{2}	2.9706×10^{1}	6.9922×10^{2}	2.0480×10	1.2892	3.5038×10	-6.7536×10^{-4}
a_{12}	-3.5025×10^{-1}	1.9290×10^{-1}	-1.5980×10	2.8768×10^{-1}	-6.4280	6.1458×10^{-1}	2.8132×10^{-2}	6.2282×10^{-1}	1.5390×10^{-5}
a_{111}	--	--	--	--	--	--	--	--	4.1446×10^{-7}
a_{222}	--	--	--	--	--	--	--	--	1.1668×10^{-6}
Temp Range (°K)	20 - 298	20 - 298	20 - 298	20 - 298	20 - 298	20 - 298	20 - 298	20 - 298	20 - 298
Loading Direction Range (°)	0 - 90	0 - 90	0 - 90	0 - 90	0 - 90	0 - 90	0 - 90	0 - 90	0 - 90
$R^2 \times 100$(%)	71.58	95.27	84.56	96.74	93.79	95.15	84.10	95.97	87.14
Remarks	HVD		HVD				HVD		Contorted surface and HVD

HVD - Highly variable data

Thus, R is a measure of the precision of fit to the data. If R^2 x 100 is low, then additional variables (x's) must be admitted into the analysis or their effects held constant for elimination in subsequent tests. The alternative is to use a different form of equation for fitting to the data.

Which alternative is used depends on judgments made upon examination of the original test data. If the variability of this data (y) is too high for fixed conditions of the test, then obviously the form of the equation is not at fault. It is more plausible that some unrecorded parameters of the test varied to an effective degree. Such situations are noted in the "Remarks" rows in Tables 1 through 4, where HVD and EVD stand for highly variable data and excessively variable data (in y). The R^2 x 100 is also recorded for each test condition in each table.

Interpretations of the statistical analysis have been made. When R^2 x 100 exceeded 90 percent, this was deemed to be a sufficiently good fit, so that no further analytical steps were necessary. For those values below the 90-percent level, raw data was reexamined. Two major reasons were found for these lower values:

(1) The data, y, for each fixed temperature and loading direction was highly variable.

(2) A severely contorted response surface, i.e., $y = f(x_1, x_2, x_3)$, was found. This meant that in one region of temperature and loading, the y-variable surface was sloped in one direction, and in the next level of temperature, it was twisted into a slope in the opposite direction. This may have been due to an abrupt change of state, which is a common chemical phenomenon.

For the properties where HVD or EVD appears in the column, either additional variables that may have produced the fluctuations of the data must be recorded and put into the fitted equation, or these variables must be held more stable and the tests repeated. Therefore, supplemental analysis or testing was needed in these areas. Additional testing was started in these areas and is reported later in this report. In the case of the tensile tests of the UFW laminate, the test results are included in the statistical analysis.

For the properties where a contorted surface prevents a good fit to the curve, the change-of-state point should be estimated, if possible, and separate equations fitted in these two regions. A good example of this may be found in Table 1 for ultimate tensile elongation in the two temperature regions of 298°K and 20 - 197°K. When originally fitted by one equation over all temperatures, the precision of the fit was only $R^2 \times 100 = 39.98$ percent. But now they are 99.25 percent and 83.17 percent, respectively. However, the temperature where the change of state may occur is not known. Additional tests were conducted on the unreinforced resin at the four test temperatures to determine if variation in the resin properties may be causing these contorted curves.

For the properties where $R^2 \times 100 > 90$ percent, the equation developed for the test data may be used safely by interpolation, but not too far outside the test ranges by extrapolation. How far extrapolation may extend has not yet been assessed.

The majority of the properties fall into this $R^2 \times 100 > 90$ percent catagory; however, the values for bearing and shear are consistently below this value. An alternate interlaminar shear test is discussed in paragraph C-3-f of this section. The bearing results, although variable within a specific material, are similar for all of the materials, and when analyzed together, more closely approach the $R^2 \times 100 = 90$ percent level. The low values of correlation noted for some of the tensile elongation data are a result of the contorted curve caused by the 45-degree direction test values. The low tensile elongation of the resin at the lower temperature (see Table 20) is the cause of this. The slightly low value for the BFW compressive strength data resulted in further testing of this property (refer to paragraph C-3-e of this section). The low correlation values recorded for the UFW tensile properties are somewhat due to the few test points (24 compared to the 48 for most properties).

The ultimate goal of a materials testing program is to use the data obtained to design a structure with the material similar to that included in the test program. Customarily, current procedures in presenting test results involve plotting the data from a small sample, usually less than 100 test specimens. Curves are then drawn for some response variable, such as ultimate tensile strength versus temperature. The curves are then used to design structural systems. For fiberglass specimens, it is widely known that if another small sample of specimens were similarly tested and a curve fitted to this data, it is very likely that another curve would result. This variation is due to the chance fluctuations in small samples.

This situation can be remedied through the use of huge samples to more accurately estimate the average material properties or, less expensively, statistical methods that include in their basis the sampling variability ignored in contemporary methods. For example, in the statistical methods applied to the problem of this program, a mathematical function can be provided for predicting a material property level that 95 percent of a large number of such specimens will equal or exceed with a confidence level of 95 percent that the estimate is correct.

To date, a mathematical function has been fitted to the test data by the least square principle. This consists of a response variable, y, such as ultimate tensile strength, which is subject to some random variations. The controllable, nonrandom parameters are temperature and direction of loading. These are the functions defined in Tables 1 through 4. However, these equations should not be used alone to predict the response, y, for specified values of x_1 (temperature) and x_2 (direction of loading), because small samples were used to fit this function. These functions should be used in combination with the following functions:

$$S_Y = s\left[\frac{1}{n} + \sum_{i=1}^{m} c_{ii}(z_i - \bar{z}_i)^2 + 2\sum_{i=1}^{m-1}\sum_{j=i+1}^{m} c_{ij}(z_i - \bar{z}_i)(z_j - \bar{z}_j)\right]^{\frac{1}{2}}, \tag{2}$$

where s, n, c_{ii}, c_{ij}, and z_i are given in Tables 5 through 8 and S_Y is the standard deviation, and

$$Y = y - K_{C,P} S_Y , \tag{3}$$

where Y is the value of the response (ultimate tensile strength) for the specified values of temperature and direction of loading which will be exceeded with the confidence, C, by a proportion, P, of such future materials, y is the mean value of the test data as defined by the functions of Tables 1 through 4, and $K_{C,P}$ is a constant obtained from Table 9.

The steps by which these lower tolerance limits may be computed are as follows:

a. From Table 9 choose a confidence level, C, and the properties of the distribution, P, that you wish to exceed your predicted response.

b. For the sample size, n, listed in Table 5, 6, 7, or 8, locate the $K_{C,P}$ value from Table 9. For values of n not in the table, $K_{C,P}$ can be computed as follows:

$$K_{C,P} = \frac{K_{1-P} + \sqrt{K^2_{1-P} - ab}}{a} \tag{4}$$

where

K_{1-P} is obtained from tables of the Normal Curve, i.e.,

Table 5. Factors for Computing S_Y - BFW Laminates

Factor	Interlaminar Shear Strength	Ultimate Tensile Strength	Ultimate Flexural Strength	Flexural Modulus	Tensile Modulus	Ultimate Compressive Strength	Ultimate Tensile Elongation (20 - 197°K)	Ultimate Tensile Elongation (298°K)	Bearing Strength
s	1.17558×10^{3}	1.18709×10^{4}	1.59522×10^{4}	2.98231×10^{5}	2.74072×10^{5}	1.40707×10^{4}	8.91788×10^{-1}	3.08176×10^{-1}	6.64323×10^{3}
n	49	37	53	52	36	48	26	10	48
$\bar{z}_1$	1.54000×10^{2}	1.50078×10^{2}	1.57981×10^{2}	1.59538×10^{2}	1.55722×10^{2}	1.48000×10^{2}	94.192308	--	1.48000×10^{2}
$\bar{z}_2$	3.24000×10	1.65789×10	3.56603×10	3.63461×10	1.62500×10	3.37500×10	15.57692	1.8×10	3.37500×10
$\bar{z}_3$	3.56982×10^{4}	8.55626×10^{3}	3.71405×10^{4}	3.77407×10^{4}	3.59411×10^{4}	3.34855×10^{4}	1.41320×10^{4}	--	3.34855×10^{4}
$\bar{z}_4$	2.43000×10^{3}		2.67452×10^{3}	2.72596×10^{3}	7.31250×10^{2}	2.53125×10^{3}	7.00961×10^{2}	--	2.53125×10^{3}
$\bar{z}_5$	4.79124×10^{3}		6.04962×10^{3}	6.16478×10^{3}	2.57601×10^{3}	4.99500×10^{3}	1.52653×10^{3}	--	4.99500×10^{3}
c_{11}	3.74325×10^{-5}	3.59769×10^{-6}	3.59681×10^{-5}	3.60381×10^{-5}	5.11563×10^{-5}	3.75982×10^{-5}	1.99539×10^{-4}	1.43481×10^{-1}	3.75984×10^{-5}
c_{22}	2.49216×10^{-4}	1.64958×10^{-4}	2.17073×10^{-4}	2.19844×10^{-4}	2.02500×10^{3}	2.49495×10^{-4}	1.00000×10^{11}		2.49495×10^{-4}
c_{33}	3.28291×10^{-10}	4.75018×10^{-9}	3.19216×10^{-10}	3.21510×10^{-10}	4.55496×10^{-10}	3.38614×10^{-10}	3.74548×10^{-9}	--	3.38616×10^{-10}
c_{44}	2.77760×10^{-8}		2.43541×10^{-8}	2.4424×10^{-8}	1.00000	2.79428×10^{-8}	4.93827×10^{7}	--	2.79428×10^{-8}
c_{55}	1.22467×10^{-9}		1.11904×10^{-9}	1.12879×10^{-9}	4.98595×10^{-9}	1.29210×10^{-9}	1.57266×10^{-8}	--	1.29210×10^{-9}
c_{12}	6.23894×10^{-6}	1.18324×10^{-5}	6.72288×10^{-6}	6.28230×10^{-6}	-3.92731×10^{-4}	6.45400×10^{-6}	6.19242×10^{-5}	--	6.45403×10^{-6}
c_{13}	-1.06505×10^{-7}	-7.99486×10^{-8}	-1.02365×10^{-7}	-1.02766×10^{-7}	-1.46817×10^{-7}	-1.07813×10^{-7}	-8.39406×10^{-7}	--	-1.07814×10^{-7}
c_{14}	5.25766×10^{-9}		-1.20737×10^{-8}	-9.84720×10^{-9}	9.05236×10^{-6}	-7.24377×10^{-13}	-8.86420×10^{-7}	--	-3.58822×10^{-13}
c_{15}	-4.69511×10^{-8}		-3.00593×10^{-8}	-2.92331×10^{-8}	-7.66252×10^{-8}	-4.36076×10^{-8}	-2.22283×10^{-7}	--	-4.36081×10^{-8}
c_{23}	1.69725×10^{-9}	-7.19807×10^{-7}	-6.75822×10^{-9}	-4.23699×10^{-9}	9.02225×10^{-7}	1.67671×10^{-13}	-3.08669×10^{-7}	--	-3.30652×10^{-14}
c_{24}	-2.39372×10^{-6}		-2.06762×10^{-6}	-2.08162×10^{-6}	-4.50002×10	-2.40054×10^{-6}	-2.22222×10^{9}	--	-2.40054×10^{-6}
c_{25}	-1.95568×10^{-9}		-1.54209×10^{-7}	-1.59406×10^{-7}	5.89242×10^{-6}	-1.91231×10^{-7}	-1.38064×10^{-8}	--	-1.91230×10^{-7}
c_{34}	-4.14927×10^{-11}		9.63562×10^{-11}	8.36145×10^{-11}	-2.01557×10^{-8}	1.89236×10^{-15}	6.16121×10^{-9}	--	1.89238×10^{-15}
c_{35}	2.63810×10^{-11}		-3.68879×10^{-11}	-4.16161×10^{-11}	-2.65679×10^{-11}	-2.23136×10^{-15}	-1.40365×10^{-10}	--	-9.18805×10^{-16}
c_{45}	1.06048×10^{-10}		-2.62143×10^{-10}	-2.35878×10^{-10}	-1.48356×10^{-7}	3.61048×10^{-15}	-3.32060×10^{-8}	--	-7.22100×10^{-15}

Table 6. Factors for Computing S_Y - UFW Laminates

Factor	Bearing Strength	Ultimate Compressive Strength	Flexural Modulus	Ultimate Flexural Strength	Ultimate Tensile Strength	Tensile Modulus	Interlaminar Shear Strength
s	7.47702×10^{3}	2.35375×10^{4}	2.80073×10^{5}	3.41098×10^{4}	3.06900×10^{4}	2.67453×10^{5}	1.71419×10^{3}
n	20	48	46	48	24	24	24
z_1	1.38828×10^{2}	1.48000×10^{2}	1.52326×10^{2}	1.48000×10^{2}	148	148	148
z_2	4.32364×10^{4}	3.37500×10	3.13043×10	3.37500×10	3.34855×10^{4}	3.34855×10^{4}	1.88350×10
z_3	1.696212×10^{7}	3.34855×10^{4}	3.48038×10^{4}	3.34855×10^{4}		8.64337×10^{6}	3.34855×10^{4}
z_4		2.53125×10^{3}	2.28913×10^{3}	2.53125×10^{3}			3.54780×10^{2}
z_5		4.99500×10^{3}	5.02219×10^{3}	4.99500×10^{3}			2.78717×10^{3}
c_{11}	8.47577×10^{-4}	3.75982×10^{-5}	3.85399×10^{-5}	3.75982×10^{-5}	7.22539×10^{-5}	5.77328×10^{-4}	5.84652×10^{-2}
c_{22}	4.54012×10^{-8}	2.49495×10^{-4}	2.49759×10^{-4}	2.49495×10^{-4}	6.77237×10^{-10}	3.23015×10^{-8}	5.11237×10^{5}
c_{33}	1.81580×10^{-13}	3.38614×10^{-10}	3.48930×10^{-10}	3.38614×10^{-10}		1.34668×10^{-13}	6.99213×10^{-10}
c_{44}		2.79428×10^{-8}	2.91289×10^{-8}	2.79428×10^{-8}			3.59323×10^{2}
c_{55}		1.29210×10^{-9}	1.45095×10^{-9}	1.29210×10^{-9}			1.64839×10^{-4}
c_{12}	-6.08217×10^{-6}	6.45400×10^{-6}	5.98536×10^{-6}	6.45400×10^{-6}	-2.15631×10^{-7}	-4.21220×10^{-6}	1.76215
c_{13}	1.17645×10^{-8}	-1.07813×10^{-7}	-1.10914×10^{-7}	-1.07813×10^{-7}		8.24728×10^{-9}	-2.08758×10^{-8}
c_{14}		-7.24377×10^{-13}	-6.25068×10^{-9}	-7.24377×10^{-13}			-3.43683×10^{-2}
c_{15}		-4.36076×10^{-8}	-3.85406×10^{-8}	-4.36076×10^{-8}			-3.10242×10^{-3}
c_{23}	-9.00239×10^{-11}	1.67671×10^{-13}	1.60016×10^{-9}	1.67671×10^{-13}		-6.52594×10^{-10}	-3.00725×10^{-3}
c_{24}		-2.40054×10^{-6}	-2.39150×10^{-6}	-2.40054×10^{-6}			-1.35535×10^{4}
c_{25}		-1.91231×10^{-7}	-1.9576×10^{-7}	-1.91231×10^{-7}			-3.86603×10^{-2}
c_{34}		1.89236×10^{-15}	3.15516×10^{-11}	1.89236×10^{-15}			7.97013×15^{-5}
c_{35}		-2.23136×10^{-15}	-2.04064×10^{-11}	-2.23136×10^{-15}			-1.07363×10^{-8}
c_{45}		3.61048×10^{-15}	-4.21709×10^{-10}	3.61048×10^{-15}			3.70056×10^{-4}

Table 7. Factors for Computing S_Y - 1543 Cloth Laminates

Factor	Ultimate Tensile Elongation	Flexural Modulus	Tensile Modulus	Tensile Notched Strength	Ultimate Flexural Strength	Ultimate Compressive Strength	Ultimate Tensile Strength	Bearing Strength	Interlaminar Shear Strength
s	1.20024 x 10	2.34450 x 10	4.08926 x 10^{5}	1.25084 x 10^{4}	1.06620 x 10^{4}	7.43415 x 10^{3}	1.29684 x 10^{4}	8.08325 x 10^{3}	1.57561 x 10^{3}
n	49	48	49	49	48	48	49	48	24
$\bar{z}_1$	1.46551 x 10^{2}	1.48000 x 10^{2}	1.30914 x 10^{2}	1.49000 x 10^{2}	1.48000 x 10^{2}	1.48000 x 10^{2}	1.46551 x 10^{2}	1.48000 x 10^{2}	1.4800 x 10^{2}
$\bar{z}_2$	3.48979 x 10	3.37500 x 10	3.30612 x 10	3.30612 x 10	3.37500 x 10	3.37500 x 10	3.48979 x 10	3.37500 x 10	3.34855 x 10^{4}
$\bar{z}_3$	3.29231 x 10^{4}	3.34855 x 10^{4}	2.96738 x 10^{4}	3.35941 x 10^{4}	3.34855 x 10^{4}	3.34850 x 10^{4}	3.29231 x 10^{4}	3.34855 x 10^{4}	
$\bar{z}_4$	2.64489 x 10^{3}	2.53125 x 10^{3}	2.47959 x 10^{3}	2.47959 x 10^{3}	2.53125 x 10^{3}	2.53125 x 10^{3}	2.64489 x 10^{3}	2.53125 x 10^{3}	
$\bar{z}_5$	-2.86988 x 10^{3}	1.29210 x 10^{-9}	4.07878 x 10^{3}	1.61999 x 10^{3}	4.95500 x 10^{3}	4.99500 x 10^{3}	2.86988 x 10^{3}	4.99500 x 10^{3}	
c_{11}	3.72981 x 10^{-5}	3.75982 x 10^{-5}	4.23436 x 10^{-5}	3.61158 x 10^{-5}	3.75982 x 10^{-5}	3.75984 x 10^{-5}	3.72981 x 10^{-5}	3.75982 x 10^{-5}	7.22539 x 10^{-5}
c_{22}	2.49471 x 10^{-4}	2.49495 x 10^{-4}	2.55258 x 10^{-4}	2.48435 x 10^{-4}	2.49495 x 10^{-4}	2.49495 x 10^{-4}	2.49471 x 10^{-4}	2.49495 x 10^{-4}	6.77237 x 10^{-10}
c_{33}	3.36109 x 10^{-10}	3.38614 x 10^{-10}	3.91321 x 10^{-10}	3.27453 x 10^{-10}	3.38614 x 10^{-10}	3.38616 x 10^{-10}	3.36109 x 10^{-10}	3.38614 x 10^{-10}	
c_{44}	2.75652 x 10^{-8}	2.79428 x 10^{-8}	2.95600 x 10^{-8}	2.78453 x 10^{-8}	2.79428 x 10^{-8}	2.79428 x 10^{-8}	2.75652 x 10^{-8}	2.79428 x 10^{-8}	
c_{55}	1.26835 x 10^{-9}	1.29210 x 10^{-9}	1.20498 x 10^{-9}	1.28789 x 10^{-9}	1.29210 x 10^{-9}	1.29210 x 10^{-9}	1.26835 x 10^{-9}	1.29210 x 10^{-9}	
c_{12}	6.53789 x 10^{-6}	6.45400 x 10^{-6}	2.89319 x 10^{-5}	7.70755 x 10^{-6}	6.45400 x 10^{-6}	6.45403 x 10^{-6}	6.53789 x 10^{-6}	6.45400 x 10^{-6}	-2.15631 x 10^{-7}
c_{13}	-1.06946 x 10^{-7}	-1.07813 x 10^{-7}	-1.23957 x 10^{-7}	-1.03746 x 10^{-7}	-1.07813 x 10^{-7}	-1.07814 x 10^{-7}	-1.06946 x 10^{-7}	-1.07813 x 10^{-7}	
c_{14}	-1.06463 x 10^{-8}	-7.24377 x 10^{-13}	-2.45173 x 10^{-7}	-1.20240 x 10^{-8}	-7.24377 x 10^{-13}	-3.58822 x 10^{-13}	-1.06463 x 10^{-8}	-7.24377 x 10^{-13}	
c_{15}	4.09377 x 10^{-8}	-4.36076 x 10^{-8}	-3.68614 x 10^{-8}	-4.11103 x 10^{-8}	-4.36076 x 10^{-8}	-4.36081 x 10^{-8}	-4.09377 x 10^{-8}	-4.36076 x 10^{-8}	
c_{23}	-2.42255 x 10^{-10}	1.67671 x 10^{-13}	-6.57835 x 10^{-8}	-3.43942 x 10^{-9}	1.67671 x 10^{-13}	-3.30652 x 10^{-14}	-2.42255 x 10^{-10}	1.67671 x 10^{-13}	
c_{24}	-2.39756 x 10^{-6}	-2.40054 x 10^{-6}	-2.53803 x 10^{-6}	-2.39037 x 10^{-6}	-2.40054 x 10^{-6}	-2.40054 x 10^{-6}	-2.39756 x 10^{-6}	-2.40054 x 10^{-6}	
c_{25}	-1.91977 x 10^{-7}	-1.91231 x 10^{-7}	-1.54455 x 10-7	-1.93343 x 10^{-7}	-1.91231 x 10^{-7}	-1.91230 x 10^{-7}	-1.91977 x 10^{-7}	-1.91231 x 10^{-7}	
c_{34}	3.07604 x 10^{-11}	1.89236 x 10^{-15}	6.94641 x 10^{-10}	3.29925 x 10^{-11}	1.89236 x 10^{-15}	1.89238 x 10^{-15}	3.07604 x 10^{-11}	1.89236 x 10^{-15}	
c_{35}	-7.71638 x 10^{-12}	-2.23136 x 10^{-15}	-1.39992 x 10^{-11}	-6.85475 x 10^{-12}	-2.23136 x 10^{-15}	-9.18805 x 10^{-16}	-7.71638 x 10^{-12}	-2.23136 x 10^{-15}	
c_{45}	9.46941 x 10^{-11}	3.61048 x 10^{-15}	-1.14732 x 10^{-10}	2.02590 x 10^{-11}	1.29210 x 10^{-9}	-7.22100 x 10^{-15}	9.46941 x 10^{-11}	3.61048 x 10^{-15}	

Table 8. Factors for Computing S_Y - 1581 Cloth Laminates

Factor	Ultimate Tensile Elongation	Flexural Modulus	Bearing Strength	Ultimate Compressive Strength	Ultimate Flexural Strength	Tensile Modulus	Tensile Notched Strength	Interlaminar Shear Strength	Ultimate Tensile Strength
s	3.47398×10^{-1}	2.77318×10^{5}	7.34784×10^{3}	5.35726×10^{3}	7.64235×10^{3}	2.07168×10^{5}	5.92015×10^{3}	9.22024×10^{2}	7.90004×10^{3}
n	42	48	48	48	48	48	48	48	48
$\bar{z}_1$	1.33785×10^{2}	1.48000×10^{2}	1.48000×10^{2}	1.48000×10^{2}	1.48000×10^{2}	1.48000×10^{2}	1.48000×10^{2}	1.48000×10^{2}	1.48000×10^{2}
$\bar{z}_2$	3.21428×10	3.37500×10	3.37500×10	3.37500×10	3.37500×10	3.37500×10	3.37500×10	3.37500×10	3.37500×10
$\bar{z}_3$	2.91539×10^{4}	3.34855×10^{4}	3.34855×10^{4}	3.34855×10^{4}	3.34855×10^{4}	3.34855×10^{4}	3.34855×10^{4}	3.34855×10^{4}	3.34855×10^{4}
$\bar{z}_4$	2.60357×10^{3}	2.53125×10^{3}	2.53125×10^{3}	2.53125×10^{3}	2.53125×10^{3}	2.53125×10^{3}	2.53125×10^{3}	2.53125×10^{3}	2.53125×10^{3}
$\bar{z}_5$	-13.97544×10^{3}	4.99500×10^{3}	4.99500×10^{3}	4.99500×10^{3}	4.99500×10^{3}	4.99500×10^{3}	4.99500×10^{3}	4.99500×10^{3}	4.99500×10^{3}
c_{11}	2.98041×10^{-4}	3.75982×10^{-5}	3.75980×10^{-5}	3.75984×10^{-5}	3.75982×10^{-5}	3.75984×10^{-5}	3.75982×10^{-5}	3.75982×10^{-5}	3.75982×10^{-5}
c_{22}	2.00033×10	2.49495×10^{-4}	2.49495×10^{-4}	2.49495×10^{-4}	2.49495×10^{-4}	2.49495×10^{-4}	2.49495×10^{-4}	2.49495×10^{-4}	2.49495×10^{-4}
c_{33}	1.74106×10^{-8}	3.38614×10^{-10}	3.38612×10^{-10}	3.38616×10^{-10}	3.38614×10^{-10}	3.38616×10^{-10}	3.38614×10^{-10}	3.38614×10^{-10}	3.38614×10^{-10}
c_{44}	2.22256×10^{-2}	2.79428×10^{-8}	2.79428×10^{-8}	2.79428×10^{-8}	2.79428×10^{-8}	2.79428×10^{-8}	2.79428×10^{-8}	2.79428×10^{-8}	2.79428×10^{-8}
c_{55}	7.53640×10^{-14}	1.29210×10^{-9}	1.29210×10^{-9}	1.29210×10^{-9}	1.29210×10^{-9}	1.29210×10^{-9}	1.29210×10^{-9}	1.29210×10^{-9}	1.29210×10^{-9}
c_{12}	3.63965×10^{-5}	6.45400×10^{-6}	6.45399×10^{-6}	6.45403×10^{-6}	6.45400×10^{-6}	6.45403×10^{-6}	6.45400×10^{-6}	6.45400×10^{-6}	6.45400×10^{-6}
c_{13}	-2.20559×10^{-6}	-1.07813×10^{-7}	-1.07813×10^{-7}	-1.07814×10^{-7}	-1.07813×10^{-7}	-1.07814×10^{-7}	-1.07813×10^{-7}	-1.07813×10^{-7}	-1.07813×10^{-7}
c_{14}	-1.63159×10^{-6}	-7.24377×10^{-13}	-4.23113×10^{-13}	-3.58822×10^{-13}	-7.24377×10^{-13}	-3.58822×10^{-13}	-7.24377×10^{-13}	-7.24377×10^{-13}	-7.24377×10^{-13}
c_{15}	4.37167×10^{-9}	-4.36076×10^{-8}	-4.36078×10^{-8}	-4.36081×10^{-8}	-4.36076×10^{-8}	-4.36081×10^{-8}	-4.36076×10^{-8}	-4.36076×10^{-8}	-4.36076×10^{-8}
c_{23}	-5.28349×10^{-8}	1.67671×10^{-13}	1.90678×10^{-13}	-3.30652×10^{-14}	1.67671×10^{-13}	-3.30652×10^{-14}	1.67671×10^{-13}	1.67671×10^{-13}	1.67671×10^{-13}
c_{24}	-6.66769×10^{-1}	-2.40054×10^{-6}	-2.40054×10^{-6}	-2.40054×10^{-6}	-2.40054×10^{-6}	-2.40054×10^{-6}	-2.40054×10^{-6}	-2.40054×10^{-6}	-2.40054×10^{-6}
c_{25}	-1.59679×10^{-11}	-1.91231×10^{-7}	-1.91231×10^{-7}	-1.91230×10^{-7}	-1.91231×10^{-7}	-1.91230×10^{-7}	-1.91231×10^{-7}	-1.91231×10^{-7}	-1.91231×10^{-7}
c_{34}	1.01540×10^{-8}	1.89236×10^{-15}	9.46175×10^{-16}	1.89238×10^{-15}	1.89236×10^{-15}	1.89238×10^{-15}	1.89236×10^{-15}	1.89236×10^{-15}	1.89236×10^{-15}
c_{35}	-3.57963×10^{-11}	-2.23136×10^{-15}	-1.79383×10^{-15}	-9.18805×10^{-16}	-2.23136×10^{-15}	-9.18805×10^{-16}	-2.23136×10^{-15}	-2.23136×10^{-15}	-2.23136×10^{-15}
c_{45}	-1.56967×10^{-11}	3.61048×10^{-15}	3.61049×10^{-15}	-7.22100×10^{-15}	3.61048×10^{-15}	-7.22100×10^{-15}	3.61048×10^{-15}	3.61048×10^{-15}	3.61048×10^{-15}

Table 9. Factors for One-Sided Tolerance Limits for Normal Distributions

Factors K such that the probability is C that at least a proportion P of the distribution will be greater than y - KS_Y, where y and S_Y are estimates of the mean and the standard deviation computed from a sample size of n.

	C = 0.95					C = 0.99				
	P					P				
n	0.75	0.90	0.95	0.99	0.999	0.75	0.90	0.95	0.99	0.999
3	3.804	6.158	7.655	10.552	13.857	--	--	--	--	--
4	2.619	4.163	5.145	7.042	9.215	--	--	--	--	--
5	2.149	3.407	4.202	5.741	7.501	--	--	--	--	--
6	1.895	3.006	3.707	5.062	6.612	2.849	4.408	5.409	7.334	9.540
7	1.732	2.755	3.399	4.641	6.061	2.490	3.856	4.730	6.411	8.348
8	1.617	2.582	3.188	4.353	5.686	2.252	3.496	4.287	5.811	7.566
9	1.532	2.454	3.031	4.143	5.414	2.085	3.242	3.971	5.389	7.014
10	1.465	2.355	2.911	3.981	5.203	1.954	3.048	3.739	5.075	6.603
11	1.411	2.275	2.815	3.852	5.036	1.854	2.897	3.557	4.828	6.284
12	1.366	2.210	2.736	3.747	4.900	1.771	2.773	3.410	4.633	6.032
13	1.329	2.155	2.670	3.659	4.787	1.702	2.677	3.290	4.472	5.826
14	1.296	2.108	2.614	3.585	4.690	1.645	2.592	3.189	4.336	5.651
15	1.268	2.068	2.566	3.520	4.607	1.596	2.521	3.102	4.224	5.507
16	1.242	2.032	2.523	3.463	4.534	1.553	2.458	3.028	4.124	5.374
17	1.220	2.001	2.486	3.415	4.471	1.514	2.405	2.962	4.038	5.268
18	1.200	1.974	2.453	3.370	4.415	1.481	2.357	2.906	3.961	5.167
19	1.183	1.949	2.423	3.331	4.364	1.450	2.315	2.855	3.893	5.078
20	1.167	1.926	2.396	3.295	4.319	1.424	2.275	2.807	3.832	5.003
21	1.152	1.905	2.371	3.262	4.276	1.397	2.241	2.768	3.776	4.932
22	1.138	1.887	2.350	3.233	4.238	1.376	2.208	2.729	3.727	4.866
23	1.126	1.869	2.329	3.206	4.204	1.355	2.179	2.693	3.680	4.806
24	1.114	1.853	2.309	3.181	4.171	1.336	2.154	2.663	3.638	4.755
25	1.103	1.838	2.292	3.158	4.143	1.319	2.129	2.632	3.601	4.706
30	1.059	1.778	2.220	3.064	4.022	1.249	2.029	2.516	3.446	4.508
35	1.025	1.732	2.166	2.994	3.934	1.195	1.957	2.431	3.334	4.364
40	0.999	1.697	2.126	2.941	3.866	1.154	1.902	2.365	3.250	4.255
45	0.978	1.669	2.092	2.897	3.811	1.122	1.857	2.313	3.181	4.168
50	0.961	1.646	2.065	2.863	3.766	1.096	1.821	2.296	3.124	4.096

$$1 - P = \sqrt{\frac{1}{2\pi}} \int_{K_{1-P}}^{\infty} e^{-x^2/2} dx,$$

$$a = 1 - \frac{K_{1-C}^2}{2(n-1)}, \text{ where } 1 - C = \sqrt{\frac{1}{2\pi}} \int_{K_{1-C}}^{\infty} e^{-x^2/2} dx,$$

$$b = K_{1-P}^2 - \frac{K_{1-C}^2}{n};$$

or $K_{C,P}$ can be interpolated (see Reference 1).

c. Select the x_1 and x_2 values for which you want to predict the response.

d. From these values of x_1 and x_2, calculate the values of z_i:

$$z_1 = x_1, \ z_2 = x_2, \ z_3 = x_1^2, \ z_4 = x_2^2, \ z_5 = x_1 x_2.$$

e. Compute y from the equation $y = a_0 + a_1 z_1 + a_2 z_2 + a_{11} z_3 + a_{22} z_4 + a_{12} z_5$, using the coefficients of Table 1, 2, 3, or 4.

f. Using the same z_i values and obtaining s, n, c_{ii}, c_{ij} and z_i from Table 5, 6, 7, or 8, compute S_Y.

g. Finally compute Y using y from step "e," K_{CP} from step "b," and S_Y from step "f."

The assumptions and rationale behind the above methodology may be found in References 2 and 3. The somewhat complicated procedures and lengthy calculations have been programmed for GAC's IBM-1401/1410 computer. The results of these calculations are given in Tables 10 through 13. The lower 95 percent tolerance limits of the 95 percent confidence level are given for each material, test temperature, and test. These values can be interpreted as follows: 95 percent or more of a large number of future, similarly produced specimens when tested in the same manner as the specimens of this program will exceed this lower tolerance

Table 10. Lower Tolerance Limits - 298°K

Material	Specimen Direction	Tension (psi)	Compression (psi)	Flexure (psi)	Shear (psi)	Bearing Yield (psi)	Tensile Modulus (psi)
UFW	Parallel	252, 463	131, 188	206, 123	7, 344	38, 862	7, 949, 774
BFW	Parallel	137, 965	87, 445	165, 523	5, 901	46, 021	5, 008, 400
	45°	16, 492	12, 230	22, 443	3, 338	39, 342	2, 927, 700
	Normal	-	63, 242	134, 747	3, 392	42, 982	-
1581 Cloth	Parallel	82, 202	58, 225	99, 278	7, 396	39, 652	3, 062, 848
	45°	14, 196	26, 782	35, 836	4, 631	35, 245	1, 552, 381
	Normal	65, 006	53, 118	91, 353	6, 925	34, 804	2, 837, 151
1543 Cloth	Parallel	160, 773	83, 240	126, 491	8, 127	46, 947	5, 042, 851
	45°	-	25, 660	26, 922	-	34, 747	1, 797, 918
	Normal	18, 816	27, 455	30, 573	-	25, 613	1, 615, 171

Table 11. Lower Tolerance Limits - 197°K

Material	Specimen Direction	Tension (psi)	Compression (psi)	Flexure (psi)	Shear (psi)	Bearing Yield (psi)	Tensile Modulus (psi)
UFW	Parallel	312, 874	170, 636	307, 626	12, 439	39, 998	8, 831, 456
BFW	Parallel	138, 858	119, 621	217, 784	7, 349	58, 718	5, 887, 400
	45°	20, 570	41, 768	62, 986	4, 945	52, 291	4, 032, 500
	Normal	-	93, 988	168, 387	5, 472	57, 997	-
1581 Cloth	Parallel	108, 319	77, 209	132, 351	10, 257	45, 851	3, 409, 360
	45°	37, 675	44, 407	66, 913	7, 282	42, 375	1, 909, 457
	Normal	86, 016	70, 847	122, 523	9, 617	44, 873	3, 261, 401
1543 Cloth	Parallel	187, 464	102, 372	161, 922	11, 994	56, 790	5, 465, 120
	45°	13, 107	43, 146	51, 152	-	44, 564	2, 247, 822
	Normal	28, 661	45, 328	47, 920	-	37, 612	2, 286, 452

Table 12. Lower Tolerance Limits - 77°K

Material	Specimen Direction	Tension (psi)	Compression (psi)	Flexure (psi)	Shear (psi)	Bearing Yield (psi)	Tensile Modulus (psi)
UFW	Parallel	310, 574	207, 999	423, 696	13, 630	44, 382	8, 582, 807
BFW	Parallel	155, 337	127, 820	232, 041	7, 135	72, 796	6, 207, 000
	45°	22, 410	48, 310	66, 501	4, 975	67, 365	4, 620, 400
	Normal	-	98. 421	160, 303	6, 027	73, 854	-
1581 Cloth	Parallel	124, 978	98, 297	163, 798	11, 712	57, 908	3, 890, 137
	45°	51, 641	64, 442	96, 790	8, 583	56, 307	2, 424, 511
	Normal	96, 410	89, 658	150, 585	10, 735	60, 445	3, 804, 086
1543 Cloth	Parallel	209, 449	118, 798	196, 790	13, 808	68, 413	5, 708, 631
	45°	24, 829	58, 398	73, 680	-	57, 003	2, 654, 755
	Normal	29, 774	59, 166	61, 611	-	50, 608	2, 807, 542

Table 13. Lower Tolerance Limits - 20°K

Material	Specimen Direction	Tension (psi)	Compression (psi)	Flexure (psi)	Shear (psi)	Bearing Yield (psi)	Tensile Modulus (psi)
UFW	Parallel	271, 669	218, 378	471, 670	11, 857	44, 981	9, 299, 958
BFW	Parallel	162, 864	118, 048	217, 912	6, 129	78, 041	6, 083, 100
	45°	15, 755	38, 703	48, 532	4, 097	73, 532	4, 623, 900
	Normal	-	86, 607	135, 634	5, 410	79, 824	-
1581 Cloth	Parallel	126, 938	106, 902	174, 531	11, 517	64, 247	4, 111, 763
	45°	51, 733	72, 910	107, 296	8, 377	69, 035	2, 676, 441
	Normal	95, 515	97, 085	159, 574	10, 363	68, 323	4, 051, 399
1543 Cloth	Parallel	214, 595	123, 017	209, 181	13, 117	72, 618	5, 654, 482
	45°	25, 609	62, 562	80, 627	-	62, 143	2, 750, 595
	Normal	23, 933	62, 022	63, 805	-	55, 320	2, 883, 510

limit; the confidence probability that this statement is true is 95 percent. In making these calculations, care must be taken that the results desired are within the specific range of the variables originally defined by the test results, and also the dangers of rounding off numbers cannot be ignored.

C. SUPPLEMENTAL TESTING

1. General

As a part of Task I, further testing of simple test specimens was performed to supplement the data gather during the first year's effort. This supplemental testing can be grouped as follows:

(1) Continuation of tests not completed during the first year's effort. These tests include tensile testing of UFW material and thermal conductivity testing.

(2) Additional tests that were considered necessary to complete the data. These tests include further thermal expansion testing; tension, compression, and flexure tests of the cast resins; additional compression tests of BFW material; and a modified shear test.

The specimens for mechanical and thermal testing are as shown in Figures 1 and 2 unless otherwise noted.

2. Fabrication

Wherever possible, the flat laminates produced and documented during the first year's effort of this contract were used for the specimens of the second year's effort. However, Task I required the fabrication of some additional laminate materials. These materials have been fabricated with the same meticulous quality and process control as used in the first year's effort. The basic raw material quality control test reports on the material used for the additional sheets are presented in Tables 14 and 15. The additional panels were fabricated in accordance with the process sheets included as Figures 3 through 11. Table 16 gives the resin content of the panels.

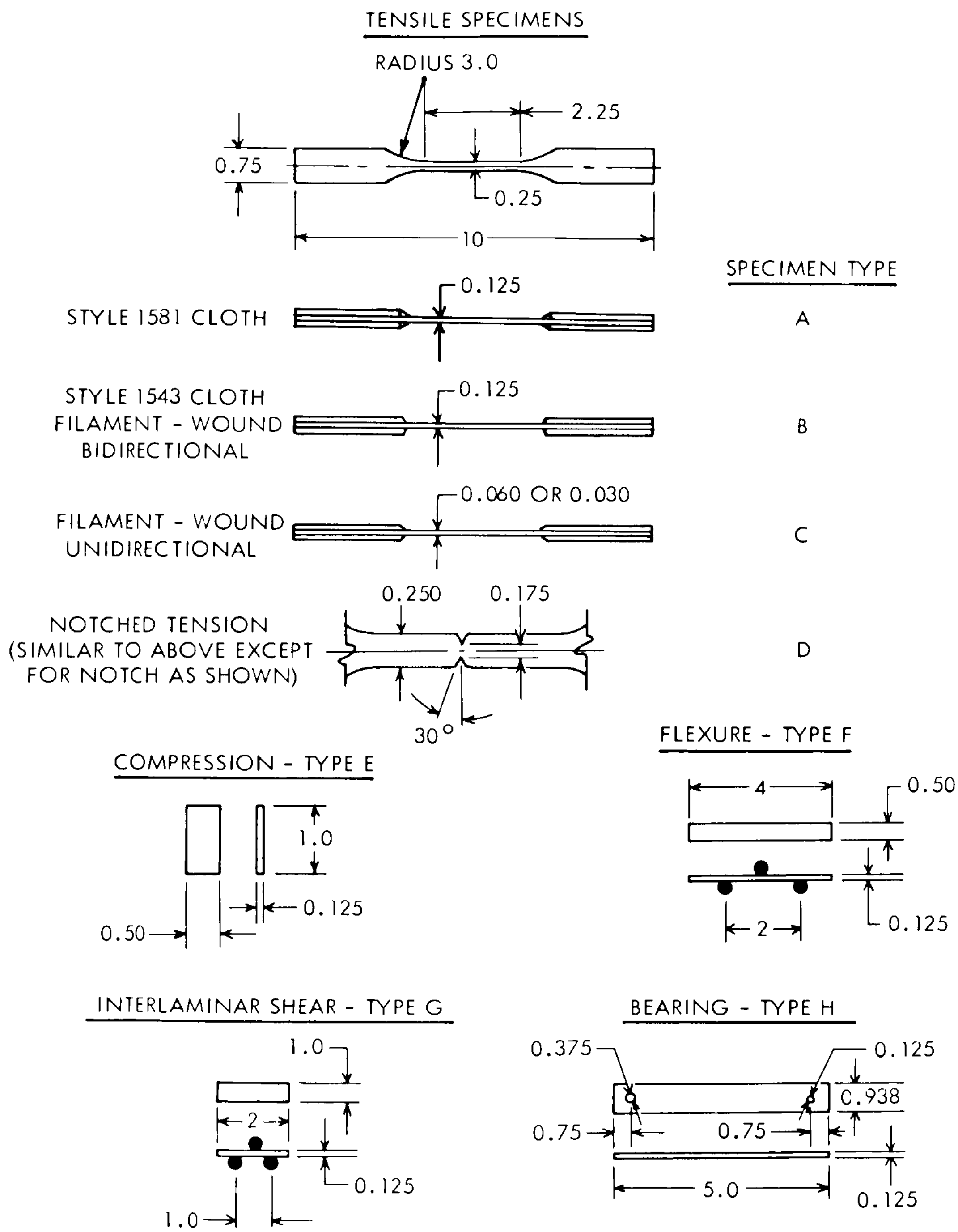

Figure 1. Specimens for the Mechanical Properties Test Program

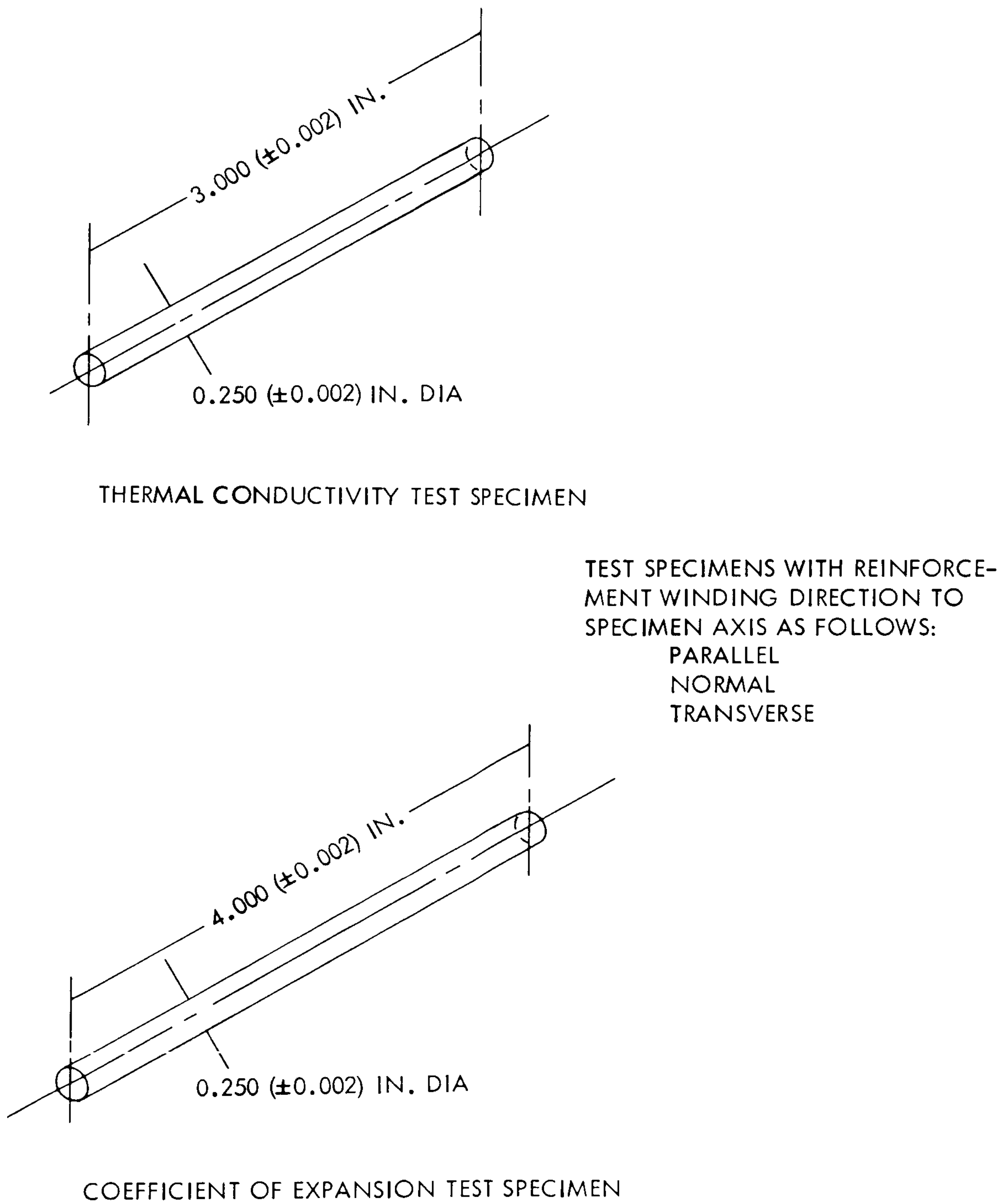

Figure 2. Specimens for the Thermal Properties Test Program

Table 14. E-787 Prepreg Roving Quality Control Test Report (Sheet 1)

Roving Lot No. F1620, U.S. Polymeric, Specification WS-1028A

Property	Roll No. 209-41			Roll No. 206-37			Roll No. 77-7		
	1	2	3	1	2	3	1	2	3
% VOLATILES									
Original Wt (g/yd)	1.547	1.552	1.550	1.566	1.564	1.560	1.529	1.520	1.525
Less Volatile Wt (g/yd)	1.539	1.534	1.530	1.552	1.550	1.546	1.516	1.503	1.510
Difference	0.008	0.018	0.020	0.014	0.014	0.014	0.013	0.017	0.015
% Volatiles	0.51	1.1	1.29	0.89	0.89	0.9	0.85	1.1	0.98
Average	0.97			0.89			0.98		
IGNITION LOSS									
Less Volatile Wt (g/yd)	1.539	1.534	1.530	1.552	1.550	1.546	1.516	1.503	1.510
Final Wt (g/yd)	1.218	1.218	1.215	1.223	1.224	1.222	1.229	1.229	1.227
Difference	0.321	0.316	0.315	0.329	0.326	0.324	0.287	0.274	0.283
% Ignition Loss	20.8	20.6	20.6	21.2	21.0	20.9	18.9	18.2	18.7
Average	20.7			21.0			18.6		
Wt per Yd (g)	0.6090	0.6090	0.6075	0.6115	0.6120	0.6110	0.6145	0.6145	0.6135
Average	0.6085			0.6115			0.6141		
RESIN FLOW									
Original Wt (g/yd)	0.127	0.127	0.127	0.130	0.131	0.131	0.128	0.128	0.128
Wt after Curing (g/yd)	0.117	0.115	0.115	0.116	0.117	0.117	0.117	0.117	0.115
Difference	0.010	0.012	0.012	0.014	0.014	0.014	0.011	0.011	0.013
% Flow	7.8	9.4	9.4	10.7	10.7	10.7	8.6	8.6	10.1
Average	8.9			10.7			9.1		
GEL-TIME at 325°F (Minutes & Seconds)	2'54"	2'25"	2'15"	2'28"	2'22"	2'24"	1'50"	1'52"	1'37"
Average	2'31"			2'25"			1'46"		
TENSILE STRENGTH (psi)	424,157			422,076			396,678		
HORIZ SHEAR STRENGTH At 250°F (psi)	3,287	3,287	3,227	3,406	3,324	3,155	3,394	3,155	3,227
Average (psi)	3,267			3,295			3,259		
After 2-hr Water Boil	12,071	11,773	12,060	10,040	10,279	10,458	11,713	11,235	11,833
Average	11,968			10,259			11,594		

Table 14. E-787 Prepreg Roving Quality Control Test Report (Sheet 2)

Roving Lot No. F1620, U.S. Polymeric, Specification WS-1028A

Roll No. 9-49			Roll No. 100-30			Roll No. 5-47			Roll No. 151-20		
1	2	3	1	2	3	1	2	3	1	2	3
1.475 1.460 0.015 1.0	1.487 1.473 0.014 0.94	1.474 1.460 0.014 1.0	1.510 1.495 0.015 0.99	1.491 1.480 0.011 0.74	1.505 1.493 0.013 0.79	1.497 1.484 0.013 0.87	1.501 1.485 0.016 1.0	1.495 1.483 0.012 0.80	1.524 1.510 0.014 0.92	1.526 1.508 0.018 1.18	1.520 1.504 0.016 1.05
0.98			0.84			0.89			1.05		
1.460 1.198 0.262 17.9	1.473 1.179 0.294 18.6	1.460 1.196 0.264 17.9	1.495 1.210 0.285 19.0	1.480 1.200 0.280 18.9	1.493 1.200 0.293 19.6	1.484 1.210 0.274 18.4	1.485 1.211 0.274 18.4	1.483 1.210 0.273 18.4	1.510 1.210 0.300 19.8	1.508 1.214 0.294 19.5	1.504 1.215 0.289 19.2
18.1			19.1			18.4			19.5		
0.5990	0.5995	0.5980	0.6050	0.6000	0.6000	0.6050	0.6055	0.6050	0.6050	0.6070	0.6075
0.5955			0.6017			0.6052			0.6065		
0.122 0.112 0.010 8.2	0.124 0.115 0.009 7.2	0.122 0.113 0.009 7.4	0.122 0.113 0.009 7.4	0.121 0.113 0.008 6.6	0.122 0.113 0.009 7.4	0.123 0.112 0.011 8.9	0.123 0.113 0.010 8.1	0.122 0.112 0.010 8.2	0.122 0.113 0.009 7.4	0.123 0.114 0.009 7.3	0.123 0.113 0.010 8.1
7.6			7.1			8.4			7.6		
1'27"	1'48"	1'26"	1'54"	2'00"	1'41"	1'23"	1'55"	1'37"	1'47"	1'54"	1'43"
1'33"			1'52"			1'35"			1'48"		
450,377			453,049			440,846			432,646		
3,359	3,466	3,394	2,760	2,688	2,614	3,526	3,494	3,140	3,108	3,133	3,205
3,406			2,687			3,387			3,149		
12,240	12,000	12,307	10,380	10,920	10,482	11,760	10,757	10,964	9,639	9,360	9,578
12,182			10,594			11,160			9,526		

Table 15. E-787 Prepreg Cloth Quality Control Test Report
Dated 7 September 1964

Test	U. S. Polymeric Lot No. D5942			U.S. Polymeric Lot No. D5942		
PROPERTIES	S/HTS, S-901, 81/38,32(±2)% Ignition Loss			S/HTS, S-901, 43/38, 32(±2)% Ignition Loss		
% Resin Solids	34.35			36.38		
% Volatiles	1.08			1.72		
% Flow	9.9			14.8		
Gel Time	1 minute			30 seconds		
FLEXURE TEST RESULTS	Dimension	Ult Load (psi)	Ult PSI	Dimension	Ult Load (psi)	Ult PSI
	0.120 x 1.002	532	110,603	0.134 x 0.982	827	140,726
	0.125 x 1.002	512	98,084	0.136 x 1.002	909	147,167
	0.122 x 1.001	508	100,661	0.137 x 0.998	911	145,916
	0.116 x 0.999	528	117,857	0.138 x 0.999	881	138,959
	Avg		106,804	Avg		143,192

PROCESS SHEET NO. 1
SPOOL WIND FLAT PANELS
BIDIRECTIONAL - 1/1 DISPERSION

W. O. No. 866732
U. S. O. No. 558
Date 7/22/64

Panel No: 1000
1001
1002
1003

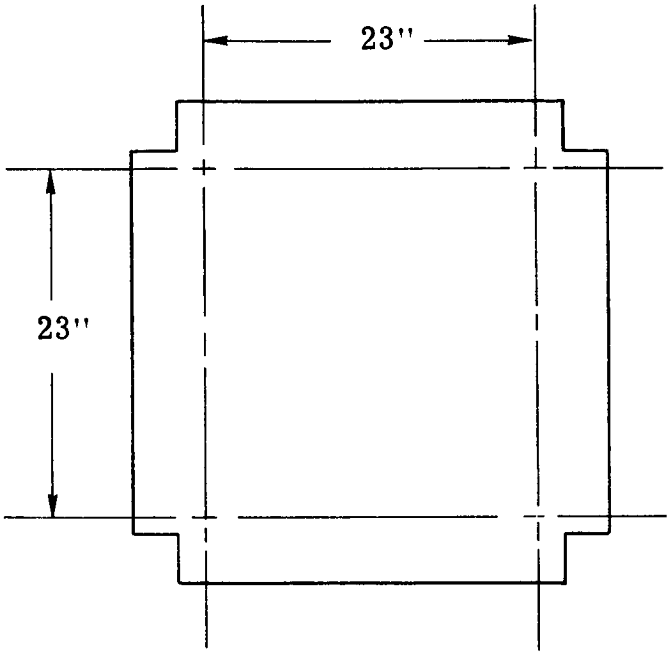

U. S. Polymeric Lot No. F1620
Packages 7, 131, 197

FABRICATION INSTRUCTIONS

1. Laminate Thickness - 0.125
2. No. of Layers - 15
3. Indexing - 0.2499 (using three 20-end rovings)
4. Material - 20-end roving, S/HTS with E-787 resin pre-preg
5. Tension - 5 lb/20-end

AFTER WINDING

1. Cut filaments and remove from flat mandrel.
2. Trim ends of panels, making them approximately 23 x 23 inches.
3. Number panels and mark filament direction.
4. Store in freezer, if necessary, in a sealed bag.
5. Cure panels per process card (4 hours at 325°F, 50 psi pressure).

Figure 3. Process Sheet No. 1

PROCESS SHEET NO. 2
SPOOL WIND FLAT PANELS
BIDIRECTIONAL - 1/1 DISPERSION

W. O. No. - 866732
U. S. O. No. - 569
Date - 7/24/64

Panel No: 1004
1005
1006
1007

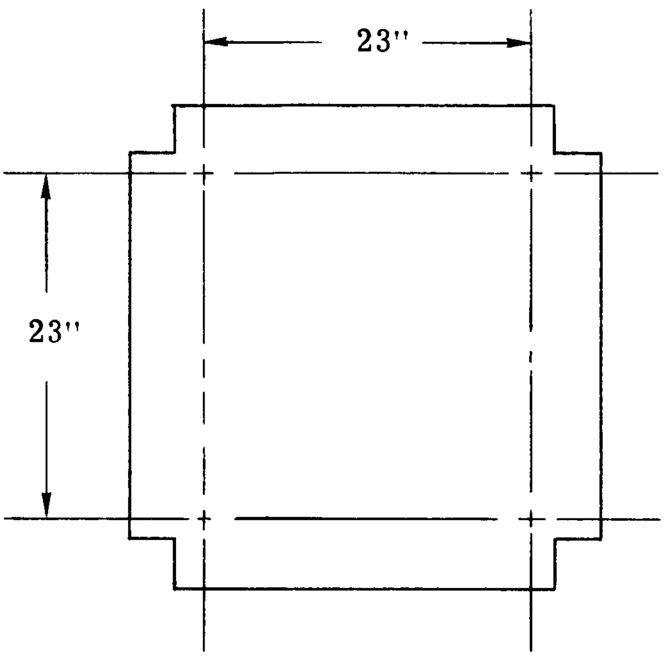

U. S. Polymeric Lot No. F1620
Packages 214, 111, 21

FABRICATION INSTRUCTIONS

1. Laminate Thickness - 0.125
2. No. of Layers - 15
3. Indexing - 0.2499 (using three 20-end rovings)
4. Material - 20-end roving S/HTS with E-787 resin pre-preg
5. Tension - 5 lb/20-end

AFTER WINDING

1. Cut filaments and remove from flat mandrel.
2. Trim ends of panels making them approximately 23 x 23 inches.
3. Number panels and mark filament direction.
4. Store in freezer, if necessary, in a sealed bag.
5. Cure panels per process card (4 hours at 325°F, 50 psi pressure).

Figure 4. Process Sheet No. 2

PROCESS SHEET NO. 3
SPOOL WIND FLAT PANELS
UNIDIRECTIONAL

W. O. No. - 866732
U. S. O. No. - 569
Date - 7/24/64

Panel No. 1008
1009
1010
1011

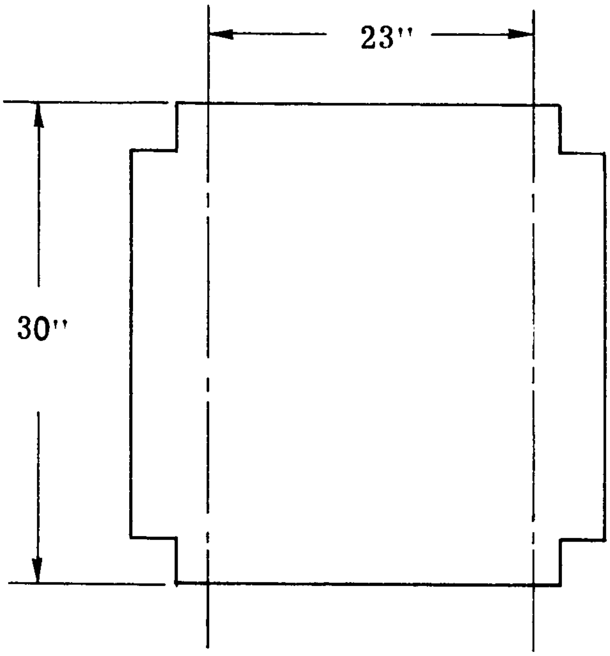

U. S. Polymeric Lot No. F1620
Packages 23, 86, 223, 75, 101, 186

FABRICATION INSTRUCTIONS

1. Laminate Thickness - 0.250
2. No. of Layers - 35
3. Indexing - 0.2499 (using three 20-end rovings)
4. Material - 20-end roving S/HTS with E-787 resin pre-preg
5. Tension - 5 lb/20-end

AFTER WINDING

1. Cut filaments and remove from flat mandrel.
2. Trim ends of panels making them approximately 23 x 23 inches.
3. Number panels and mark filament direction.
4. Store in freezer, if necessary, in a sealed bag.
5. Cure panels per process card (4 hours at 325^{o}F, 50 psi pressure).

Figure 5. Process Sheet No. 3

PROCESS SHEET NO. 4
SPOOL WIND FLAT PANELS
BIDIRECTIONAL - 1/1 DISPERSION

W. O. No. - 866732
U. S. O. No. - 569
Date - 7/24/64

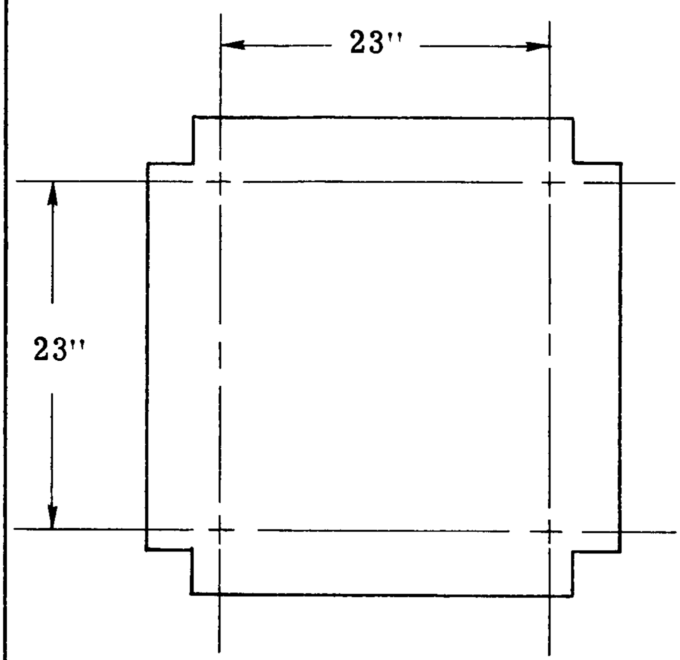

Panel No. 1012
1013
1014
1015

U.S. Polymeric Lot No. F1620
Packages 9, 11, 83, 126, 198, 213

FABRICATION INSTRUCTIONS

1. Laminate Thickness - 0.250
2. No. of Layers - 33
3. Indexing - 0.2499 (using three 20-end rovings)
4. Material - 20 end roving, S/HTS with E-787 resin pre-preg
5. Tension - 5 lb/20-end

AFTER WINDING

1. Cut filaments and remove from flat mandrel.
2. Trim ends of panels making them approximately 23 x 23 inches.
3. Number panels and mark filament direction.
4. Store in freezer, if necessary, in a sealed bag.
5. Cure panels per process card (4 hours at 325^{o}F, 50 psi pressure).

Figure 6. Process Sheet No. 4

PROCESS SHEET NO. 5
CLOTH REINFORCED LAMINATES
PARALLEL LAYER ORIENTATION

W. O. No. - 866732
U. S. O. No. - 788
Date - 9/14/64

Panel No. 1018

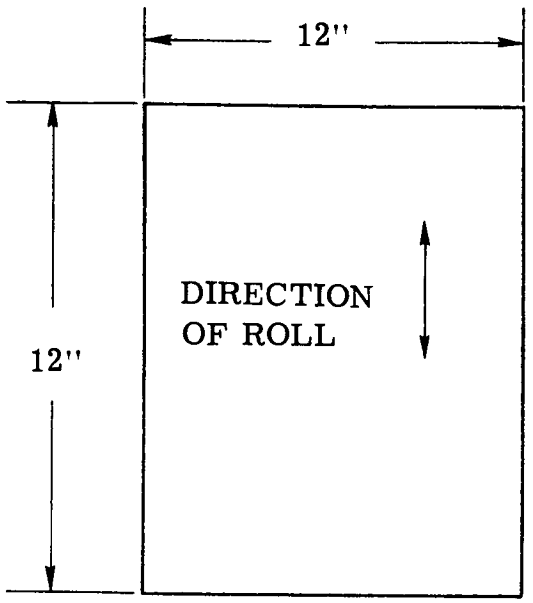

U. S. Polymeric Roll Batch
No. D5943

FABRICATION INSTRUCTIONS

1. Laminate Thickness - 0.250
2. No. of Layers - 25
3. Material - 1543, S/HTS, S-901, 43/38, E-787 pre-preg cloth, 32(±2)% ignition loss

LAYUP

1. Cut cloth to panel dimensions.
2. Indicate major reinforement direction on each layer using scotch tape.
3. Store in freezer, if necessary, in a sealed bag.
4. Layup panel on curing mold.
5. Cure panels per process card (4 hours at 325^{o}F, 50 psi pressure).

Figure 7. Process Sheet No. 5

PROCESS SHEET NO. 6
CLOTH REINFORCED LAMINATES
PARALLEL LAYER ORIENTATION

W. O. No. - 866732
U. S. O. No. - 788
Date - 9/16/64

Panel No. 1019

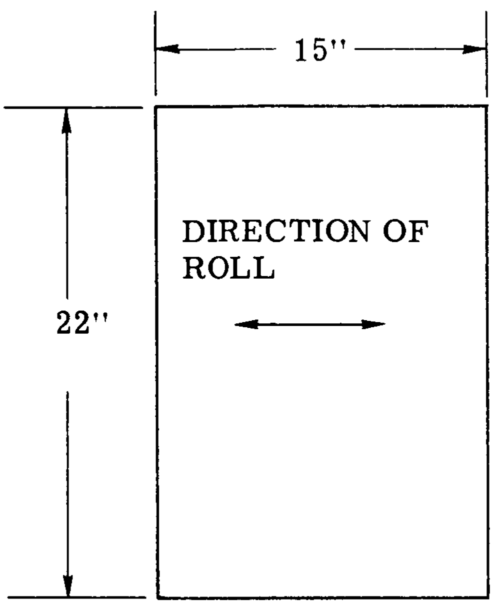

U. S. Polymeric Roll Batch No. D5943

FABRICATION INSTRUCTIONS

1. Laminate Thickness - 0.250
2. No. of Layers - 26
3. Material - 1543, S/HTS, S-901, 43/38, E-787 pre-preg cloth, 32(±2)% ignition loss

LAY-UP

1. Cut cloth to panel dimensions
2. Indicate major reinforcement direction on each layer using scotch tape.
3. Store in freezer, if necessary, in a sealed bag.
4. Lay up panel on curing mold.
5. Cure panel per process card (4 hours at 325^{O}F, 50 psi pressure)

Figure 8. Process Sheet No. 6

PROCESS SHEET NO. 7
CLOTH REINFORCED LAMINATES
PARALLEL LAYER ORIENTATION

W. O. No. - 866732
U. S. O. No. - 788
Date - 9/16/64

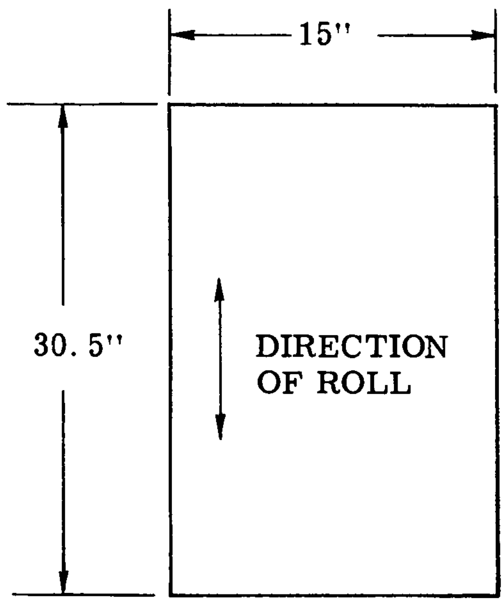

Panel No: 1020
1021
1022

U. S. Polymeric Roll Batch
No. D5943

FABRICATION INSTRUCTIONS

1. Laminate Thickness - 0.250
2. No. of Layers - 26
3. Material - 1543, S/HTS, S-901, 43/38, E-787 pre-preg cloth, 32 (±2)% ignition loss

LAY-UP

1. Cut cloth to panel dimensions.
2. Indicate major reinforcement direction on each layer using scotch tape.
3. Store in freezer, if necessary, in a sealed bag.
4. Lay up panel on curing mold.
5. Cure panels per process card (4 hours at 325°F, 50 psi pressure).

Figure 9. Process Sheet No. 7

PROCESS SHEET NO. 8
CLOTH REINFORCED LAMINATES
PARALLEL LAYER ORIENTATION

W. O. No. - 866732
U. S. O. No. - 788
Date - 9/16/64

Panel No: 1023

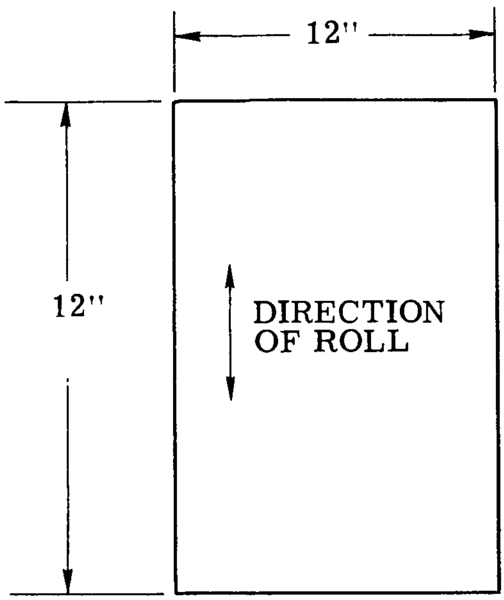

U. S. Polymeric Roll Batch
No. D5942

FABRICATION INSTRUCTIONS

1. Laminate Thickness - 0.250
2. No. of Layers - 23
3. Material - 1581, S/HTS, S-901,81/38, E-787
   pre-preg cloth, 32 (±2)% ignition loss

LAY-UP

1. Cut cloth to panel dimensions.
2. Indicate major reinforcement direction on each layer using scotch tape.
3. Store in freezer, if necessary, in a sealed bag.
4. Lay up panel on curing mold.
5. Cure panels per process card (4 hours at 325°F, 50 psi pressure)

Figure 10. Process Sheet No. 8

PROCESS SHEET NO. 9
CLOTH REINFORCED LAMINATES
PARALLEL LAYER ORIENTATION

W. O. No. - 866732
U. S. O. No. - 788
Date - 9/17/64

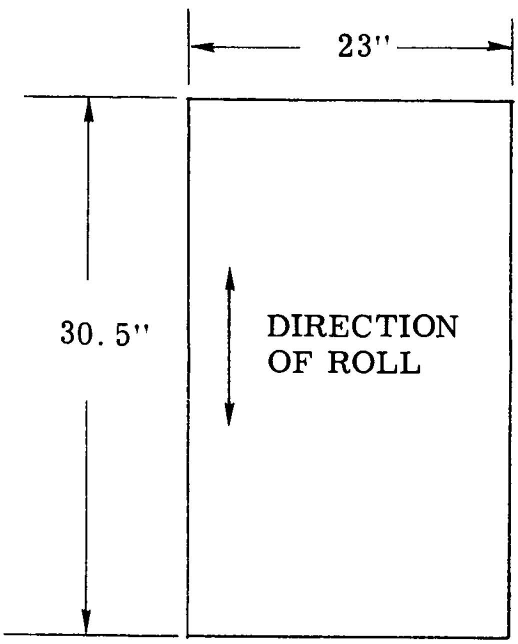

Panel No: 1024
1025
1026
1027

U. S. Polymeric Roll Batch
No. D5942

FABRICATION INSTRUCTIONS

1. Laminate Thickness - 0. 250
2. No. of Layers - 25
3. Material - 1581, S/HTS, S-901,81/38, E-787 pre-preg cloth, 32(±2)% ignition loss

LAY-UP

1. Cut cloth to panel dimensions.
2. Indicate major reinforcement direction on each layer using scotch tape.
3. Store in freezer, if necessary, in a sealed bag.
4. Lay up panel on curing mold.
5. Cure panels per process card (4 hours at 325°F, 50 psi pressure).

Figure 11. Process Sheet No. 9

Table 16. Resin Content of Panels

Panel No.	Resin Content (percent)		
	Specimen No. 1	Specimen No. 2	Average
1000	18.65	18.85	18.75
1001	18.77	18.49	18.63
1002	18.13	18.20	18.16
1003	18.16	17.98	18.07
1004	17.58	18.54	18.06
1005	19.17	19.28	19.21
1006	18.57	18.10	18.33
1007	18.58	17.90	18.24
1008	19.68	19.62	19.64
1009	18.95	19.40	19.18
1010	19.56	19.74	19.65
1011	17.62	17.63	17.62
1012	19.56	19.04	19.30
1013	19.70	19.78	19.74
1014	18.67	18.66	18.66
1015	18.56	18.70	18.63
1018	35.79	35.69	35.74
1019	35.76	35.69	35.72
1020	34.33	36.54	35.43
1021	35.52	36.31	35.91
1022	35.40	35.40	35.40
1023	35.36	34.59	34.97
1024	36.33	36.14	36.23
1025	36.30	36.27	36.28
1026	33.11	36.13	34.62
1027	35.40	35.53	35.46

3. Testing and Results

a. UFW Tensile Tests. The data on the tensile testing of UFW roving material at low temperatures was deleted from the first year's results because of premature failures in the bond of the end reinforcement to the basic specimen. The use of various adhesives that had given the desired results at room temperature met with only partial success at the liquid nitrogen temperature. Further tensile tests of this material were therefore necessary to complete the test data.

New tensile grips that would accept specimens with a longer reinforcement area were fabricated. The longer area and the use of an Adiprene L-100 and Moca adhesive system with a 160°F maximum temperature cure produced an ultimate failure in six of seven specimens at 77°K (see Figure 12). With these encouraging results, the UFW tensile and notched tensile specimens were tested at all four temperatures. The results are shown in Table 17. All failures in these tests indicated that the ultimate tensile strength had been obtained. The strength of the unidirectional panels in the normal direction at 298°K is also shown in this table.

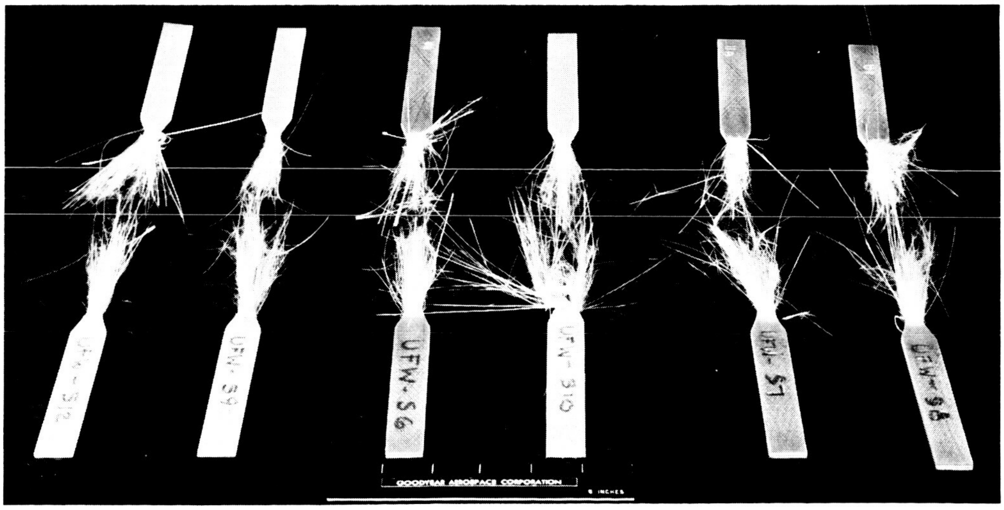

Figure 12. Ultimate Failures of Unidirectional Tensile Specimens Tested at 77°K

Table 17. Supplemental Testing - UFW Tensile Tests

Test	Test Temp (°K)	Specimen No.	Test Results (psi)	Avg Results (psi)
Ultimate Tensile Strength	298	UFW-11B-28	307,796	
		UFW-12A-28	277,778	
		UFW-12B-28	297,872	
		UFW-13B-28	277,055	
		UFW-15A-28	242,581	
		UFW-15B-28	282,258	280,890
	197	UFW-11B-28	313,476	
		UFW-12A-28	344,604	
		UFW-12B-28	375,672	
		UFW-13B-28	348,178	
		UFW-15A-28	314,516	
		UFW-15B-28	325,781	337,038
	77	UFW-11B-28	352,377	
		UFW-12A-28	347,195	
		UFW-12B-28	383,226	
		UFW-13B-28	345,994	
		UFW-15A-28	264,785	
		UFW-15B-28	290,193	330,628
	20	UFW-11B-28	252,623	
		UFW-12A-28	287,175	
		UFW-12B-28	334,147	
		UFW-13B-28	330,645	
		UFW-15A-28	295,265	
		UFW-15B-28	286,590	297,741
Tensile Notched Stength	298	UFW-11B-29	260,492	
		UFW-12A-29	287,841	
		UFW-12B-29	285,618	
		UFW-13B-29	265,269	
		UFW-15A-29	280,358	
		UFW-15B-29	284,011	277,256

Table 17. Supplemental Testing - UFW Tensile Tests (Continued)

Test	Test Temp (^oK)	Specimen No.	Test Results	Avg Results (psi)
Tensile Notched Strength	197	UFW-11B-29	302,579	
		UFW-12A-29	283,559	
		UFW-12B-29	326,049	
		UFW-13B-29	276,750	
		UFW-15A-29	315,860	
		UFW-15B-29	298,074	299,645
	77	UFW-11B-29	278,533	
		UFW-12A-29	324,324	
		UFW-12B-29	281,870	
		UFW-13B-29	308,090	
		UFW-15A-29	328,725	
		UFW-15B-29	325,736	307,880
	20	UFW-11B-29	256,286	
		UFW-12A-29	311,185	
		UFW-12B-29	289,123	
		UFW-13B-29	269,370	
		UFW-15A-29	296,703	
		UFW-15B-29	326,203	291,478
Tensile Modulus	298	UFW-11B-28	8,640,600	
		UFW-12A-28	8,000,000	
		UFW-12B-28	8,234,800	
		UFW-13B-28	8,129,600	
		UFW-15A-28	7,985,400	
		UFW-15B-28	8,215,200	8,184,000
	197	UFW-11B-28	9,005,100	
		UFW-12A-28	9,068,500	
		UFW-12B-28	9,189,000	
		UFW-13B-28	9,189,000	
		UFW-15A-28	9,240,000	
		UFW-15B-28	8,800,600	9,082,100

Table 17. Supplemental Testing - UFW Tensile Tests (Continued)

Test	Test Temp (°K)	Specimen No.	Test Results (psi)*	Avg Results (psi)*
Tensile Modulus	77	UFW-11B-28	8,968,900	
		UFW-12A-28	8,636,700	
		UFW-12B-28	8,871,000	
		UFW-13B-28	8,942,500	
		UFW-15A-28	8,945,700	
		UFW-15B-28	8,636,700	8,833,600
	20	UFW-11B-28	9,716,300	
		UFW-12A-28	9,582,600	
		UFW-12B-28	8,996,300	
		UFW-13B-28	9,915,400	
		UFW-15A-28	10,005,600	
		UFW-15B-28	9,088,500	9,550,800
Ultimate Tensile Elongation	298	UFW-11B-28	4.3%	
		UFW-12A-28	4.5	
		UFW-12B-28	4.6	
		UFW-13B-28	4.1	
		UFW-15A-28	4.9	
		UFW-15B-28	3.9	4.4%
	197	UFW-11B-28	4.4%	
		UFW-12A-28	4.3	
		UFW-12B-28	4.5	
		UFW-13B-28	4.4	
		UFW-15A-28	4.4	
		UFW-15B-28	4.4	4.4%
	77	UFW-12A-28	5.5%	
		UFW-12B-28	4.3	
		UFW-13B-28	5.0	
		UFW-15A-28	6.0	
		UFW-15B-28	5.9	5.3%

*Test results are in psi except for ultimate tensile elongation, which is in percent.

Table 17. Supplemental Testing - UFW Tensile Tests (Continued)

Test	Test Temp (°K)	Specimen No.	Test Results (psi)*	Avg Results (psi)*
Ultimate Tensile Elongation	20	UFW-11B-28	4.6%	
		UFW-12A-28	6.2	
		UFW-12B-28	5.2	
		UFW-13B-28	4.3	
		UFW-15A-28	5.3	
		UFW-15B-28	4.9	5.1%
Ultimate Tensile Strength (Normal Direction)	298	UFW-1A-1	5,844	
		UFW-1A-2	6,231	
		UFW-1A-3	5,588	
		UFW-1A-4	5,146	
		UFW-1A-5	6,355	
		UFW-1A-6	6,506	
		UFW-1A-7	6,304	
		UFW-1A-8	5,988	5,995

*Test results are in psi except for ultimate tensile elongation, which is in percent.

b. Thermal Conductivity Testing. Thermal conductivity tests at 20, 77, 197, and 300°K were performed using the axial heat flow method developed during the first year's work. This method consisted of measuring the power input and temperature gradient along the axis of an electrically heated rod specimen under thermal equilibrium conditions. These measurements combined with data on the cross-sectional area of the specimen permitted calculations of thermal conductivity from Fourier's equation for linear heat flow:

$$q = -kA \frac{\Delta T}{\Delta X} \tag{5}$$

where

q = heat flow through the specimen,

k = thermal conductivity,

A = cross-sectional area of the specimen,

$\frac{\Delta T}{\Delta X}$ = temperature gradient along the axis of the specimen.

The test specimen, a 1/4-inch diameter x 3-inch long rod, was assembled in the cryostat as shown schematically in Figure 13. Heat transfer between the specimen and radiation shield was minimized by evacuating the copper chamber and differentially heating the shield to approximately the same temperature as the specimen. Heat conduction in the lead wires from the thermocouples and heaters was minimized by wrapping the wires around the radiation shield and copper post. Vacuum-type feed-throughs at the top of the stainless steel evacuation line were used for electrical connections from the chamber to the associated measuring instruments and power supplies.

During the tests, the specimen chamber was evacuated to 10^{-5} torr or lower and completely immersed in a Dewar containing liquid hydrogen, liquid nitrogen, acetone and dry ice mixture, or water for testing at 20, 77, 197 and 330°K respectively. After thermal equilibrium was obtained, power was applied to the specimen and guard heaters to produce a temperature gradient of about 10°K. Temperatures along the axis of the specimen were measured with premium grade copper constantan thermocouples that were referenced to the liquid bath temperature. The specimen heater power was computed from measured values of the voltage and current through the heater.

Thermal conductivity test results are given in Table 18. These results indicate that the thermal conductivity of the fiberglass-reinforced epoxy resin materials investigated on this program nonlinearly decreases with temperature. The value

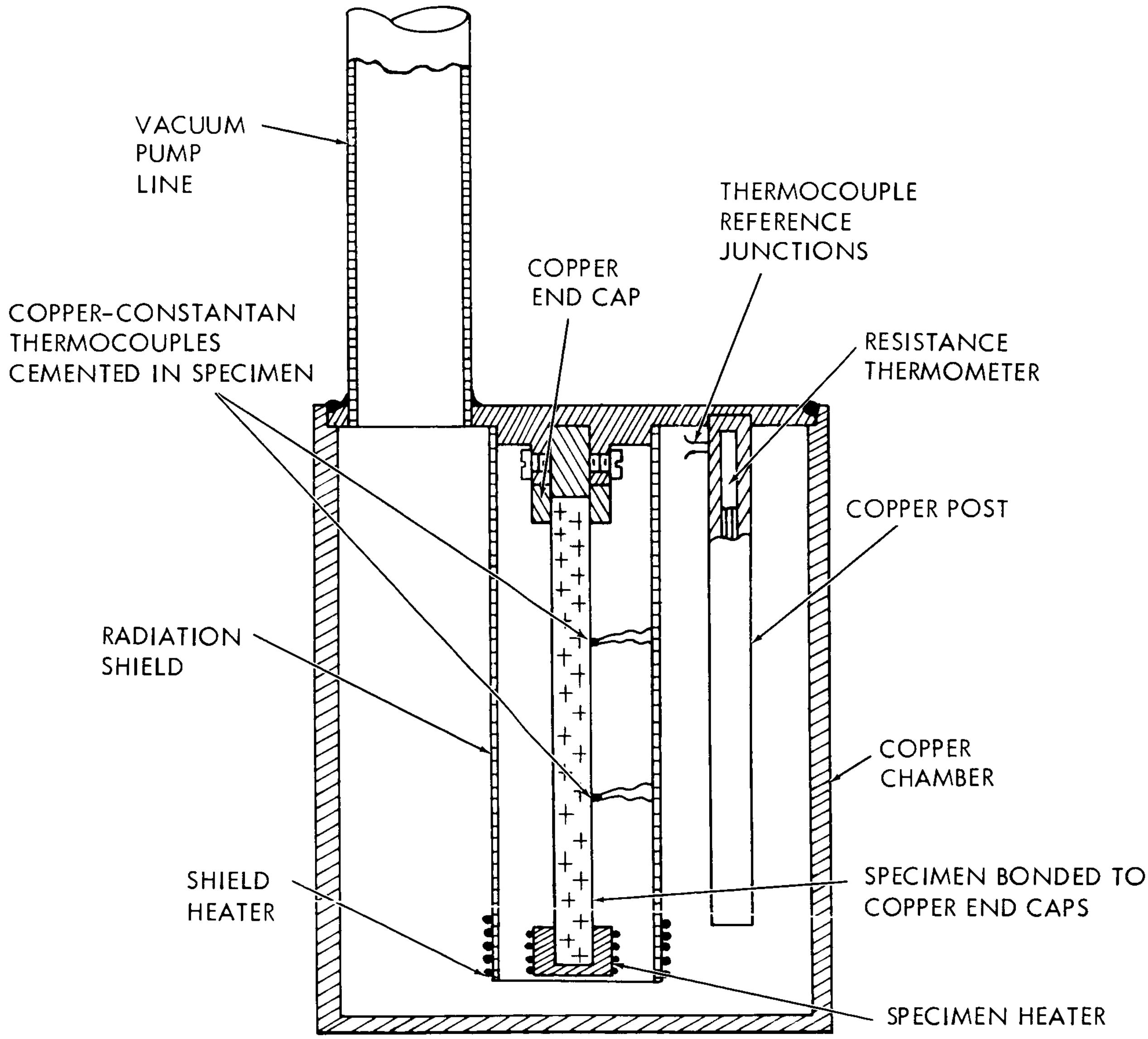

Figure 13. Thermal Conductivity Cryostat Specimen Chamber

Table 18. Thermal Conductivity Test Results

Material	Direction of Measurement	Specimen No.	Thermal Conductivity (mw cm^{-1} $^{o}K^{-1}$)			
			300°K	197°K	77°K	20°K
BFW	Parallel to reinforcement	BFW-7A and 7B-23-1	7.55	3.47	1.08	
		BFW-7A and 7B-23-2	8.57	3.20	1.09	0.75
		BFW-7A and 7B-23-3	6.40	2.01	0.90	
UFW	Parallel to reinforcement	UFW-9A and 9B-23-1	8.93	3.12	1.16	
		UFW-9A and 9B-23-2	6.66	2.11	1.27	1.15
		UFW-9A and 9B-23-3	6.69	2.53	1.33	
1543 Cloth Laminate	Parallel to reinforcement	1543-10A-23-1	7.95	2.68	0.84	
		1543-10A-23-2	6.50	2.40	1.00	0.80
		1543-10A-23-3	6.29	2.20	1.23	
1581 Cloth Laminate	Parallel to reinforcement	1581-9A and 9B-23-1	9.94	3.14	1.00	
		1581-9A and 9B-23-2	8.53	3.00	1.00	0.86
		1581-9A and 9B-23-3	8.16	2.95	1.02	
BFW	Across reinforcement	BFW-7A and 7B-31-1	10.50	2.92	0.92	
		BFW-7A and 7B-31-2	10.80	3.19	1.07	1.08
		BFW-7A and 7B-31-3	10.55	3.37	1.27	
UFW	Across reinforcement	UFW-9A and 9B-31-1	6.90	3.60	1.35	
		UFW-9A and 9B-31-2	6.79	2.99	1.32	1.19
		UFW-9A and 9B-31-3	7.80	3.30	1.30	

Table 18. Thermal Conductivity Test Results (Continued)

Material	Direction of Measurement	Specimen No.	Thermal Conductivity (mw cm^{-1} $^oK^{-1}$)			
			300°K	197°K	77°K	20°K
1543 Cloth Laminate	Across reinforcement	1543-10A-31-1 1543-10A-31-2 1543-10A-31-3	11.00 10.70 10.15	3.72 3.34 2.15	0.90 1.18 1.13	1.05
1581 Cloth Laminate	Across reinforcement	1581-9A and 9B-31-1 1581-9A and 9B-31-2 1581-9A and 9B-31-3	9.77 8.80 7.78	3.82 3.75 2.72	0.79 1.20 1.36	1.17
E-787 Resin		E-787-1	2.30	1.81	0.93	0.85

for thermal conductivity at any specific test temperature appears to be dependent on both the composition and orientation of the individual specimen material components. Variations in test results appear to be within reasonable limits considering the test method and the inherent nonhomogeneity of the materials.

c. Thermal Expansion Testing. Additional thermal expansion tests of the reinforced plastic laminates were appended to the original test schedule when it appeared that additional testing using current techniques would provide an improved set of data points for a final evaluation. All the tests conducted to obtain the data given in Table 19 used coincident test procedures and the same quartz support tube. The dilatometer cryostat (see Figure 14) with the specimen installed was allowed to stabilize overnight at 77°K. The following day, the specimen was cooled to 4.2°K with liquid helium and maintained at this temperature until no further contraction of the specimen was observed. The dial gage reading was recorded; then the specimen was heated and stabilized at each of the temperature test points - 20, 77, and 197°K. The integral expansion measurements were completed with the temperature of the specimen stabilized at 293°K. For continuity and comparative purposes, the data presented in Table 19 was adjusted for a reference temperature of 297°K.

Comparison of initial expansion test data, presented in the annual report for the first year's effort (GER 11214 S/11), with the data of Table 19 indicates that the magnitude of variation in test results for like material has been reduced. Dilatometer calibration curves using an OFHC copper rod were made periodically and, as shown in Figure 15, indicate the repeatability of the instrument and that there are no basic problems associated with the selected measurement technique or test procedures.

d. Cast E-787 Resin Testing. During this year, the mechanical properties of the cast E-787 resin without reinforcement were also obtained. The purposes of these tests are to define the properties of the resin at these temperatures in order to better understand the total laminate's properties and modes of failure, and also to be more prepared to evaluate other resin systems that might be suggested for cryogenic use. Cast sheets of the resin, obtained from U.S. Polymeric Chemicals Inc, were tested in flexure, compression, and tension. The test specimens

Table 19. Linear Thermal Contraction

Material	Direction of Reinforcement	Specimen No.	$\frac{L_{297}-L_T}{L_{297}} \times 10^5$ T = 297°K	T = 197°K	T = 77°K	T = 20°K	T = 4.2°K
BFW	Normal	BFW-7A and 7B-26-1	0	72	129	145	145
		BFW-7A and 7B-26-2	0	72	130	142	143
		BFW-7A and 7B-26-3	0	72	133	148	150
BFW	Parallel	BFW-7A and 7B-24-1	0	72	134	147	149
		BFW-7A and 7B-24-2	0	82	155	172	174
		BFW-7A and 7B-24-3	0	65	125	147	148
UFW	Normal	UFW-9A and 9B-26-1	0	177	323	363	366
		UFW-9A and 9B-26-2	0	175	317	362	364
		UFW-9A and 9B-26-3	0	171	320	354	356
UFW	Parallel	UFW-9A and 9B-24-1	0	39	69	77	78
		UFW-9A and 9B-24-2	0	36	61	75	75
		UFW-9A and 9B-24-3	0	32	52	59	61
1581 Cloth Laminate	Normal	1581-9A and 9B-26-1	0	111	216	243	246
		1581-9A and 9B-26-2	0	113	213	251	254
		1581-9A and 9B-26-3	0	113	213	245	247
1581 Cloth Laminate	Parallel	1581-9A and 9B-24-1	0	105	202	224	227
		1581-9A and 9B-24-2	0	104	201	235	236
		1581-9A and 9B-24-3	0	114	207	238	240
1543 Cloth Laminate	Normal	1543-10A-26-1	0	191	352	398	401
		1543-10A-26-2	0	194	362	407	409
		1543-10A-26-3	0	192	358	406	409
1543 Cloth Laminate	Parallel	1543-10A-24-1	0	61	111	128	129
		1543-10A-24-2	0	67	117	134	134
		1543-10A-24-3	0	58	106	121	122
E-787 Cast Resin		E-787-1	0	518	978	1104	1115
		E-787-2	0	521	993	1120	1127

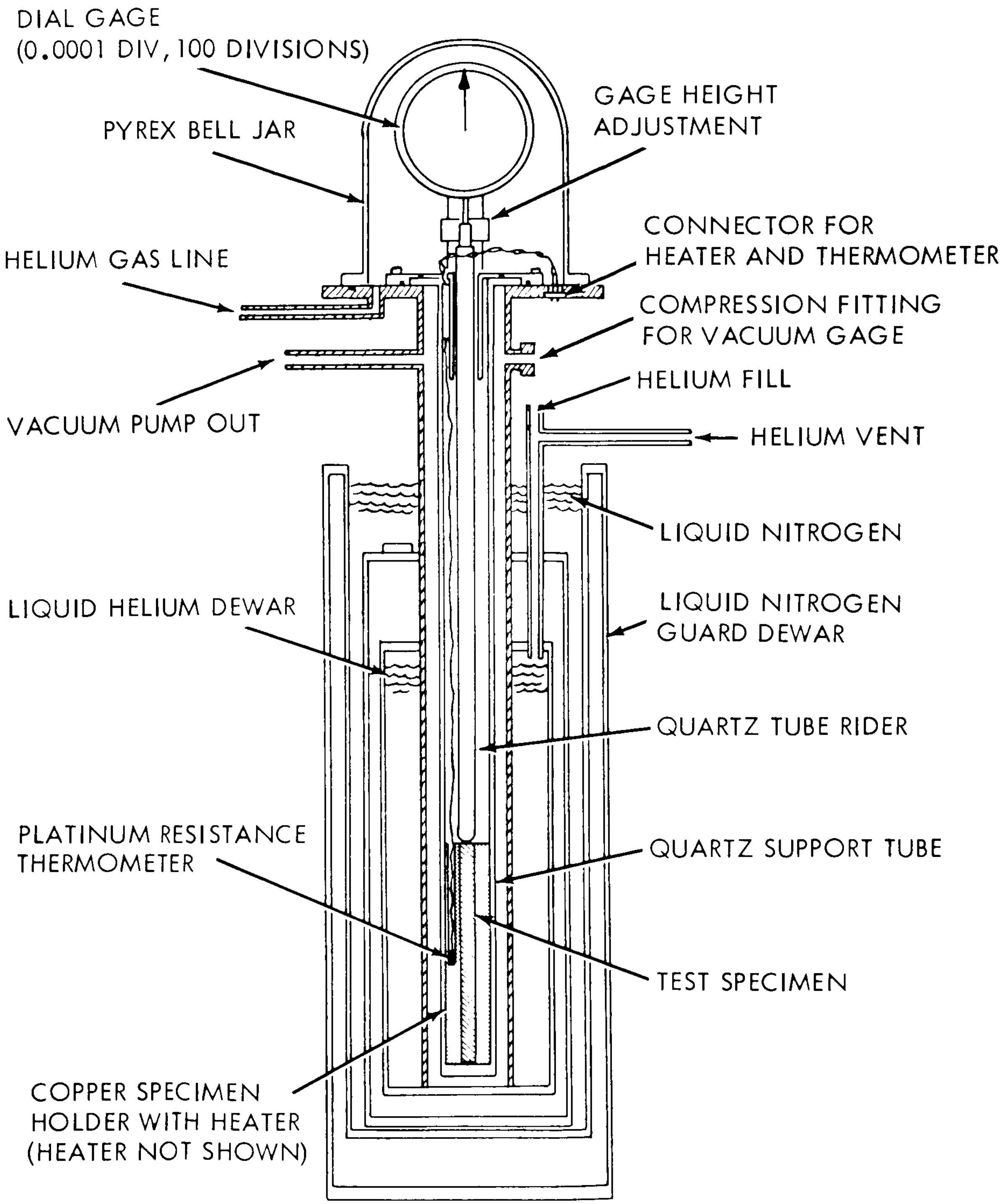

Figure 14. Dilatometer Cryostat

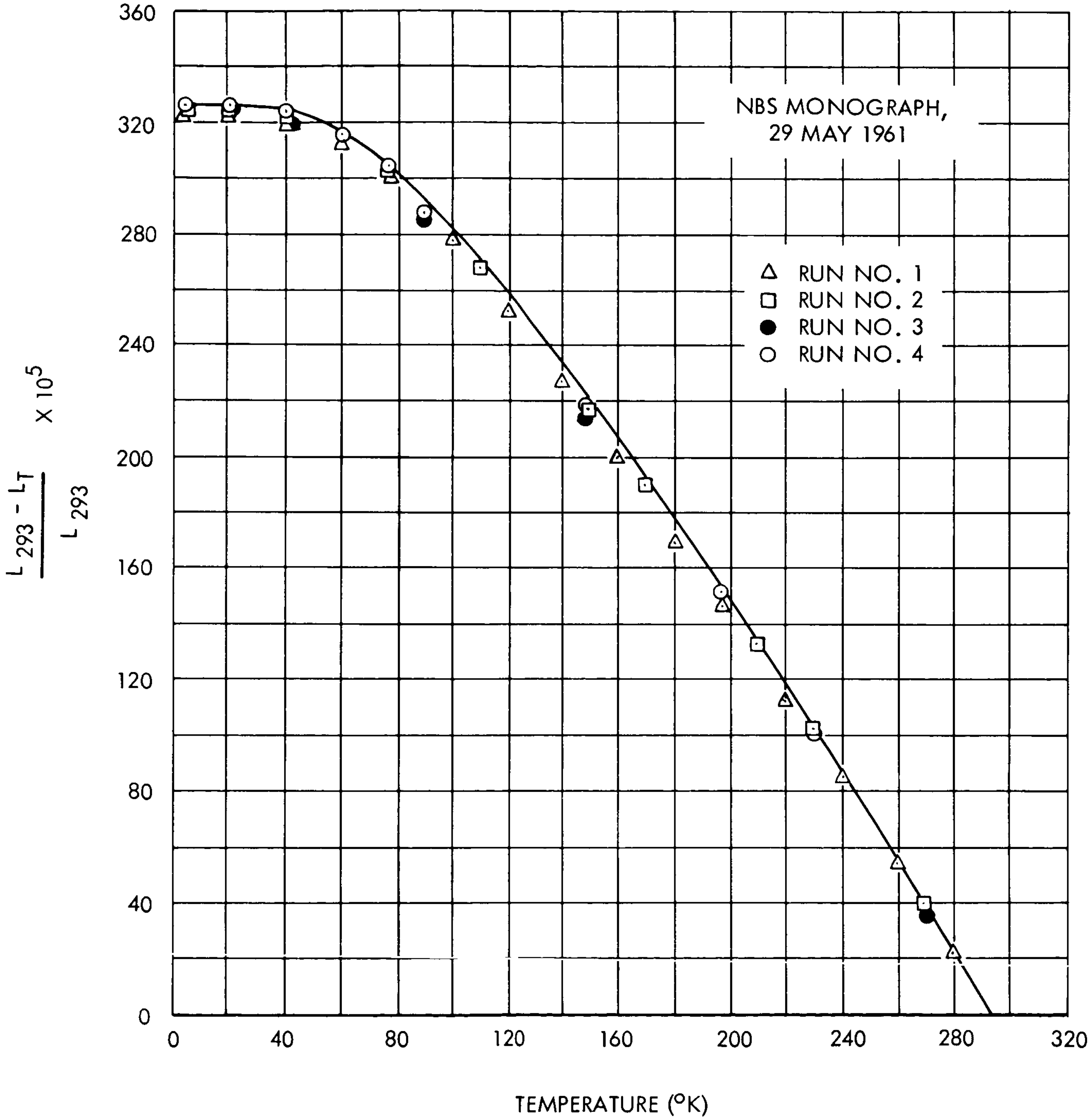

Figure 15. Dilatometer Calibration Curves Using OFHC Copper Rod

Table 20. Supplemental Testing - Mechanical Properties of E-787 Resin

Test	Test Temp (^oK)	Test Results (psi)	Avg Results (psi)
Flexure (modulus of rupture)	298	14,046 16,045 21,447	17,179
	197	12,331 26,000 17,271	18,534
	77	20,466 30,882 31,972	27,774
	20	7,030 19,890 18,525	15,148
Ultimate Compressive Strength	298	19,256 20,402 19,160	19,606
	197	38,014 37,621 37,131	37,589
	77	40,478 49,431 38,945	42,951
	20	37,304 31,681	34,492
Ultimate Tensile Strength	298	9,416 9,118	9,267
	197	8,762 9,714	9,238
	77	14,217 12,804	13,510
	20	12,025	

Table 20. Supplemental Testing - Mechanical Properties of E-787 Resin (Continued)

Test	Test Temp (^oK)	Test Results (psi)*	Avg Results (psi)*
Tensile Modulus	298	520,000 536,000	528,000
	197	788,900 724,500	756,700
	77	1,226,600 1,068,000	1,147,300
	20	1,443,000	
Ultimate Tensile Elongation	298	2.05% 2.03	2.04%
	197	1.30% 1.30	1.30%
	77	1.20% 1.20	1.20%
	20	0.70%	

*Test results are in psi except for ultimate tensile elongation, which is in percent.

and test methods used were the same as those used on the reinforced sheets. The results of these tests are shown in Table 20. The tests indicate an increase in strength through the liquid nitrogen temperature and then a reduction in strength at 20^{o}K. Also, the tensile tests indicate a continuing loss of ductility as the test temperature is lowered, which could be detrimental around flaws and discontinuities in actual fiberglass structures.

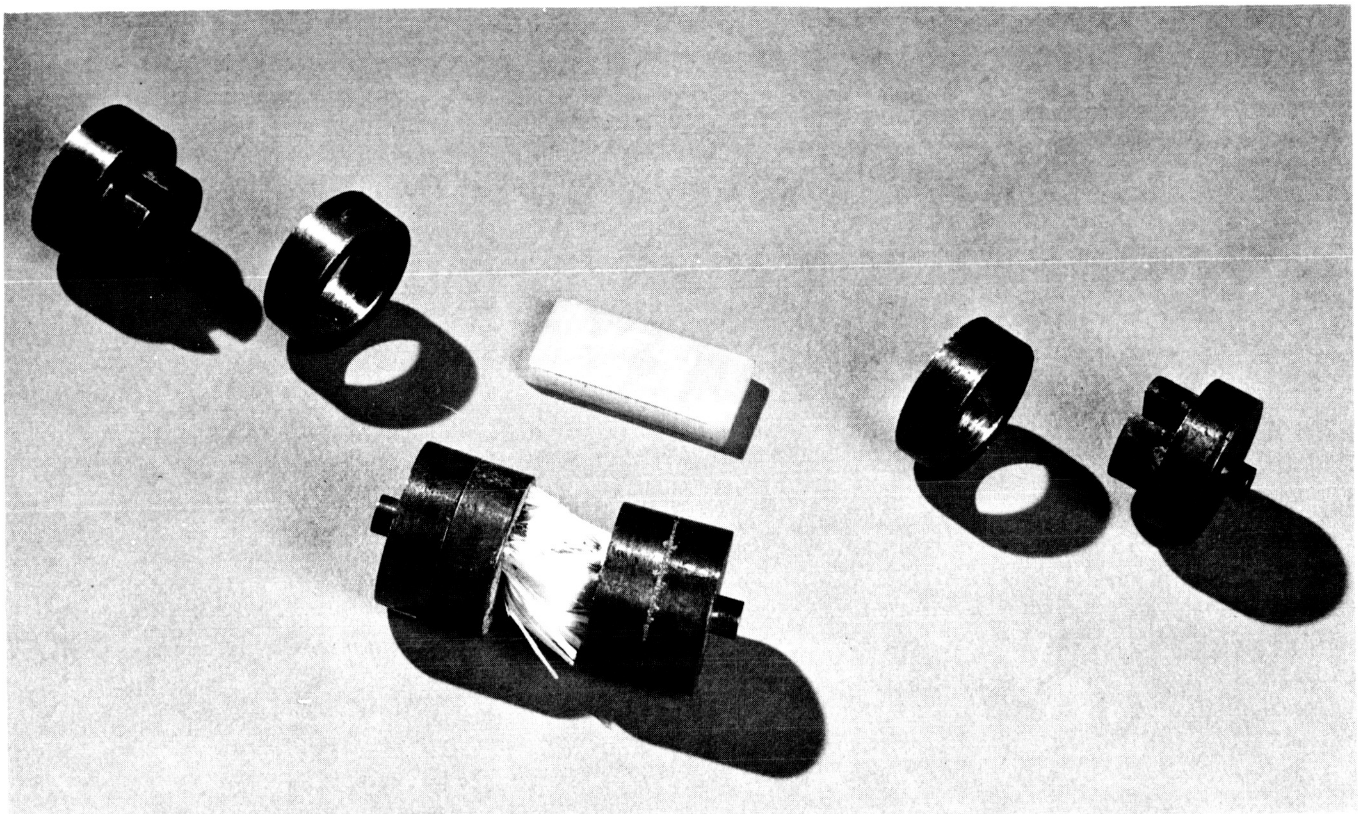

Figure 16. Details of Compression Button Assembly with Retaining Rings

e. BFW Compression Testing. The results of the compression tests on the BFW material during the first year's effort indicated more scatter in the results than was considered desirable. In the compression testing of the UFW material, it was necessary to include a retaining ring in the compression button assembly (see Figure 16) to obtain an ultimate failure. Therefore, the BFW compression tests were rerun using these compression button assemblies. A comparison of the test results with the retaining rings and without the rings is shown in Table 21. The amount of scatter has been reduced through the use of the retaining ring, especially at $77^{o}K$.

Table 21. BFW Compression Results

Temp (^{o}K)	Ultimate Compression Test Results (PSI)			
	With Ring	Avg	Without Ring	Avg
197	100,873 117,040 132,603 129,210 110,835 113,838	117,400	148,276 153,131 126,408 146,859 134,602 147,138	138,752
77	118,158 131,508 140,622 127,086 128,328 119,353	127,509	122,361 136,034 107,113 170,765 107,111 108,271	125,276
20	142,687 125,708 125,021 131,962 128,328 121,261	129,161		

f. Shear Testing. In an attempt to obtain less scatter in the ultimate interlaminar shear strength of the four materials and in the hope of obtaining values that are more representative of design values, a guillotine-type shear test method was investigated. The test specimen configuration, testing fixture, and failed specimen are shown in Figures 17, 18, and 19. One-fourth inch thick panels of each of the four materials being evaluated were fabricated, and specimens were cut. To establish the validity of the test fixtures, specimens from two BFW panels were tested in the fixture and compared with results obtained using a standard

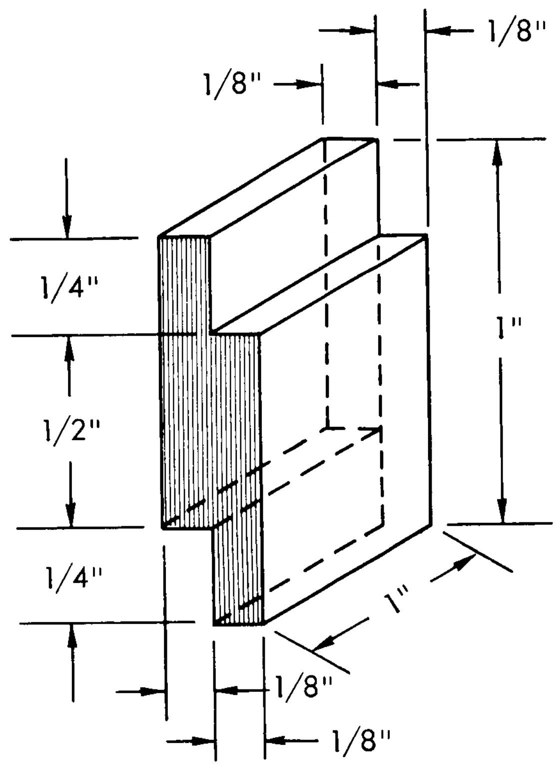

Figure 17. Guillotine-Type Shear Test Specimen

ASTM guillotine-type fixture. This comparison, shown in Table 22, indicates a close agreement of results. The results of the guillotine shear tests are shown in Table 23. This method of testing for shear strength produced results that were lower than those previously obtained by the short-beam flexure method; however, the results appear more representative of the values that could be successfully used in design. The previously noted reduction in shear strength between 77 and 20°K is again apparent; however, the shear strength at 20°K is greater than the room temperature values for each of the materials tested.

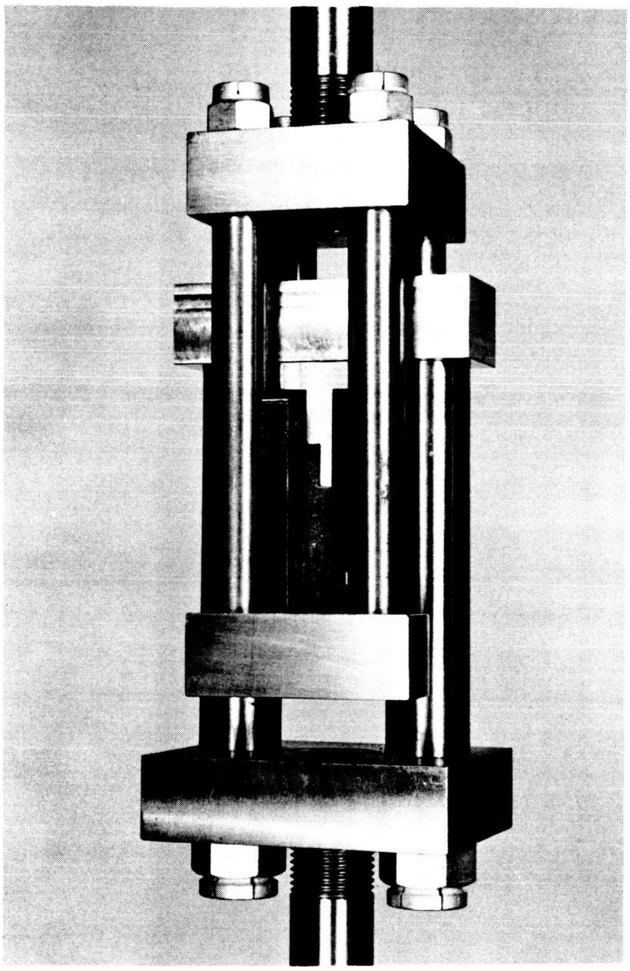

Figure 18. Guillotine Shear Specimen
in Compression Cage
before Test

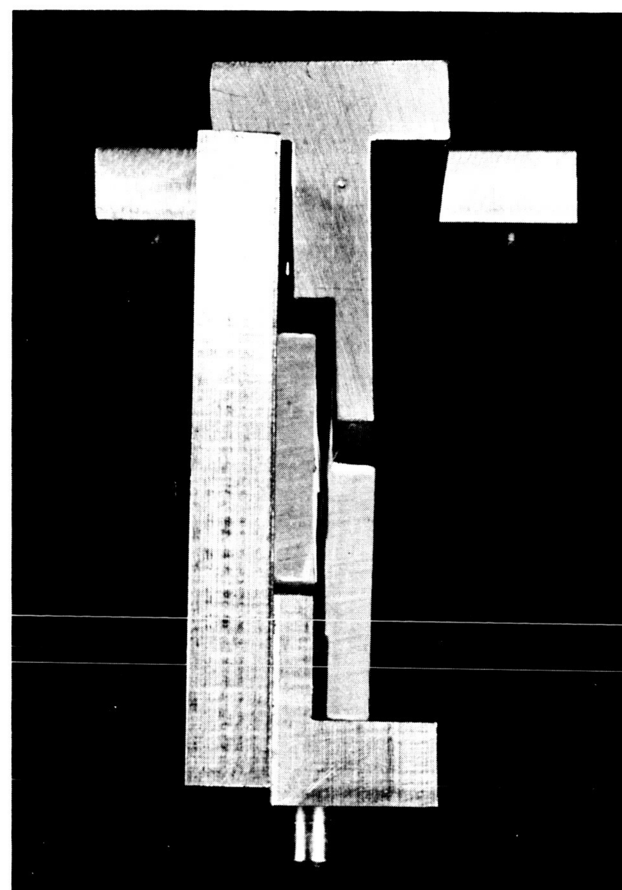

Figure 19. Failed Specimen
after Guillotine Shear Test

Table 22. Comparison of Guillotine-Type Test Fixtures

Material	Specimen No.	Test Method	Ult Interlaminar Shear (psi) Test Results	Average
Bidirectional Filament Wound	1012-1 1012-4	GAC GAC	6080 5240	5660
	1012-5 1012-6	ASTM ASTM	5020 6460	5740
	1014-1 1014-4	GAC GAC	3240 3880	3560
	1014-5 1014-6	ASTM ASTM	5260 2300	3780

Table 23. Guillotine Shear (Interlaminar Shear Strength) Test Results

Specimen Direction	Material	Test Temp (°K)	Specimen No.	Test Results (psi)	Avg Results (psi)
Parallel	1581 Cloth	298	1024-1 1025-1 1026-1 1027-1	7,478 8,441 7,597 8,247	7,941
		77	1024-2 1025-2 1026-2	14,721 12,657 11,753	13,044
		20	1024-3 1025-3 1026-3 1027-3	9,881 6,030 9,771 11,514	9,299
	1543 Cloth	298	1019-1 1020-1 1021-1 1022-1	9,145 7,729 7,211 8,056	8,035

Table 23. Guillotine Shear (Interlaminar Shear Strength) Test Results (Cont)

Specimen Direction	Material	Test Temp (^{o}K)	Specimen No.	Test Results (psi)	Avg Results (psi)
Parallel	1543 Cloth	77	1019-2	11,284	
			1020-2	11,968	
			1021-2	7,895	
			1022-2	9,564	10,178
		20	1019-3	10,446	
			1020-3	8,847	
			1021-3	10,954	
			1022-3	8,444	9,673
	UFW	298	1008-1	9,004	
			1009-1	6,514	
			1010-1	8,446	
			1011-1	7,302	7,817
		77	1008-2	7,878	
			1009-2	6,377	
			1010-2	7,421	
			1011-2	8,436	7,578
		20	1008-3	8,710	
			1009-3	7,500	
			1010-3	6,711	
			1011-3	9,644	8,141
	BFW	298	1012-1	6,050	
			1013-1	5,230	
			1014-1	3,279	
			1015-1	4,414	4,743
		77	1012-2	8,408	
			1013-2	8,583	
			1014-2	6,268	
			1015-2	5,656	7,229
		20	1012-3	6,038	
			1013-3	8,589	
			1014-3	6,320	
			1015-3	5,348	6,574

SECTION III. TASK II - ENVIRONMENTAL EFFECTS

The purpose of Task II of this year's program was to determine the effects, if any, that exposure to weather may have on the mechanical properties of fiberglass structures when used at cryogenic temperatures.

Panels of all four materials, which were fabricated during the first year's effort, were cut into two pieces. One piece of each of the four panels was placed in an Atlas Electric Company Model XW sunshine arc weatherometer. The cloth (1543 and 1581) pieces were 15 x 18 x 0.125 inches, and the filament-wound roving pieces were 12 x 24 x 0.125 inches. These pieces were exposed to a weathering cycle in accordance with ASTM specification E-42-57, Light- and Water-Exposure Apparatus for Artificial Weathering Test. The test consists essentially of exposing the pieces to 102 minutes of radiation from the open flame-type carbon arc, followed by an 18-minute exposure to water spray and radiation. The pieces were exposed to this cycle for 20 hours per day for 30 days. The other piece of each panel was stored under ambient conditions for the 30 days. Flexure and compression test specimens were then cut from both the exposed and unexposed portions of the panels and tested according to the test methods developed during the first year's effort of this program. Tests were conducted at 298, 77, and $20^{\circ}K$. The results of these tests are shown in Tables 24 and 25. The results have given no indication of any detrimental effect from the weathering exposure on the properties of any of the laminates at any temperature.

Table 24. Results of Flexure Tests on Weathered Specimens

Material	Test Temp (^oK)	Weathered Specimens Test Results (psi)	Weathered Specimens Avg (psi)	Control Specimens Test Results (psi)	Control Specimens Avg (psi)
1581 Cloth (Panel 1581-9A)	298	116,845 111,145 109,834 113,327 109,143 119,524	113,300	107,615 106,796 103,755	106,055
	77	197,754 190,882 197,468 199,299 196,143 194,790	196,056	187,244 198,512 186,759	190,838
	20	194,726 187,876 192,795 192,771 190,935 189,379	191,414	195,205 196,289 192,385 185,492	192,343
1543 Cloth (Panel 1543-9A)	298	162,525 157,216 162,070 157,845 159,490 164,296	160,574	157,438 151,527 150,000	152,988
	77	295,714 282,608 296,591 295,567 303,124 301,255	295,810	294,237 266,490 300,010	286,912
	20	312,532 304,055 264,796 258,349 314,056 282,427	289,369	309,074 282,041 246,446 306,517	286,202

Table 24. Results of Flexure Tests on Weathered Specimens (Continued)

Material	Test Temp (^{o}K)	Weathered Specimens Test Results (psi)	Weathered Specimens Avg (psi)	Control Specimens Test Results (psi)	Control Specimens Avg (psi)
BFW (Panel BFW-1004)	298	184,317 234,762 192,473 189,167 199,255 188,661	198,106	172,194 162,499 172,792	169,828
	77	265,804 266,758 253,250 275,211 270,695 254,407	264,354	229,114 265,379 262,982	252,492
	20	247,373 234,276 235,247 242,522 250,283 225,343	239,174	226,298 204,859 217,184 240,116	222,114
UFW (Panel UFW-3B)	298	242,044 254,671 247,635 245,583 251,400 245,570	247,810	242,077 244,358 288,828	238,421
	77	513,514 526,874 476,735 383,504 495,856 508,649	484,188	517,841 515,881 498,953	510,892
	20	537,162 526,466 524,751 529,176 519,630 547,695	530,813	541,103 540,444 482,645 556,644	530,209

Table 25. Results of Compression Tests on Weathered Specimens

Material	Test Temp (^{o}K)	Weathered Specimens Test Results (psi)	Weathered Specimens Average (psi)	Control Specimens Test Results (psi)	Control Specimens Average (psi)
1543 Cloth (Panel 1543-9A)	298	92,245 97,327 93,051 104,242 101,846 99,291	98,002	90,414 98,222 106,759	98,465
	77	168,427 157,550 126,154 168,439 151,127 145,877	152,929	151,030 157,120 160,086	156,079
	20	166,515 177,751 161,481 171,229 139,289 171,248	164,586	149,249 140,233 150,871	146,784
1581 Cloth (Panel 1581-9A)	298	54,572 63,258 58,815 61,061 63,814 65,224	61,124	53,116 54,558 60,324	55,999
	77	112,987 124,213 96,406 117,128 124,029 109,334	114,016	92,772 96,923 89,530	93,075
	20	123,337 106,963 93,603 120,895 132,728 119,965	116,249	121,043 110,964 106,240	112,749

Table 25. Results of Compression Tests on Weathered Specimens (Continued)

Material	Test Temp (^{o}K)	Weathered Specimens Test Results (psi)	Weathered Specimens Average (psi)	Control Specimens Test Results (psi)	Control Specimens Average (psi)
BFW (Panel BFW-1004)	298	109,618 106,784 99,767 95,648 94,394 90,452	99,444	98,846 111,170 99,075	103,030
	77	139,099 135,858 140,524 127,673 131,811 134,872	134,973	131,964 118,639 123,799	124,801
	20	115,544 129,834 111,131 122,515 139,625	122,176	108,182 104,296 124,867	112,448
UFW (Panel UFW-3B)	298	148,178 147,317 150,607 164,700 139,086 138,591	148,080	145,992 143,239 145,466	144,899
	77	215,261 277,419 252,632 319,838 258,607 261,279	264,173	236,773 201,243 207,171	215,062
	20	287,449 194,004 320,186 289,084 279,419 252,964	270,518	233,735 182,054 187,786	201,192

SECTION IV. TASK III - STRUCTURAL MODELS

A. GENERAL

The purpose of Task III of this year's effort was to determine the validity of the test data derived from small test specimens when related to actual structural shapes. During this task, rods and tubes were fabricated from the four materials being evaluated on this program and were tested in tension, compression, and flexure. The results accomplished during this task are discussed in this section.

B. FABRICATION

1. UFW Rods

a. Processing. Rod test specimens of the UFW laminate were required for the determination of tensile,compression, buckling, and flexure properties. The base laminate of this material in the form of square bars was fabricated using the filament-winding technique whereby the prepreg roving was maintained under a controlled tension of 10 pounds per 20-end roving during the winding operation. Six 20-end prepreg rovings were used side by side to form the 1/2-inch band width without the necessity for indexing.

The mandrel employed for this operation is illustrated in Figure 20. This particular mandrel produced four bars (two per side) during a single winding setup.

After winding, the uncured laminate was severed at the mandrel periphery. This was done so that the tension in the rovings would not distort the laminate bars after curing. Curing was achieved in an autoclave, using a vacuum bag and 50-psi exterior pressure. The cure temperature of 325^{o}F was applied for four hours. A 1/2-inch wide caul plate assured proper pressure transfer to the laminate during the cure cycle.

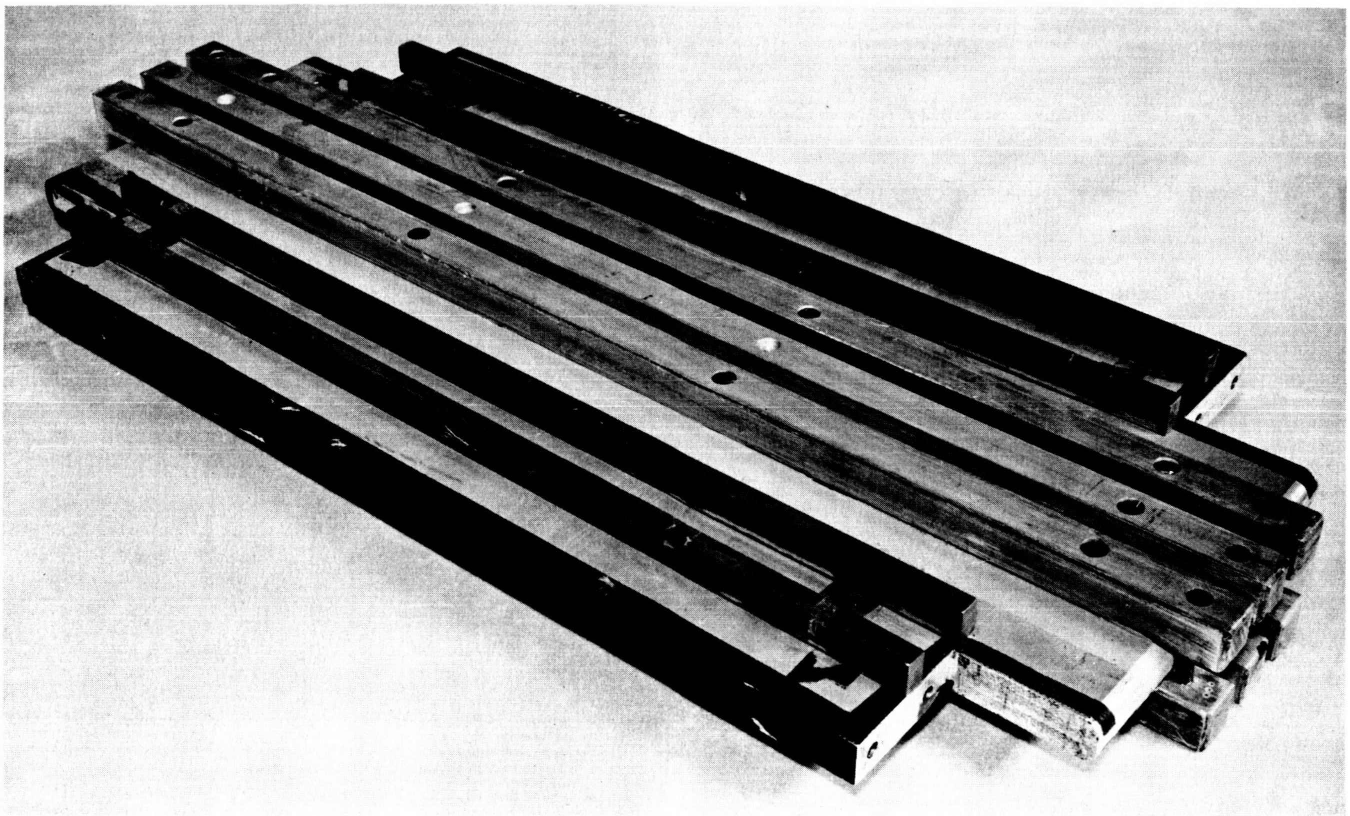

Figure 20. Mandrel for Producing Filament-Wound Bar Laminates

The resultant products from the mandrel are 1/2-inch square cured bars 24 inches long. Each of the rod test specimens was subsequently machined from these bars. The layout for providing the stock to machine a specific specimen is shown in Figure 21.

b. Rod Test Specimens. The laminate stock was machined by conventional machine shop methods. The finished dimensions and tolerances shown in Figure 22 were readily attainable. Figure 22 shows the tensile, compression, buckling, and flexure specimens as machined and subsequently used to complete the test specimen assemblies. Photographs of typical rod specimens are shown in Figure 23.

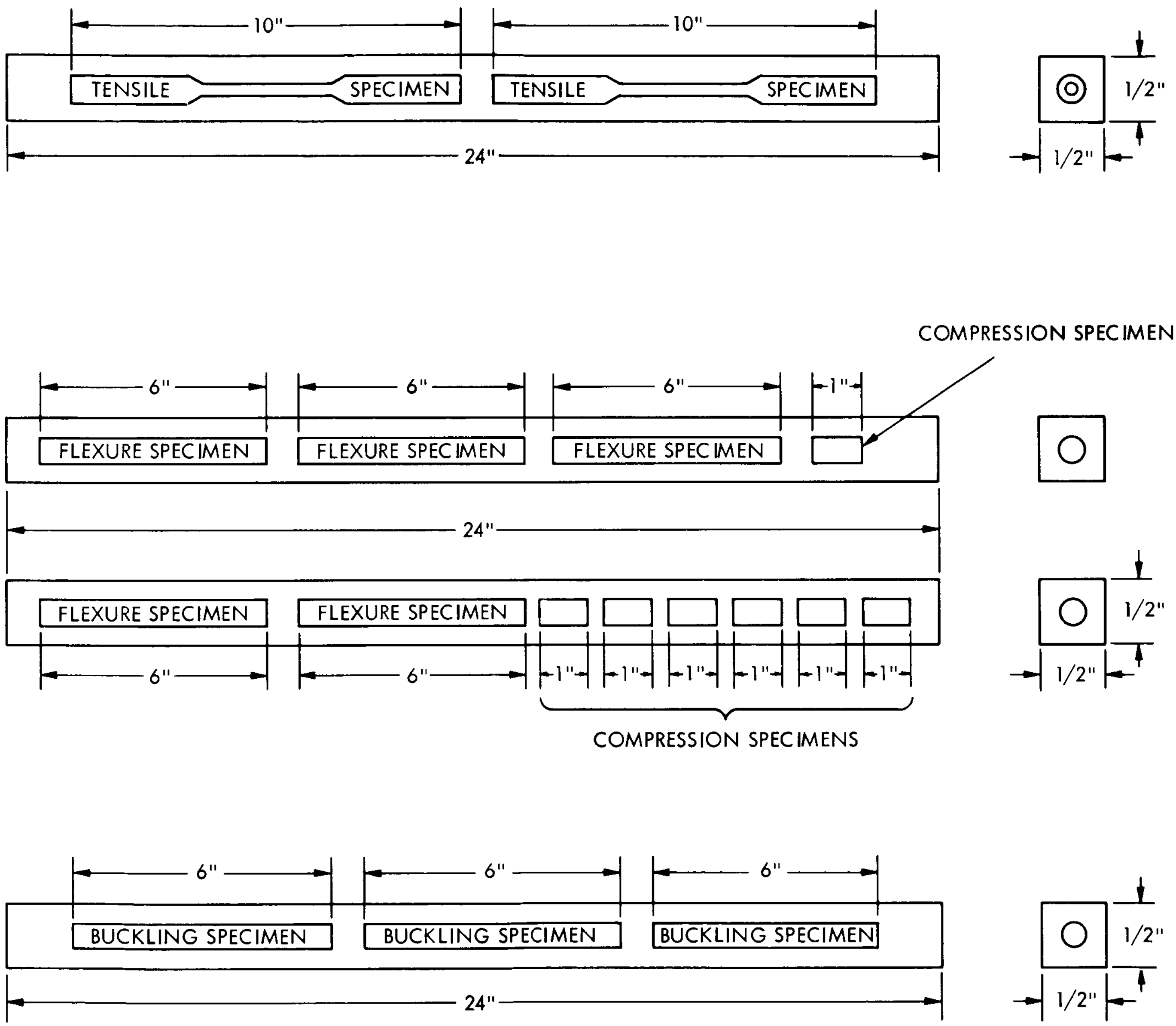

Figure 21. Layout Diagrams of Laminate Stock for Machined Rod Specimens

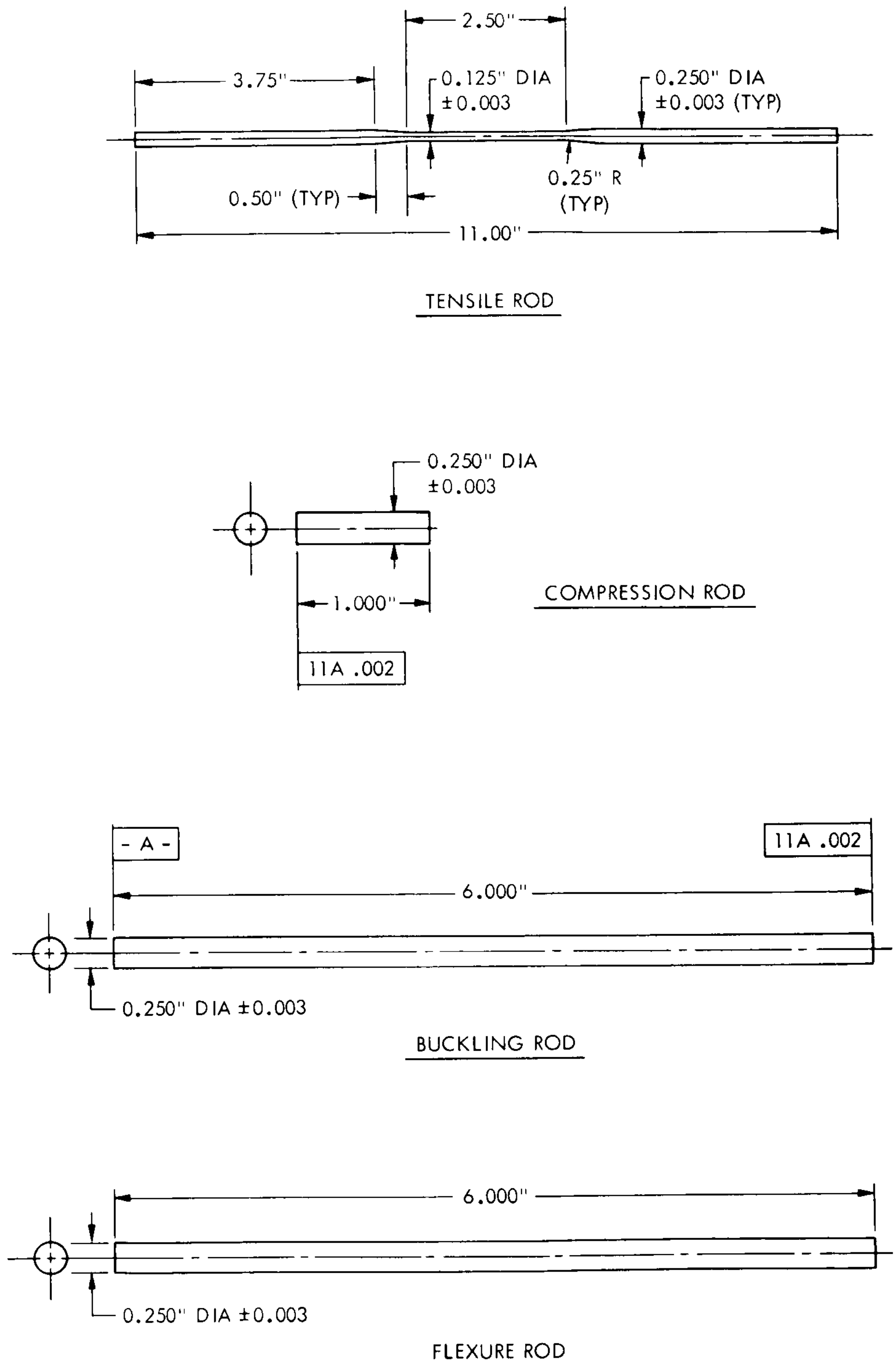

Figure 22. Dimensional Sketches of Rod Test Specimens

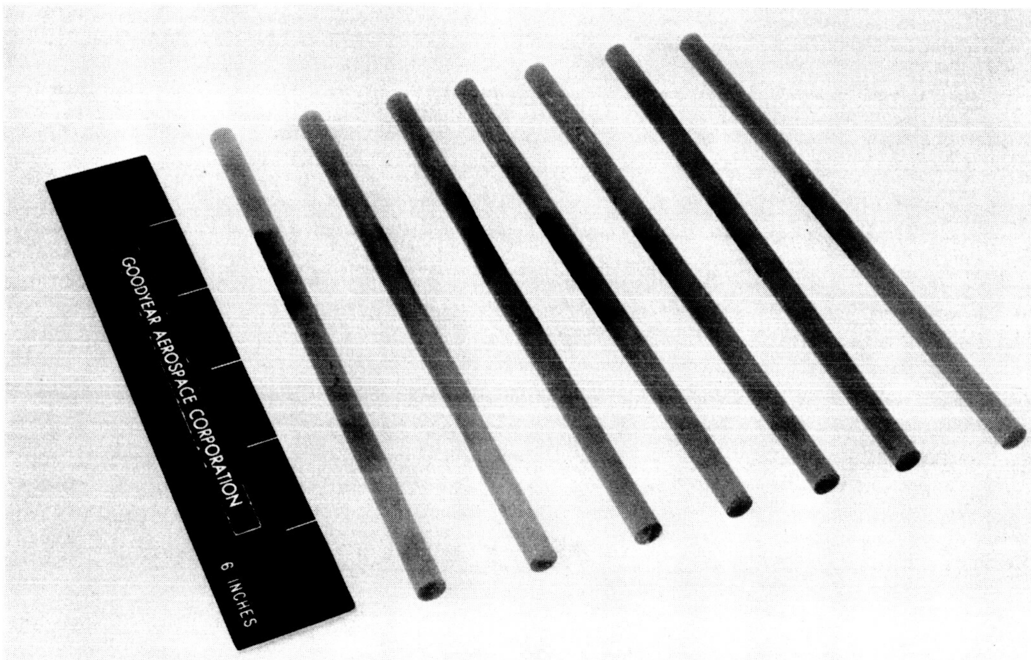

FLEXURE AND BUCKLING RODS

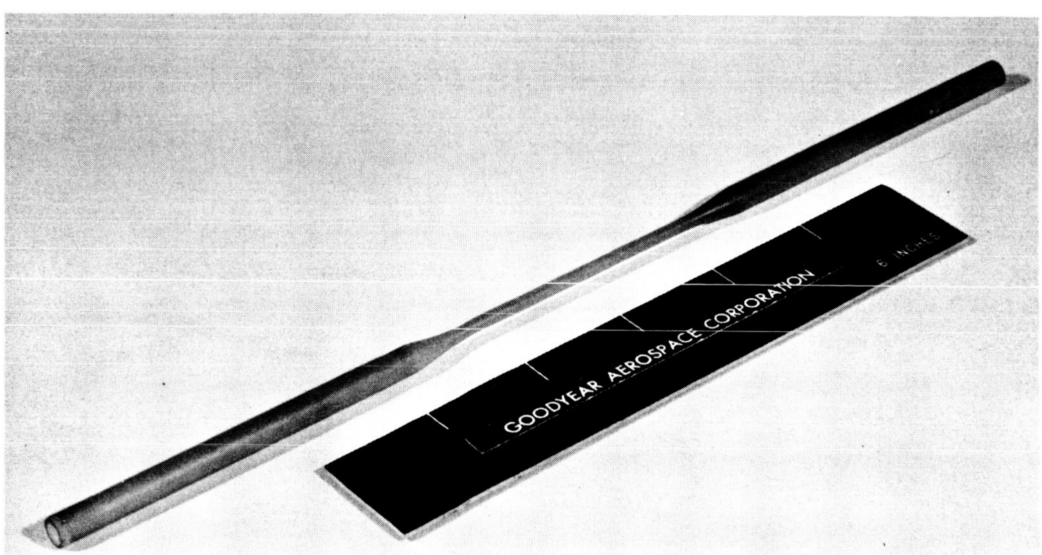

TENSILE RODS (WITHOUT HOLDERS)

Figure 23. Typical Machined Rod Specimens

c. Material Characterization. Records were maintained to document the base prepreg roving spools used to produce the required bar stock. Each specific rod specimen is identified according to a material unit. This information is summarized in Table 26.

For each raw material unit used in this program, quality control data was obtained. The quality control provisions of Specification WS-1028B were employed on the 20-end, S/HTS, epoxy resin preimpregnated roving. This information is given in Table 27.

Resin contants of a number of rod test specimens were determined. The burn-out tests were run on segments taken out of flexure and buckling specimens upon completion of the respective tests. Table 28 gives the resin content of the rod test specimens.

Table 26. Prepreg Materials Used to Fabricate UFW Bar Stock for Rod Specimens

Specimen	Prepreg Identification
Rod Tensile (see Fig. 22)	
RT-5-1 RT-5-2 RT-6-1 RT-6-2 RT-7-1 RT-7-2 RT-8-1 RT-8-2	2 spools F1718 2 spools MA22-1076 2 spools MA22-1067
RT-13-1 RT-13-2	5 spools MA22-1076 1 spool F1718

Table 26. Prepreg Materials Used to Fabricate UFW Bar Stock for Rod Specimens (Continued)

Specimen	Prepreg Identification
Rod Compression (see Fig. 22)	
RC-14-1	5 spools MA22-1076 1 spool F1718
RC-14-2	
RC-14-3	
RC-14-5	
RC-14-6	
RC-15-1	
RC-16-1	
RC-16-2	
RC-16-3	
Rod Buckling (see Fig. 22)	
RB-9-1	1 spool F1718 1 spool MA22-1067 4 spools MA22-1076
RB-9-2	
RB-9-3	
RB-10-1	
RB-10-2	
RB-10-3	
RB-11-1	
RB-11-2	
RB-11-3	
RB-12-1	
RB-12-2	
RB-12-3	
Rod Flexure (see Fig. 22)	
RF-14-1	1 spool F1718 5 spools MA22-1076
RF-14-2	
RF-15-1	
RF-15-2	
RF-15-3	
RF-16-1	
RF-16-2	
RF-16-3	

Table 27. Quality Control Data for Preimpregnated Glass Roving Used for Rod and Cylinder Specimens

Lot No.	Volatile Content Wt (%)	Ignition Loss Wt (%)	Resin Flow Wt (%)	Gel Time	Wt per Linear Yard (g)	Horizontal Shear Strength (psi)		Tensile Strength (psi)	Vendor
						At 250°F	After 2-Hour Water Boil		
F1718	1.1	19.8	9.6	2.6	0.608	8,629	19,670	398,470	U. S. Polymeric Chemicals Inc
4886	1.5	19.9	9.9	2.4	0.607	5,098	11,243	434,400	Cordo Molding Products, Inc
MA22-1067	1.4	18.9	8.7	2.7	0.602	2,233	10,507	424,700	Ripco Products Div of Chicago Printed String Company
MA22-1076	1.7	19.7	9.1	1.9	0.602	3,348	11,182	477,900	
MA22-1078	1.9	19.2	9.0	1.9	0.608	3,040	9,924	446,650	
MA22-1079	1.9	19.7	8.5	2.1	0.605	3,129	10,987	451,350	

Table 28. Resin Content of Rod Test Specimens

Rod No.	Resin Content (percent)		
	Specimen No. 1	Specimen No. 2	Average
RB-9-1	21.32	21.07	21.20
RB-9-2	19.39	21.14	20.27
RB-9-3	22.01	22.02	22.02
RB-10-1	20.92	19.88	20.40
RB-10-2	21.81	21.68	21.75
RB-12-1	21.66	21.47	21.57
RB-12-2	21.84	21.87	21.86
RB-12-3	20.60	19.49	20.05
RC-14-1	21.02	20.68	20.85
RC-14-2	20.94	20.97	20.96
RC-15-1	21.31	20.98	21.15
RC-15-2	20.81	20.88	20.85
RC-15-3	20.31	21.13	20.72
RC-16-1	19.43	20.98	20.21
RC-16-2	20.83	21.20	21.02
RF-16-3	20.90	20.98	20.94

2. Bidirectional Roving and Cloth-Reinforced Cylinders

a. Tensile Test Cylinders. Test cylinders fabricated from the three test materials were required for tensile tests. The three types of test cylinders fabricated were as follows:

(1) BFW roving reinforcement; interspersed three-ply circo and two-ply longo; 0.038-inch wall thickness.
(2) Style 1543 glass cloth reinforcement; three-ply wrap; 0.038-inch wall thickness.
(3) Style 1581 glass cloth reinforcement; three-ply wrap; 0.038-inch wall thickness.

Fabrication of these tensile cylinders requires suitable mandrels with a salt insert between the metal end fittings. The faying surfaces of the metal end fittings prior to assembly into mandrel form are processed as follows:

(1) Degrease.
(2) Prime with two coats of Bondmaster M602 primer.
(3) Oven Cure: 1/2 hour at 225°F
1 hour at 325 - 340°F.

Upon completion of the machine winding operation and subsequent cure of the part, the salt insert is dissolved, leaving a hollow cylinder in the test section and the metal fittings securely in place.

Figure 24 is an engineering drawing of the mandrel assembly. Figure 25 shows a number of these mandrels in completed form.

The machine winding operations used in the fabrication of tensile test cylinders of the three materials are illustrated in Figure 26. Typical stages in the processing of these cylinders after winding are shown in Figures 27 through 29. Figure 30 lists the process controls employed for the roving tensile test cylinders. Figure 31 lists those used for the cloth tensile test cylinders.

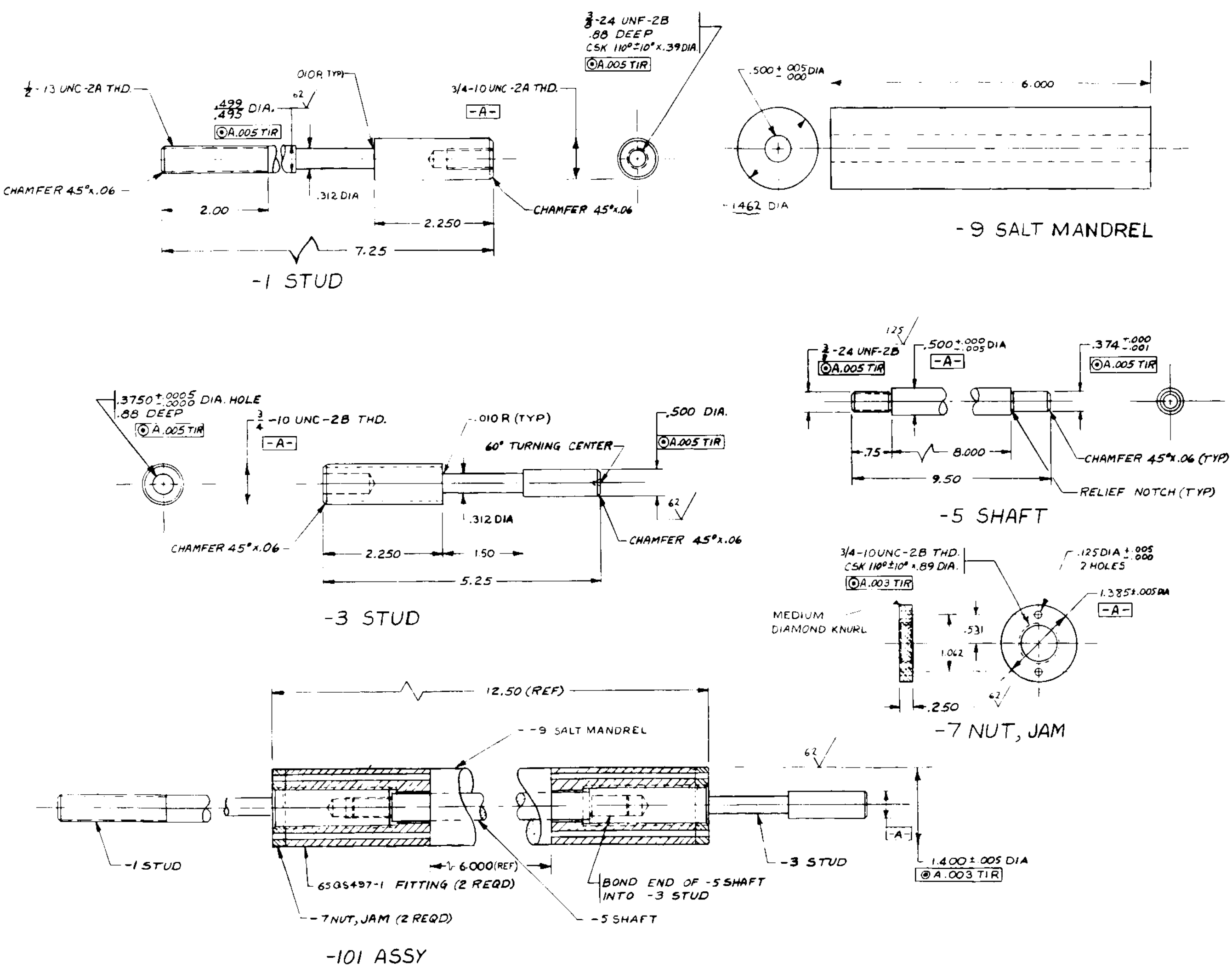

Figure 24. Tensile Cylinder Winding Mandrel

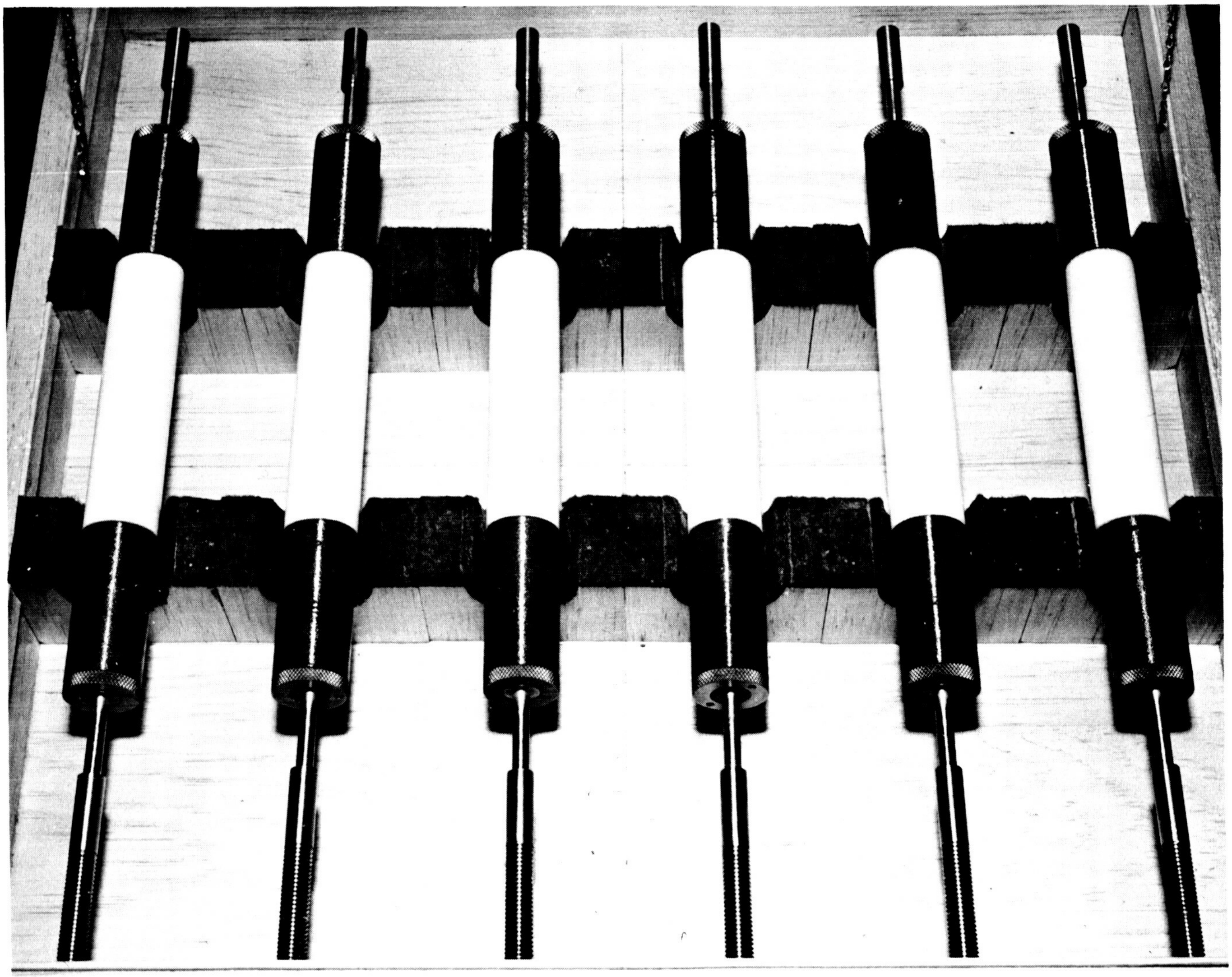

Figure 25. Mandrel Assemblies Used for Fabricating Tensile Cylinders

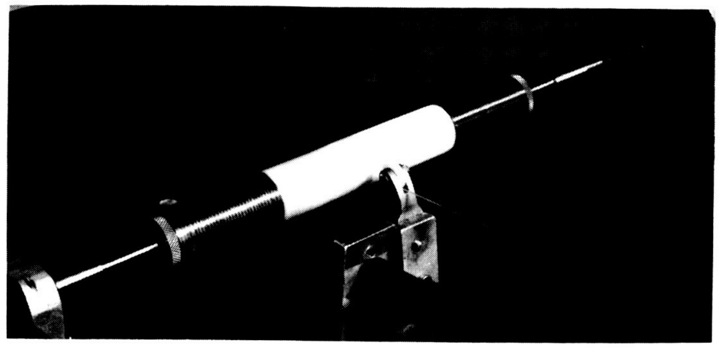

CIRCUMFERENTIAL WINDING OF PREPREG ROVING

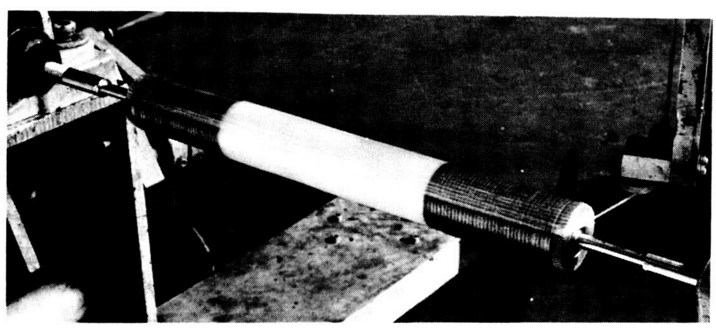

LONGITUDINAL WINDING OF PREPREG ROVING

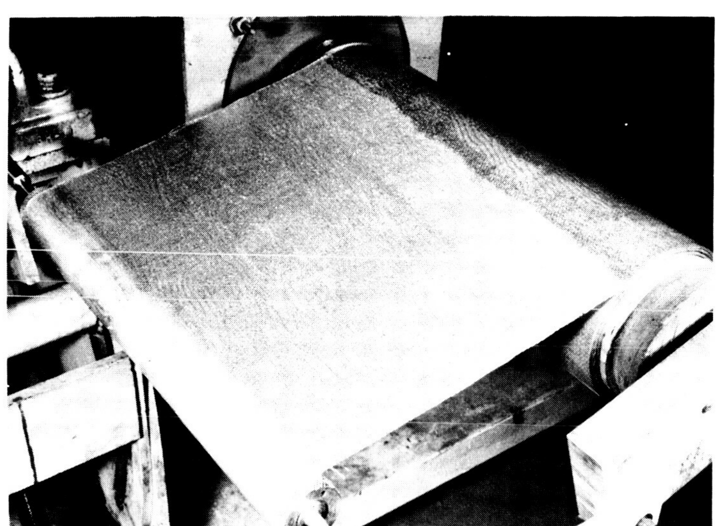

CONVOLUTE WINDING OF CLOTH PREPREG

Figure 26. Winding Operations in Fabrication of Tensile Test Cylinders

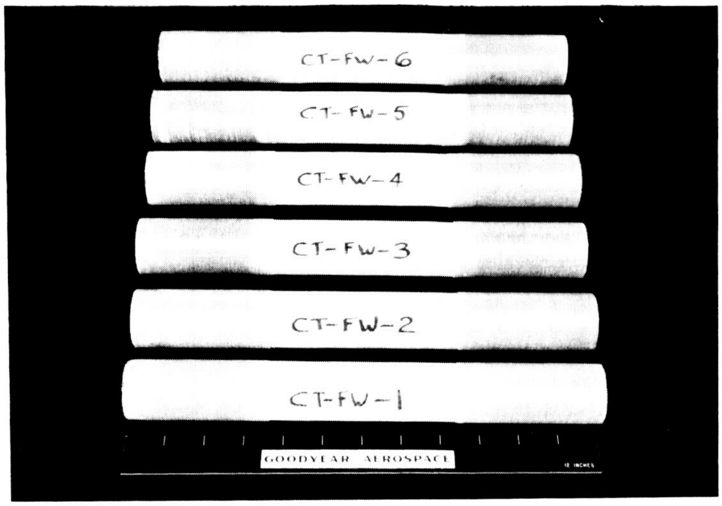

Figure 27. Filament-Wound Tensile Cylinders Ready for Metal Sleeve

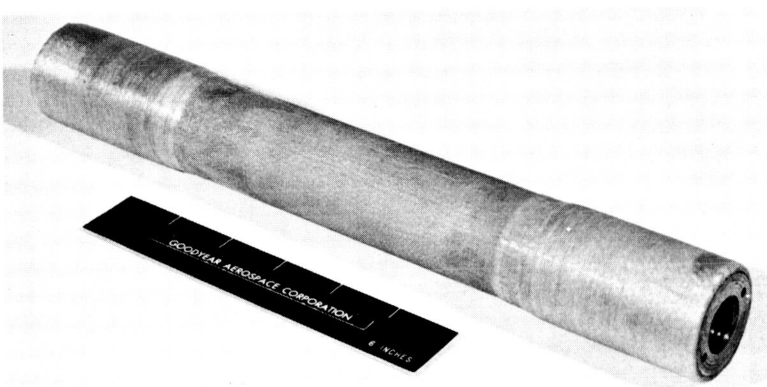

Figure 28. Glass Cloth Tensile Cylinder Ready for Metal Sleeve

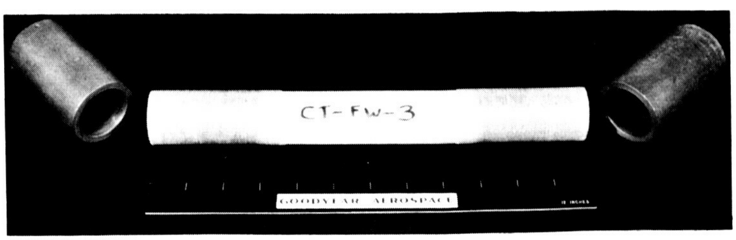

Figure 29. Filament-Wound Tensile Cylinder prior to Bonding of Outer Metal Reinforcement Sleeve

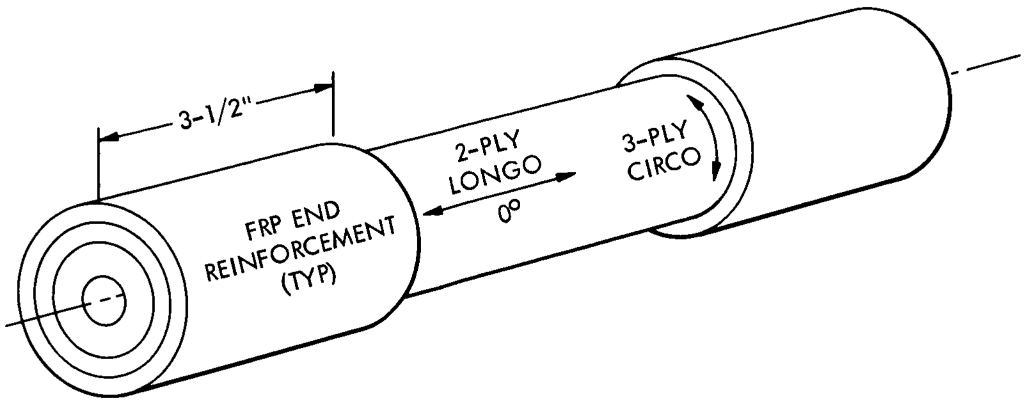

FABRICATION

OOOOOOO	CIRCO -10-LB TENSION/20 END (TYP)
▭	LONGO - 5-LB TENSION/20 END (TYP)
OOOOOOO	CIRCO
▭	LONGO
OOOOOOO	CIRCO

INDEXING

CIRCO - 0.0869"/20 END
LONGO - 0.0758"/20 END

FIBERGLASS-REINFORCED PLASTIC (FRP) END REINFORCEMENT

6 SEQUENCES OF
2-PLY, STYLE 341, E-787 PREPREG CLOTH
2-PLY, 20-END, S/HTS, E-787 PREPREG ROVING

PREPARATION FOR CURE	CURE
DACRON PEEL PLY	25" HG VACUUM PRESSURE
CELLOPHANE CURE PLY	1 HOUR AT 175°F
DRY ROVING OVERWRAP	1 HOUR AT 250°F
VACUUM BAG	4 HOURS AT 300°F

PART ALLOWED TO COOL DOWN TO 125°F UNDER VACUUM BEFORE REMOVAL FROM MANDREL.

Figure 30. Roving Filament-Wound Tension Cylinder Process Controls

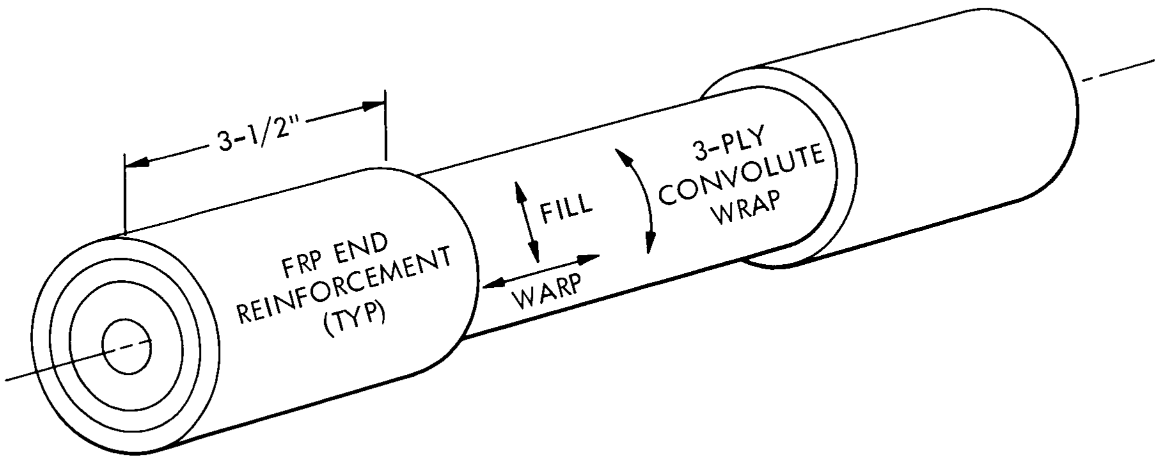

FABRICATION

3-PLY PREPREG CLOTH WOUND UNDER 1-1/2 LB/IN. TENSION

FRP END REINFORCEMENT

6 SEQUENCES OF
2-PLY, STYLE 341, E-781 PREPREG CLOTH
2-PLY, 20-END, S/HTS, E-787 PREPREG ROVING

PREPARATION FOR CURE	CURE
DACRON PEEL PLY	25" HG VACUUM PRESSURE
CELLOPHANE CURE PLY	1 HOUR AT 175°F
DRY ROVING OVERWRAP	1 HOUR AT 250°F
VACUUM BAG	4 HOURS AT 300°F

PART ALLOWED TO COOL DOWN TO 125°F UNDER VACUUM BEFORE REMOVAL FROM MANDREL.

Figure 31. Cloth Machine-Wound Tension Cylinder Process Controls

b. Compression and Buckling Test Cylinders. Test cylinders fabricated from the three test materials were required for compression and buckling tests. The three types of test cylinders fabricated were as follows:

(1) BFW roving reinforcement; interspersed four-ply circo and three-ply longo; 0.050-inch wall thickness.
(2) Style 1543 glass cloth reinforcement; four-ply wrap; 0.050-inch wall thickness.
(3) Style 1581 glass cloth reinforcement; four-ply wrap; 0.050-inch wall thickness.

The cylinders for the compression and buckling specimens were fabricated on a metal mandrel (see Figure 32). The cylinder as fabricated is 24 inches long. The cured cylinder is easily removed from the metal mandrel. The basic compression and buckling test cylinders are cut from these 24-inch lengths as shown in Figure 33.

The machine winding operations of the basic 24-inch long cylinders are shown in Figure 34. These operations are performed under controlled process conditions as listed in Figures 35 and 36.

c. Material Characterization. Raw materials were recorded according to pre-preg used in specific test pieces. This information is presented in Table 29. The quality control data in accordance with Specification WS-1028B for the epoxy impregnated roving used in the cylinders is included in Table 27. The provisions of Specification WS-1070A-1 were used for the S/HTS epoxy resin preimpregnated glass cloth. This information is summarized in Table 30. Representative resin contents of the tested specimens are given in Table 31.

3. Test Specimen Assemblies

As a result of this program, successful structural model test specimens were developed. Drawings of each of these test specimens are included as Figures 37 and 38.

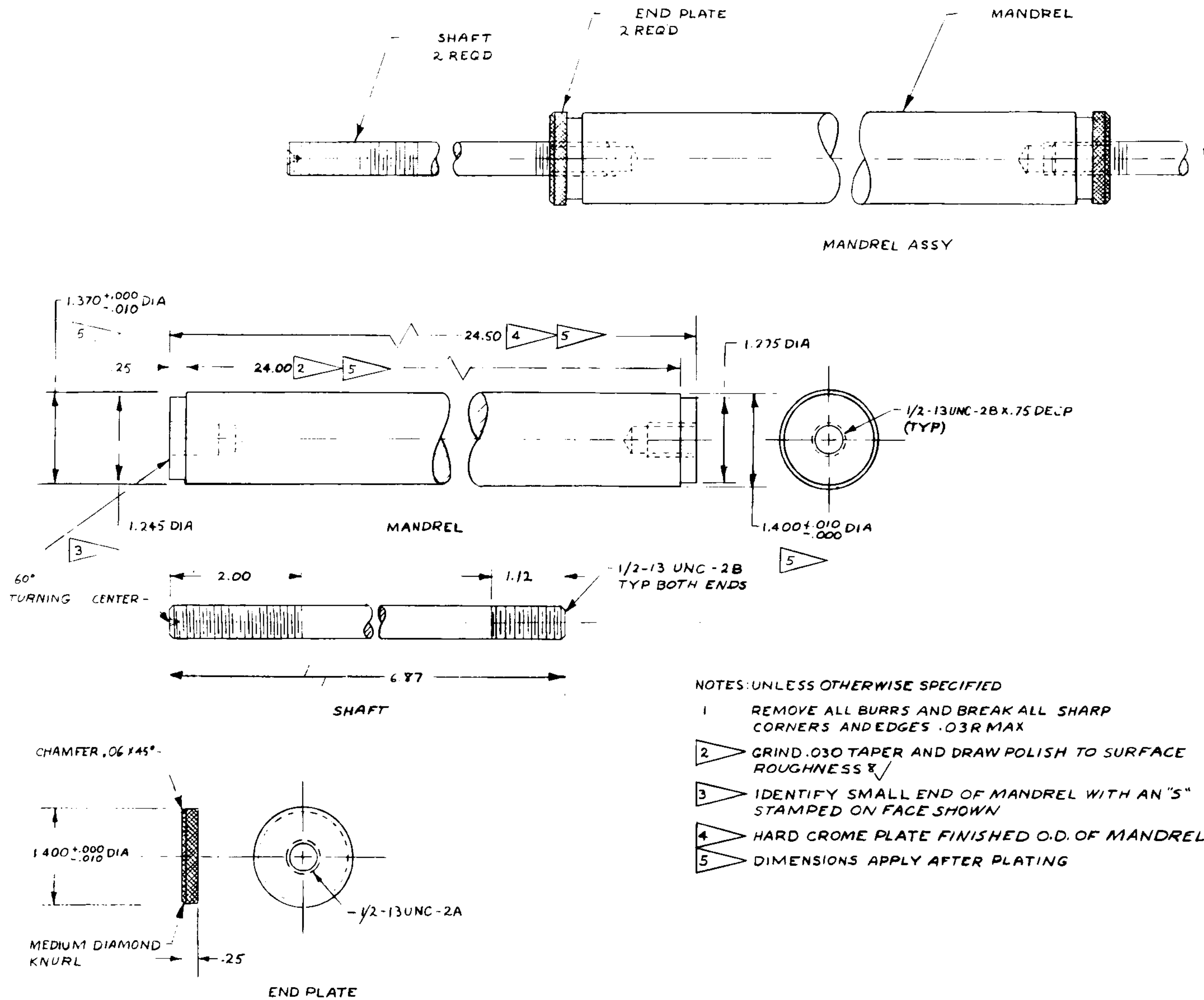

Figure 32. Assembly Drawing of the Compression Tube Mandrel

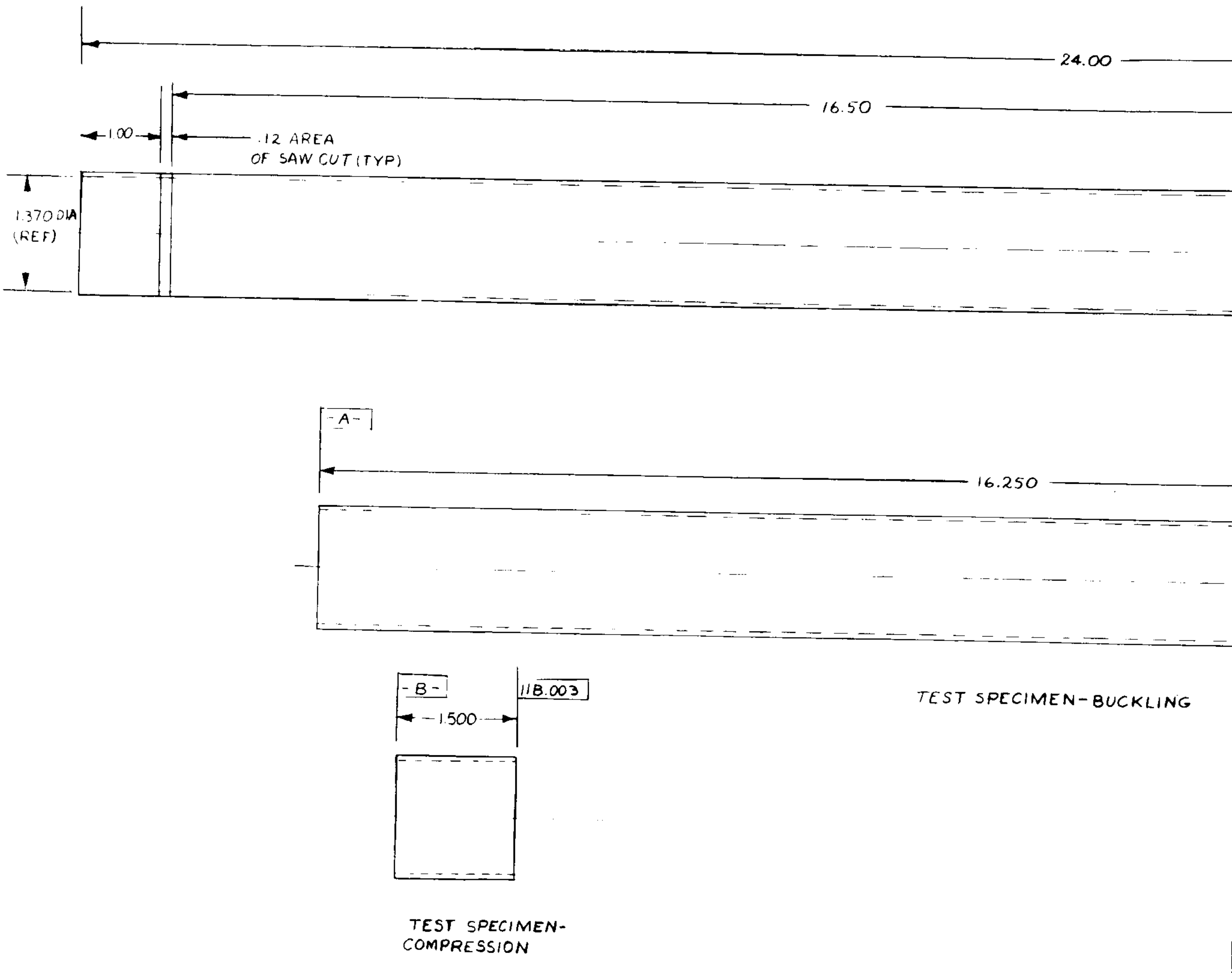
24.00
16.50
1.00
.12 AREA
OF SAW CUT (TYP)
1.370 DIA
(REF)
-A-
16.250
-B-
1.500
11B.003
TEST SPECIMEN-BUCKLING
TEST SPECIMEN-
COMPRESSION

Figure

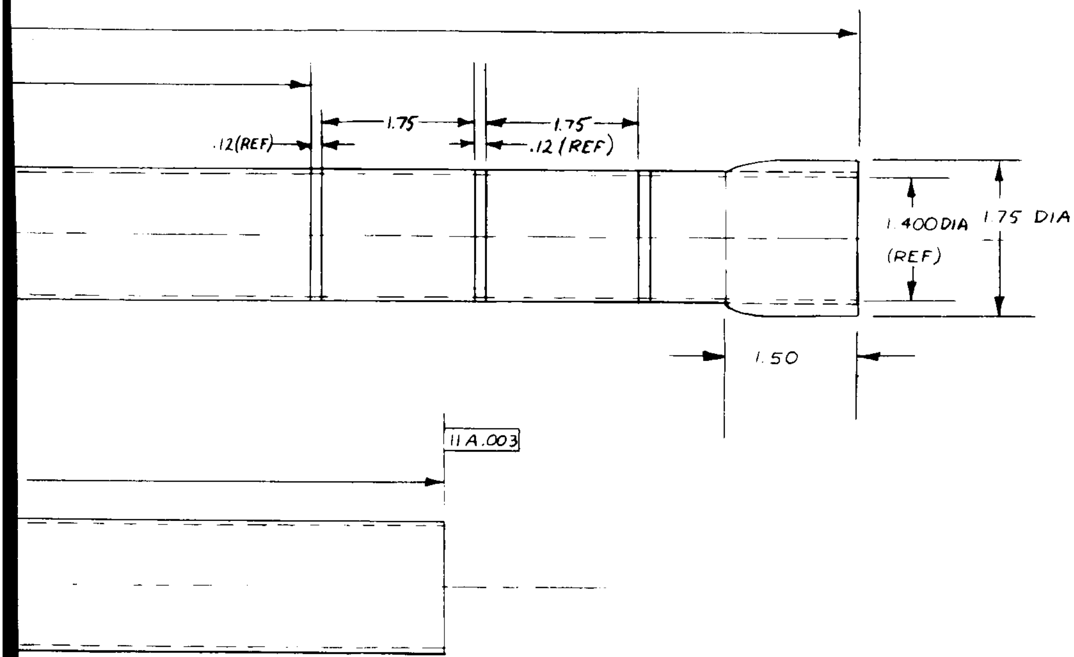

33. Cylinder Compression and Buckling Test Specimens

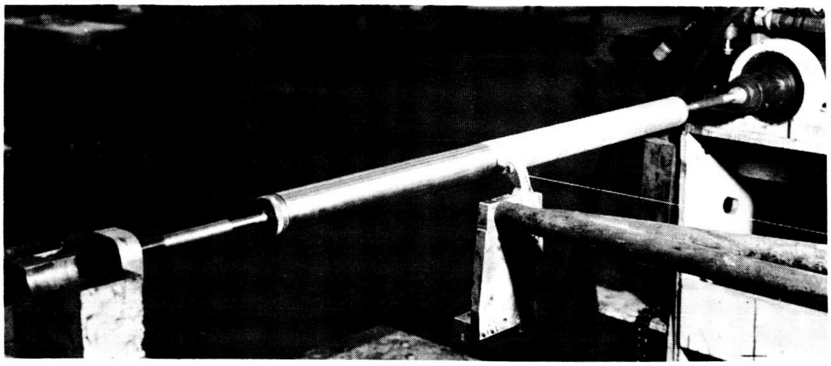

FILAMENT WINDING CIRCUMFERENTIAL PLY
FOR ROVING-REINFORCED CYLINDER

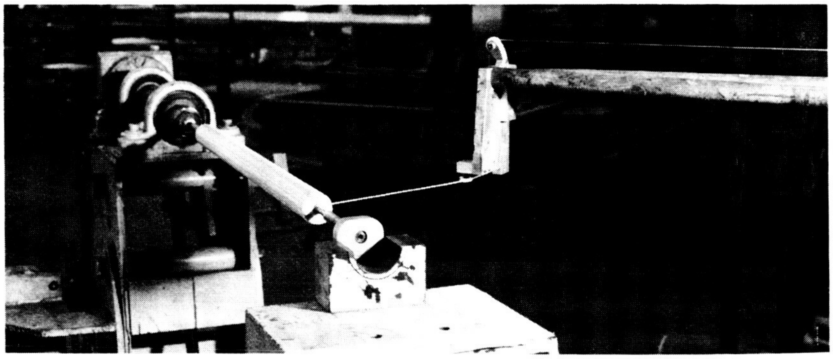

FILAMENT WINDING LONGITUDINAL PLY
FOR ROVING-REINFORCED CYLINDER

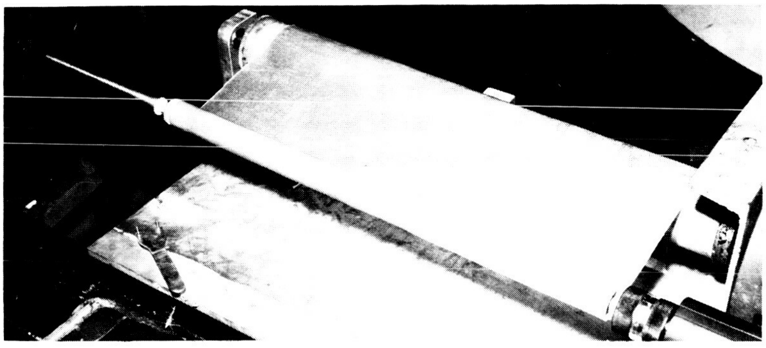

MACHINE WINDING OF GLASS CLOTH CYLINDER

Figure 34. Machine Winding of Compression and Buckling Test Cylinders

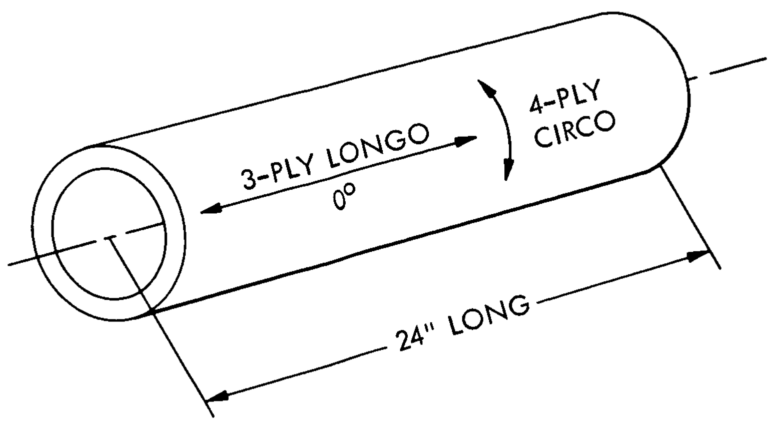

FABRICATION

OOOOOOO	1 CIRCO	- 10-LB TENSION/20 END (TYP)
▭	1 LONGO	- 5-LB TENSION/20 END (TYP)
OOOOOOO	1 CIRCO	
▭	1 LONGO	
OOOOOOO	1 CIRCO	
▭	1 LONGO	
OOOOOOO	1 CIRCO	

INDEXING

CIRCO - 0.0869"/20 END
LONGO - 0.0758"/20 END

PREPARATION FOR CURE

DACRON PEEL PLY
CELLOPHANE CURE PLY
DRY ROVING OVERWRAP
VACUUM BAG

CURE

25" HG VACUUM PRESSURE
1 HOUR AT 175°F
1 HOUR AT 250°F
4 HOURS AT 300°F

PART ALLOWED TO COOL DOWN TO 125°F UNDER VACUUM BEFORE REMOVAL FROM MANDREL.

Figure 35. Roving Filament-Wound Buckling and Compression Cylinder Process Controls

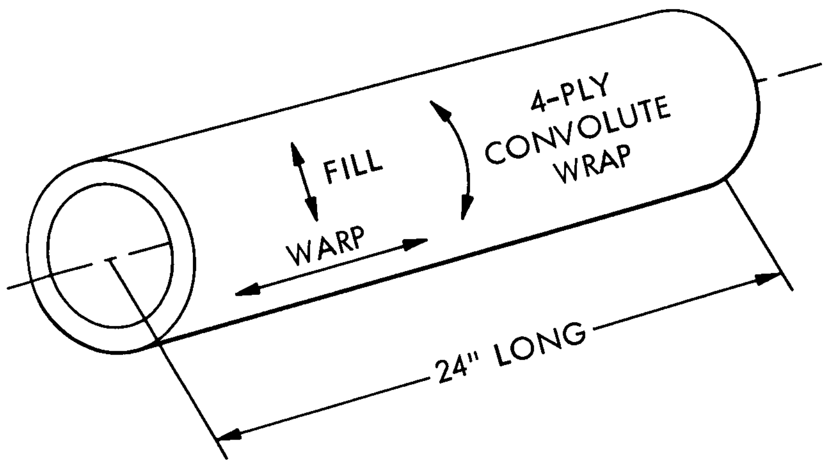

FABRICATION

4-PLY CLOTH WOUND AT 3/4 LB/INCH TENSION.

PREPARATION FOR CURE

DACRON PEEL PLY
CELLOPHANE CURE PLY
DACRON TAPE (2" WIDE)
OVERWRAP FOR 1581 ONLY
VACUUM BAG FOR 1543 ONLY

CURE

25" HG VACUUM PRESSURE
(FOR 1543 ONLY)
1 HOUR AT 175°F
1 HOUR AT 250°F
4 HOURS AT 300°F

PART COOLED DOWN TO 125°F BEFORE MANDREL REMOVAL.

Figure 36. Cloth Machine-Wound Buckling and Compression Cylinder Process Controls

Table 29. Material Characterization Summary of Cylinder Specimens

Specimen	Prepreg Identification
Tensile Cylinder (see Fig. 38)	
CT-FW-1	MA22-1078
CT-FW-2	MA22-1078
CT-FW-3	MA22-1078
CT-FW-4	MA22-1078
CT-FW-5	MA22-1078
CT-FW-6	MA22-1078
CT-1581-1	D-6233-1
CT-1581-2	D-6233-1
CT-1581-3	D-6233-1
CT-1581-4	D-6233-1
CT-1581-5	D-6233-1
CT-1581-6	D-6233-1
CT-1543-1	D-6232-1
CT-1543-2	D-6232-1
CT-1543-3	D-6232-1
CT-1543-4	D-6232-1
CT-1543-5	D-6232-1
CT-1543-6	D-6232-1
Compression Cylinder (see Fig. 38)	
CC-FW-1	MA22-1078
CC-FW-2	4886
CC-FW-3	4886
CC-FW-4	4886
CC-FW-5	4886
CC-FW-6	4886
CC-FW-7	4886
CC-FW-8	MA22-1079
CC-FW-9	4886
CC-1581-1	D-6233-1
CC-1581-2	D-6233-1
CC-1581-3	D-6233-1
CC-1581-4	D-6233-1

Table 29. Material Characterization Summary of Cylinder Specimens (Continued)

Specimen	Prepreg Identification
Compression Cylinder (see Fig. 38)	
CC-1581-5	D-6233-1
CC-1581-6	D-6233-1
CC-1581-7	D-6233-1
CC-1581-8	D-6233-1
CC-1581-9	D-6233-1
CC-1543-1	D-6232-1
CC-1543-2	D-6232-1
CC-1543-3	D-6232-1
CC-1543-4	D-6232-1
CC-1543-5	D-6232-1
CC-1543-6	D-6232-1
CC-1543-7	D-6232-1
CC-1543-8	D-6232-1
CC-1543-9	D-6232-1
Buckling Cylinder (see Fig. 38)	
CB-FW-1	MA22-1078
CB-FW-2	4886
CB-FW-3	4886
CB-FW-4	4886
CB-FW-5	4886
CB-FW-6	4886
CB-FW-7	4886
CB-FW-8	MA22-1079
CB-FW-9	4886
CB-1581-1	D-6233-1
CB-1581-2	D-6233-1
CB-1581-3	D-6233-1
CB-1581-4	D-6233-1
CB-1581-5	D-6233-1
CB-1581-6	D-6233-1
CB-1581-7	D-6233-1
CB-1581-8	D-6233-1
CB-1581-9	D-6233-1

Table 29. Material Characterization Summary of Cylinder Specimens (Continued)

Specimen	Prepreg Identification
Buckling Cylinder (see Fig. 38)	
CB-1543-1	D-6232-1
CB-1543-2	D-6232-1
CB-1543-3	D-6232-1
CB-1543-4	D-6232-1
CB-1543-5	D-6232-1
CB-1543-6	D-6232-1
CB-1543-7	D-6232-1
CB-1543-8	D-6232-1
CB-1543-9	D-6232-1

Table 30. Quality Control Data for Preimpregnated Glass Cloth

Batch No.	Mfg Date	Fabric Style	Percent Resin	Percent Volatiles	Percent Flow	Gel Time	Flexural Strength	
							Plies	Ult (psi)
D-6232-1	11-18-64	1543	39.03	6.69	23.61	5' 40"	15	164,788
D-6233-1	11-18-64	1581	32.96	5.17	17.35	3' 58"	15	107,965

Table 31. Resin Content of Cylinder Test Specimens

Tube No.	Resin Content (percent)		
	Specimen No. 1	Specimen No. 2	Average
1581-CB-1	34.84	34.81	34.83
1581-CB-2	34.81	34.62	34.72
1581-CB-3	35.24	35.21	35.23
1581-CB-4	34.95	35.08	35.02
1581-CB-5	35.24	35.14	35.19
1581-CB-6	34.95	34.44	34.70
1581-CB-8	34.64	34.85	34.75
1581-CB-9	34.43	34.47	34.45
1581-CT-1	39.56	35.71	37.64
1581-CT-2	39.81	35.66	37.74
1581-CT-3	38.41	39.12	38.77
1543-CB-6	34.85	34.81	34.83
1543-CB-7	32.94	32.76	32.85
1543-CB-8	34.41	36.66	35.54
1543-CB-11	36.14	35.14	35.64
BFW-CB-2	17.77	17.80	17.79
BFW-CB-3	16.98	16.98	16.98
BFW-CB-4	17.14	17.07	17.11
BFW-CB-5	17.25	17.34	17.30
BFW-CB-6	18.00	17.92	17.96
BFW-CB-7	18.29	18.16	18.23
BFW-CB-8	17.90	17.94	17.92
BFW-CB-9	20.35	20.70	20.53
BFW-CT-1	18.16	18.19	18.18
BFW-CT-2	18.30	18.70	18.50
BFW-CT-3	18.11	18.39	18.25
BFW-CT-4	17.34	17.58	17.46
BFW-CT-5	17.74	18.16	17.95
BFW-CT-6	18.75	18.62	18.69

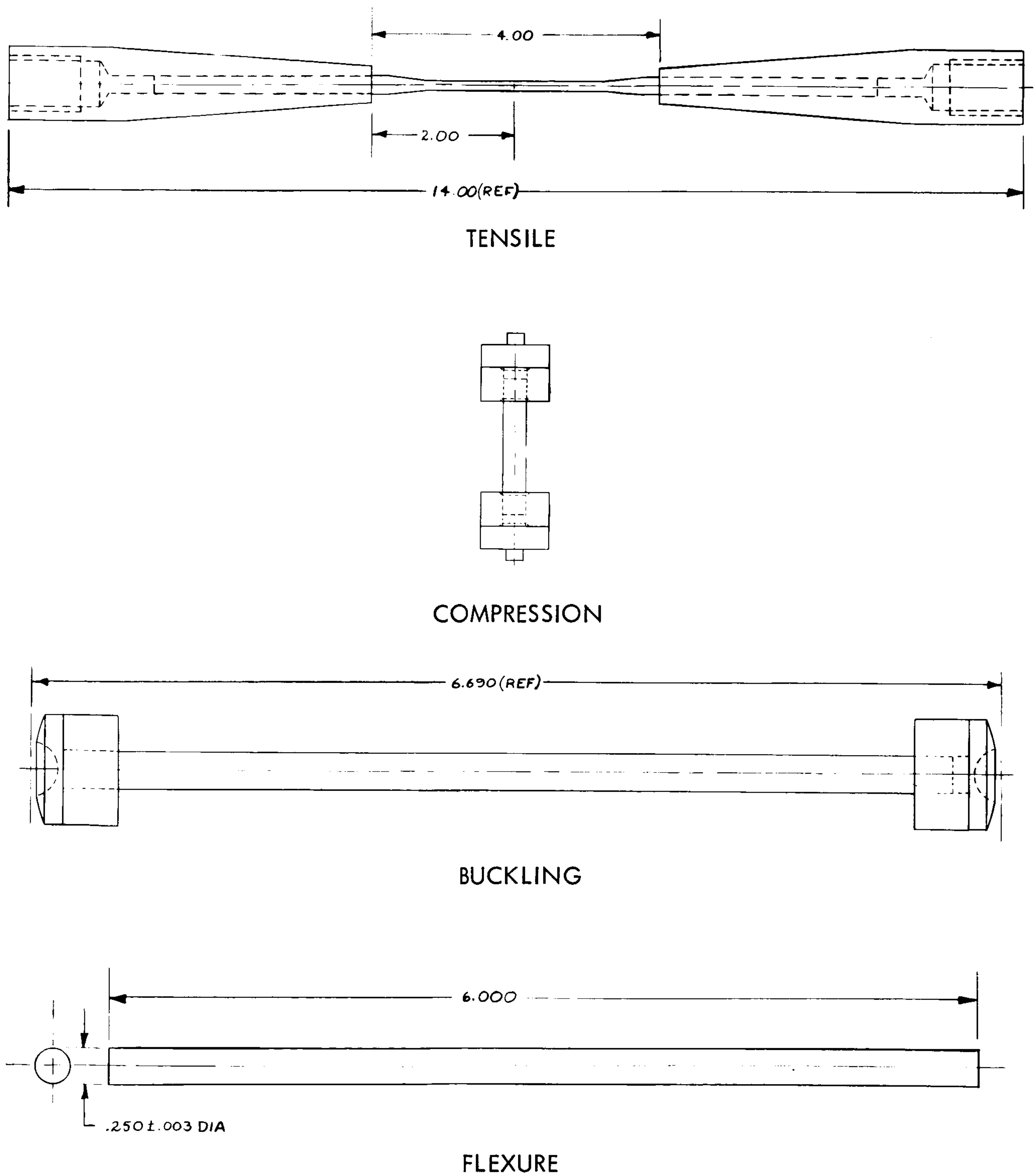

Figure 37. Filament-Wound Rod Assemblies

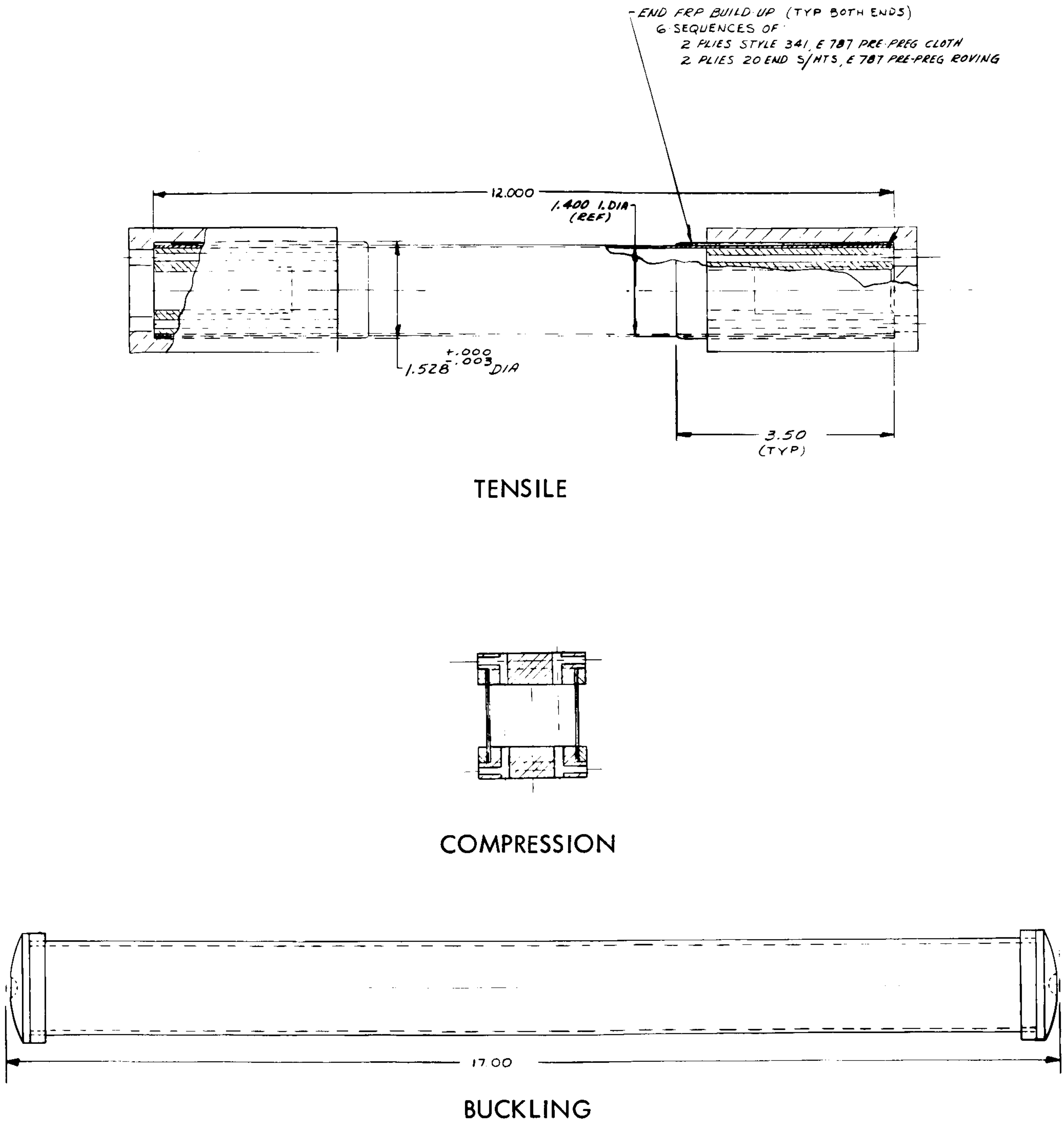

Figure 38. Machine-Wound Cylinder Assemblies

C. TESTING

Just as special test fixtures and methods were required for the mechanical properties testing program during the first year's effort, the testing of the structural tubes and rods required that new test fixtures and methods be developed to transmit the expected loads. The engineering drawings of the test fixtures fabricated to test the structural models in tension, compression, buckling, and flexure are shown in Figures 39 through 43. To enable the load to be transferred from these test fixtures into the specimens, special end fittings had to be bonded to the as-fabricated specimens. The tensile specimens required that external sleeves be bonded to the specimens. Figure 44 shows the sleeves bonded to the tensile rods, and Figure 45 shows the assembly for the tensile tubes. The compression buckling specimens required end fittings that provide a socket for the load-transmitting metal balls. The fittings for the rod and tube specimens are shown in Figures 46 and 47. To provide proper alignment of the compression buckling specimens, special centering devices were fabricated and attached to the cryostat as shown in Figures 48 and 49. After a small initial preload is applied to the specimen (see Figure 50), these centering rigs are removed for the actual test (see Figure 51). The end fittings for the ultimate compression rod and tube specimens are shown in Figures 52 and 53. These specimens are sufficiently short that the ultimate compressive strength is reached before column buckling occurs; however, uniform loading is required so the end fittings must be maintained parallel to each other and perpendicular to the axial direction of the specimen. The test setup for the flexural test of the rod specimens is shown in the cryostat in Figure 54. The test setup after the addition of liquid nitrogen is shown in Figure 55. All of the specimens were tested in either an Instron testing machine or a Baldwin testing machine, depending on the availability and loads required. The rate of loading for each test was selected so that failure of the specimen would occur within a time span of two to three minutes, the same as for the mechanical properties testing program.

The test temperature of 77°K was obtained by submerging the assembled test specimen in liquid nitrogen contained in a cryostat during the entire test.

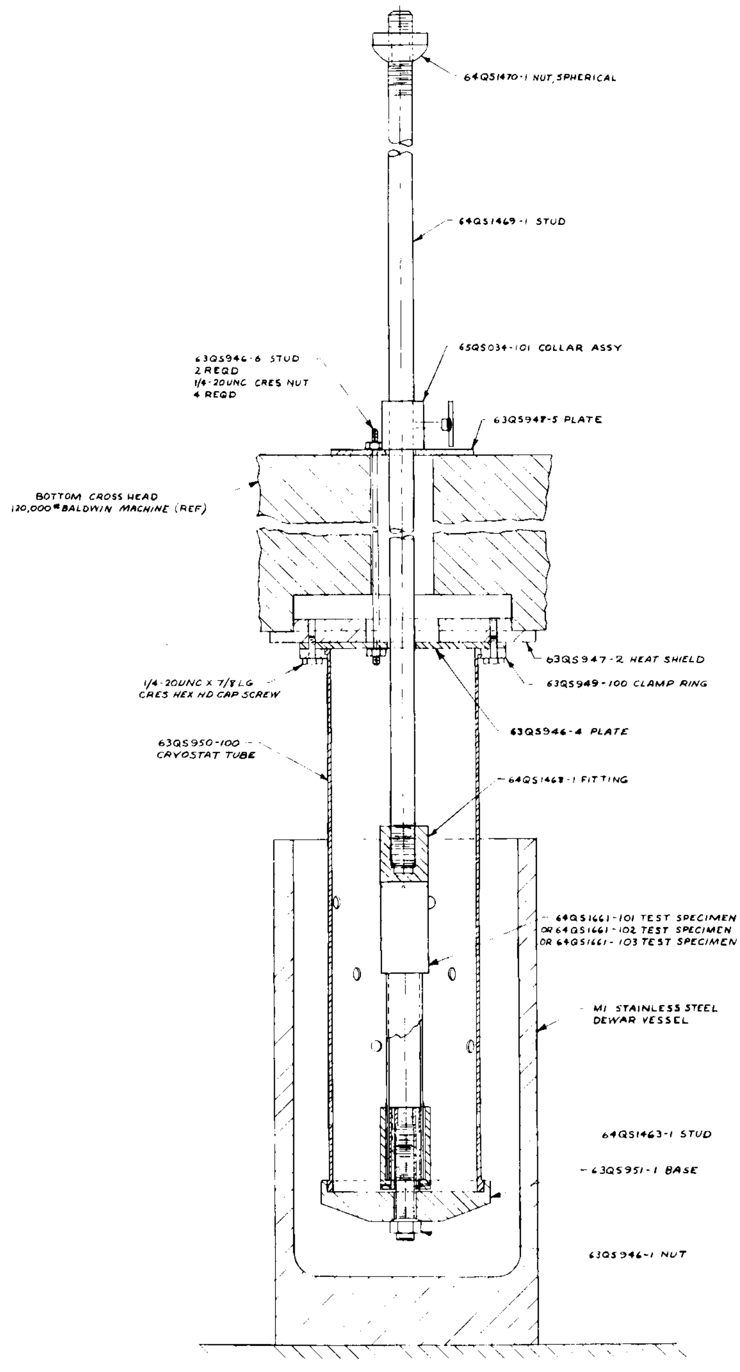

Figure 39. Tensile Tube Test Setup

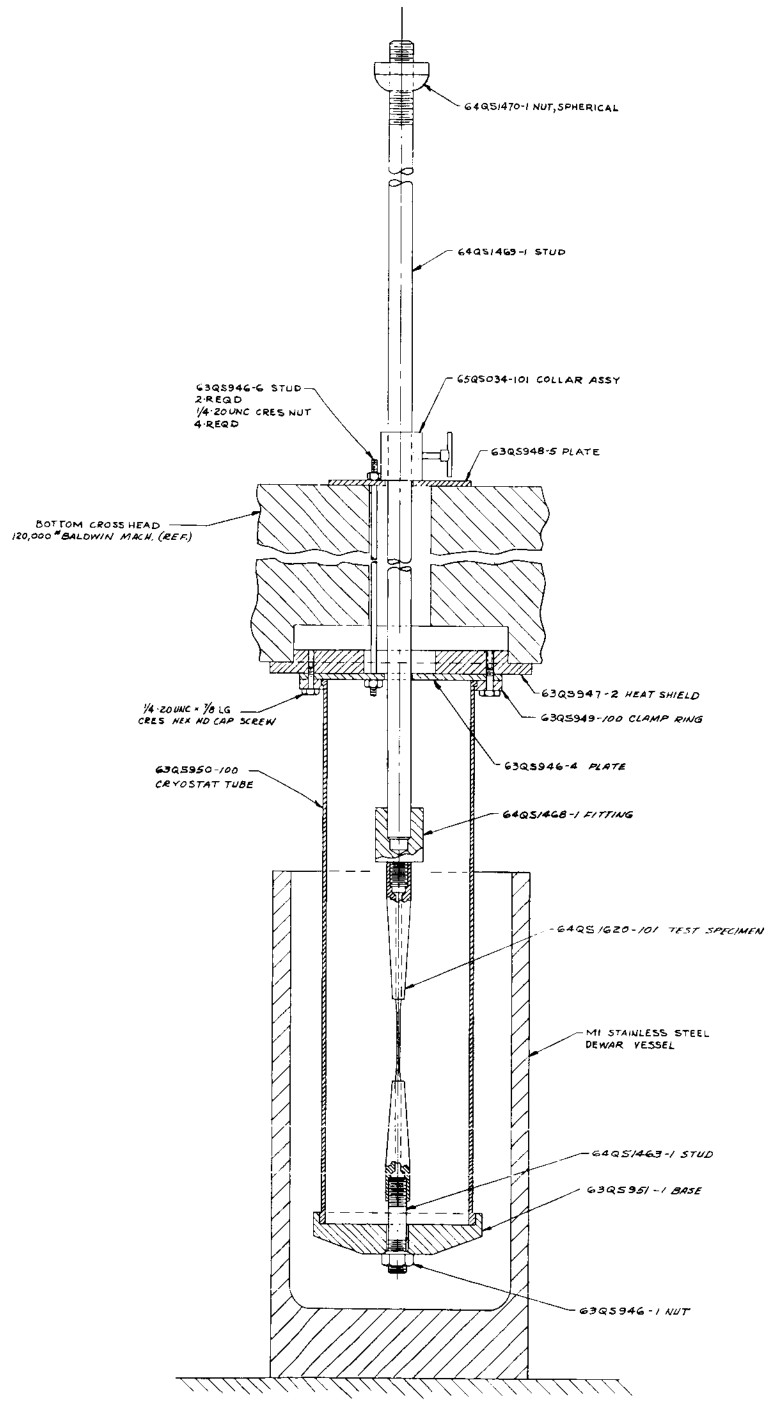

Figure 40. Tensile Rod Test Setup

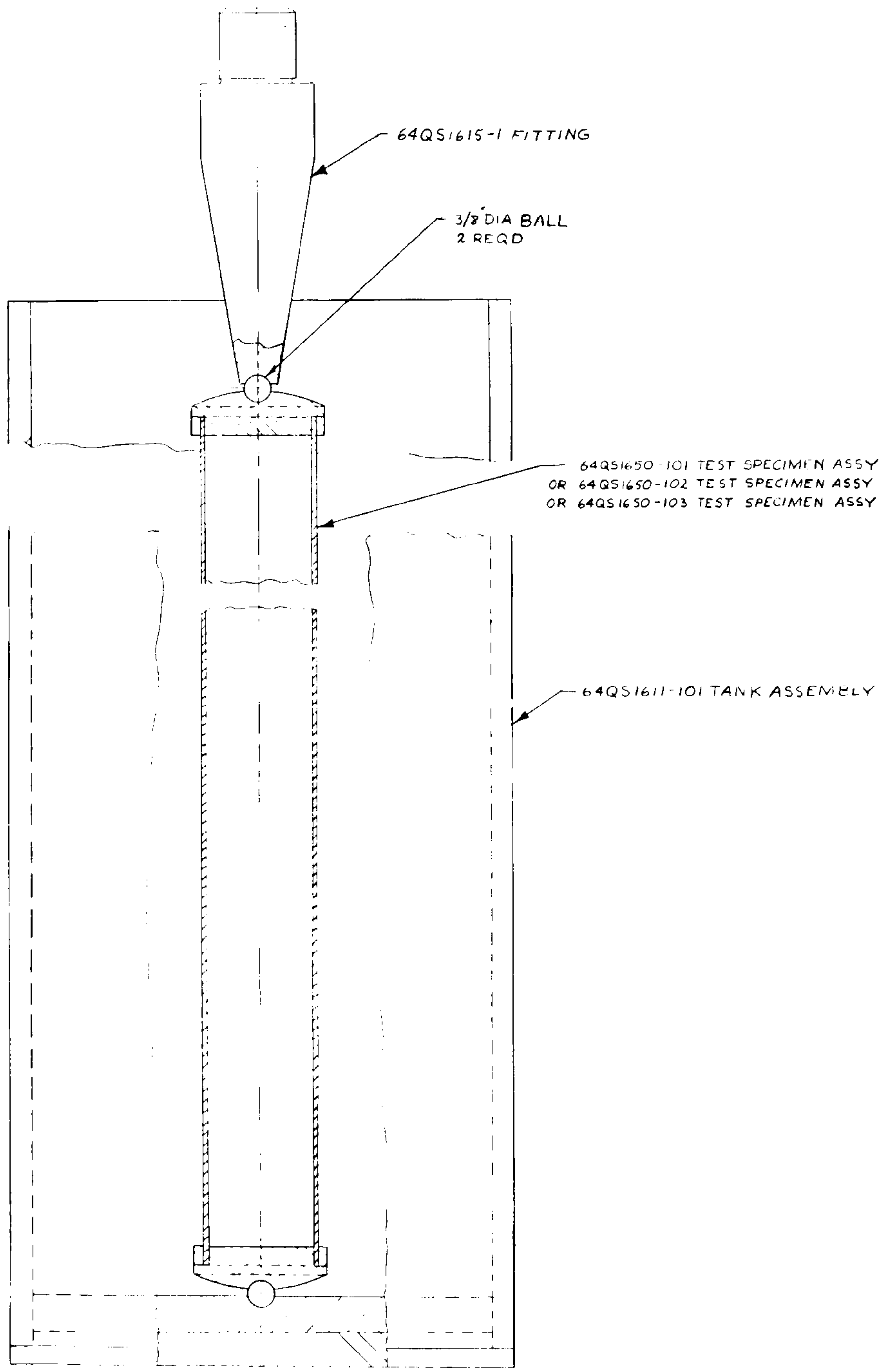

Figure 41. Buckling Tube Test Setup

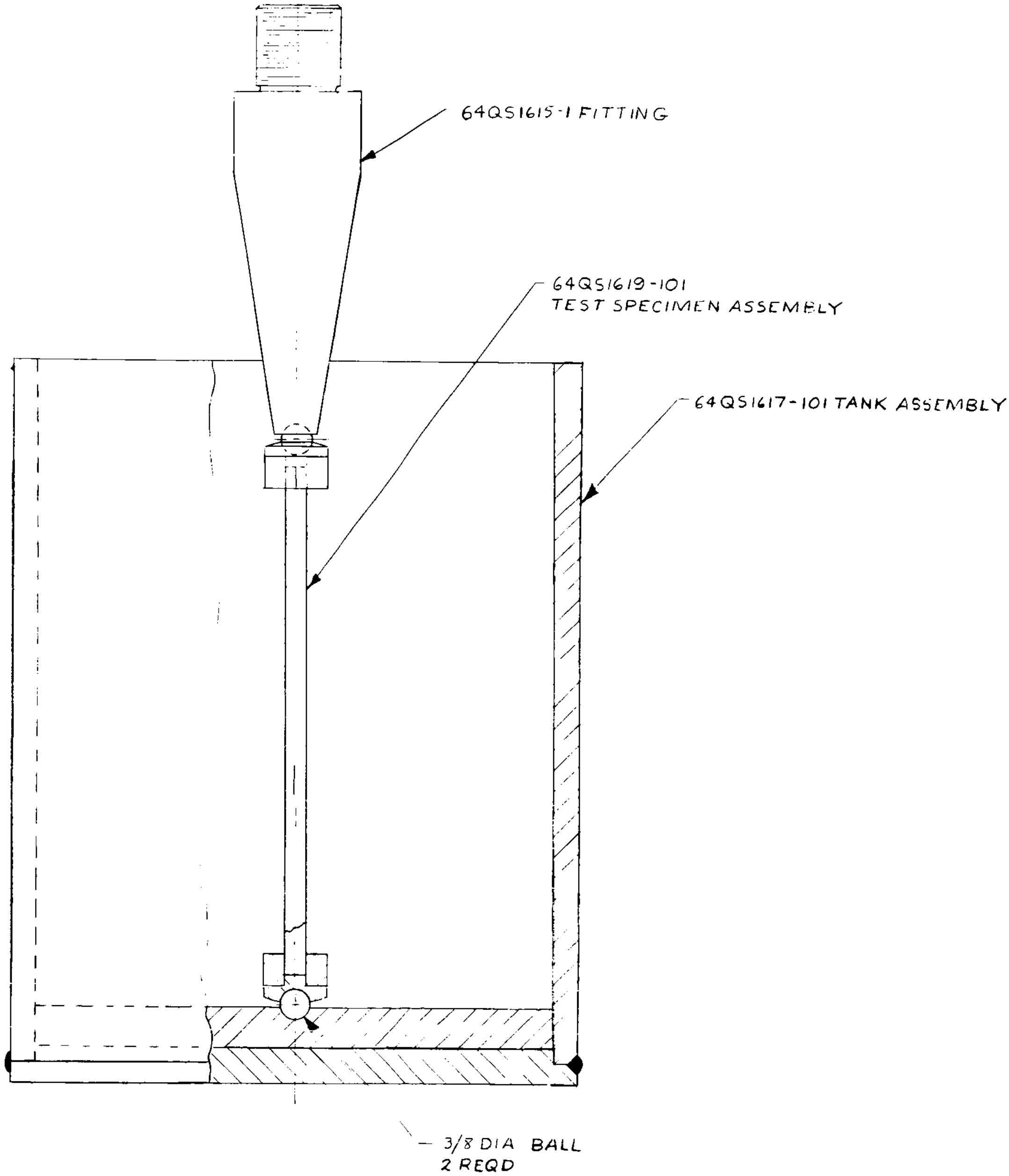

Figure 42. Buckling Rod Test Setup

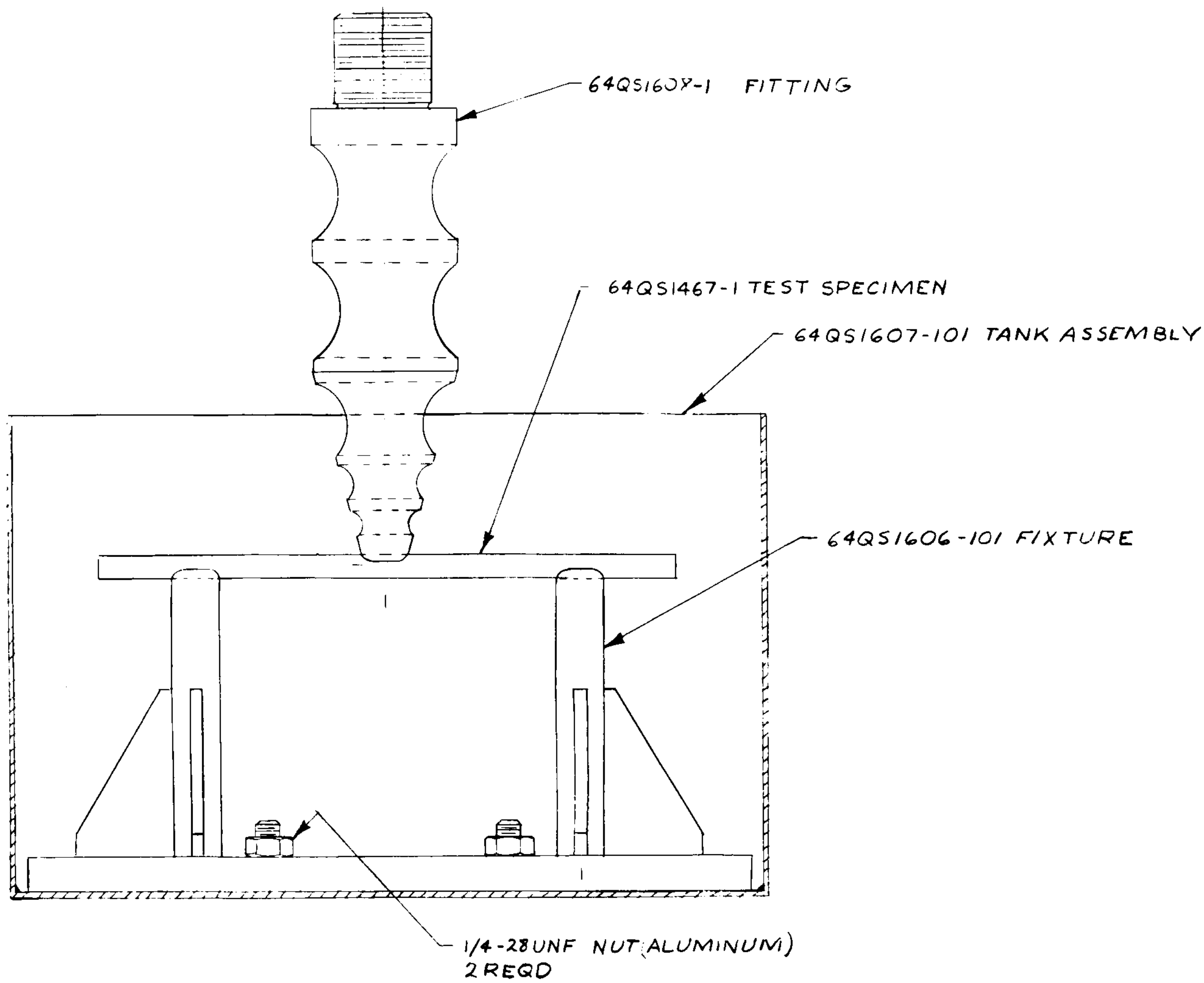

Figure 43. Flexural Rod Test Setup

Figure 44. UFW Tensile Rods before Test

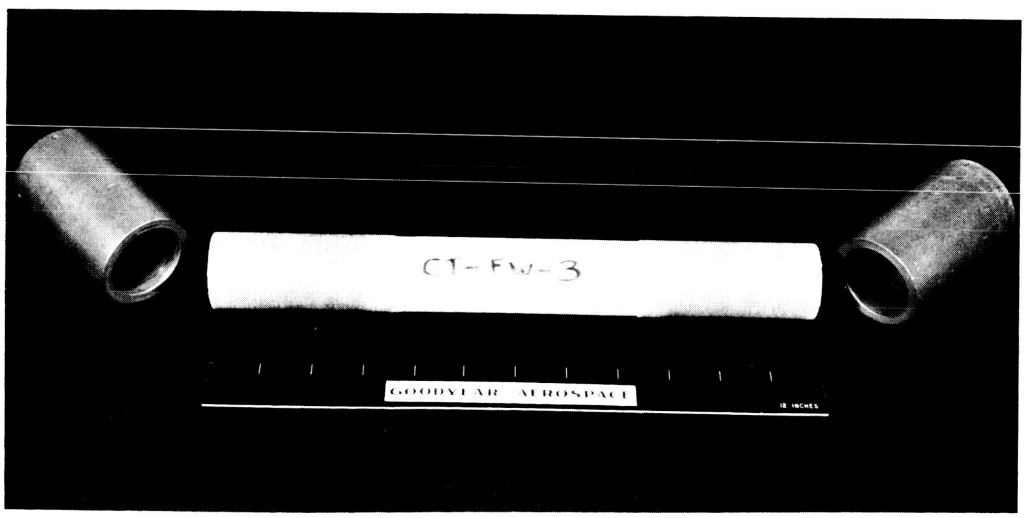

Figure 45. Tensile Tubes with Sleeves

Figure 46. Buckling Rods before Test

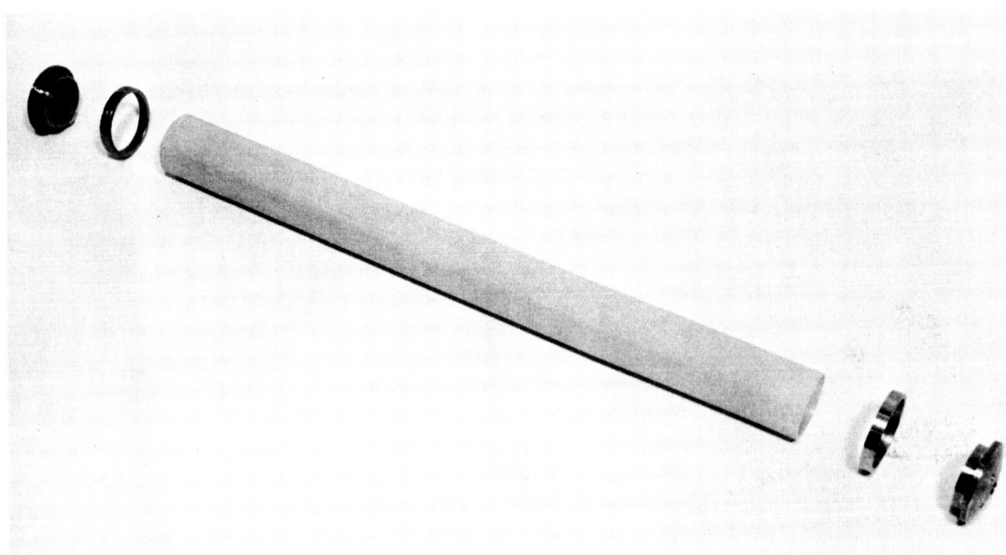

Figure 47. Buckling Tube Showing End Fittings

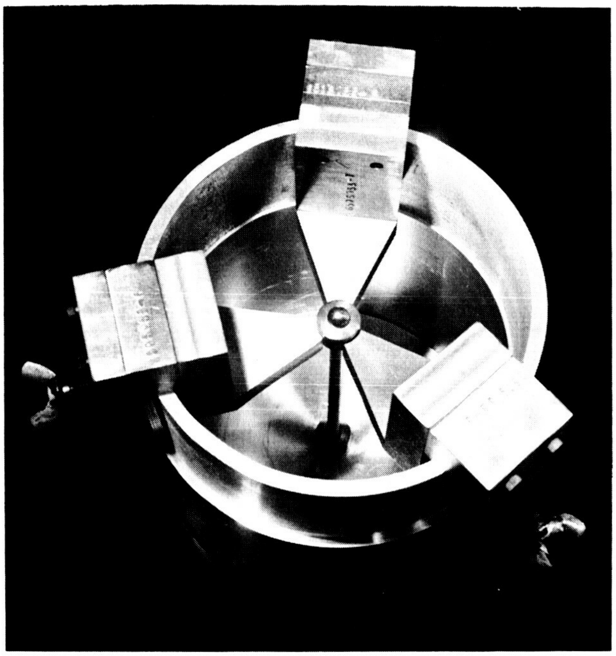

Figure 48. UFW Buckling Rod in Cryostat with Centering Rig

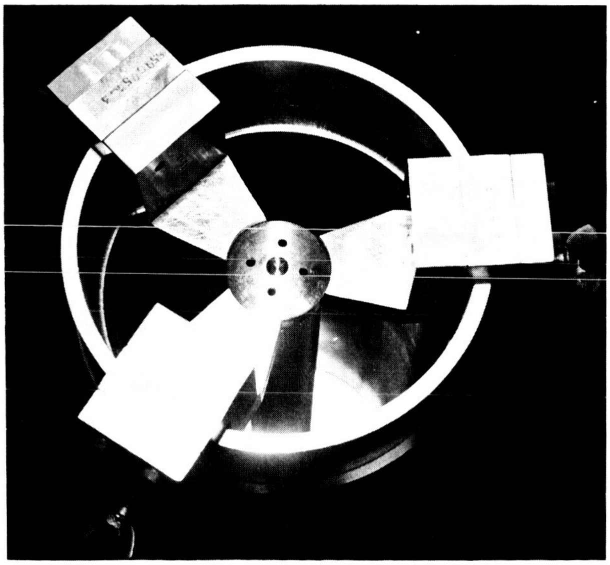

Figure 49. Buckling Tube in Cryostat with Centering Rig

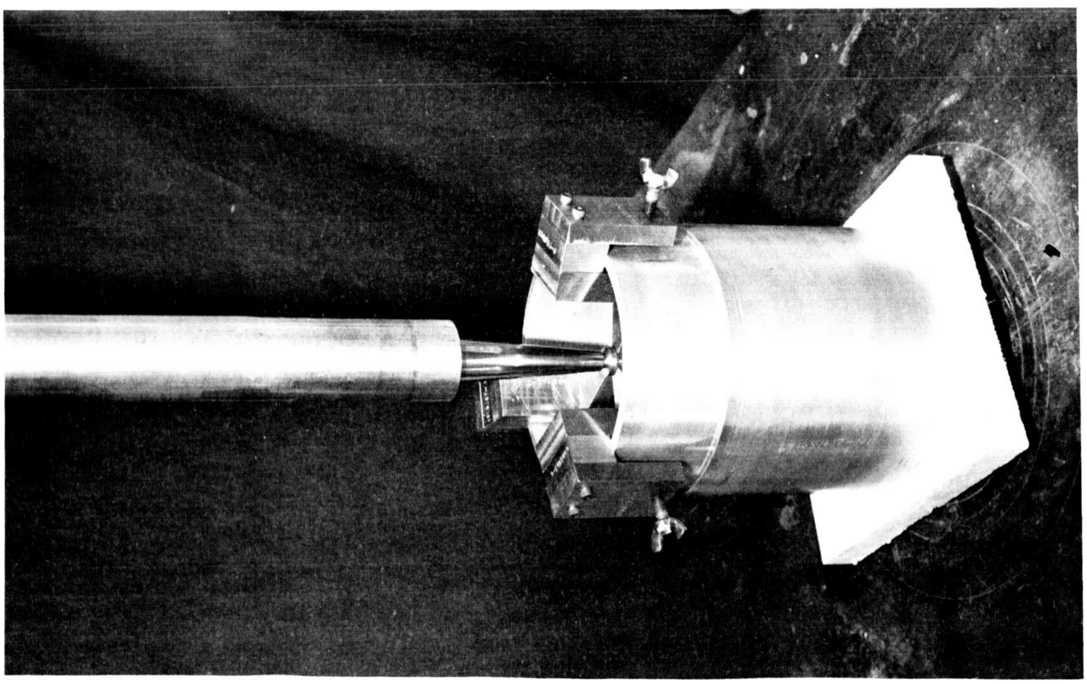

Figure 50. Buckling Rod with Initial Load Applied

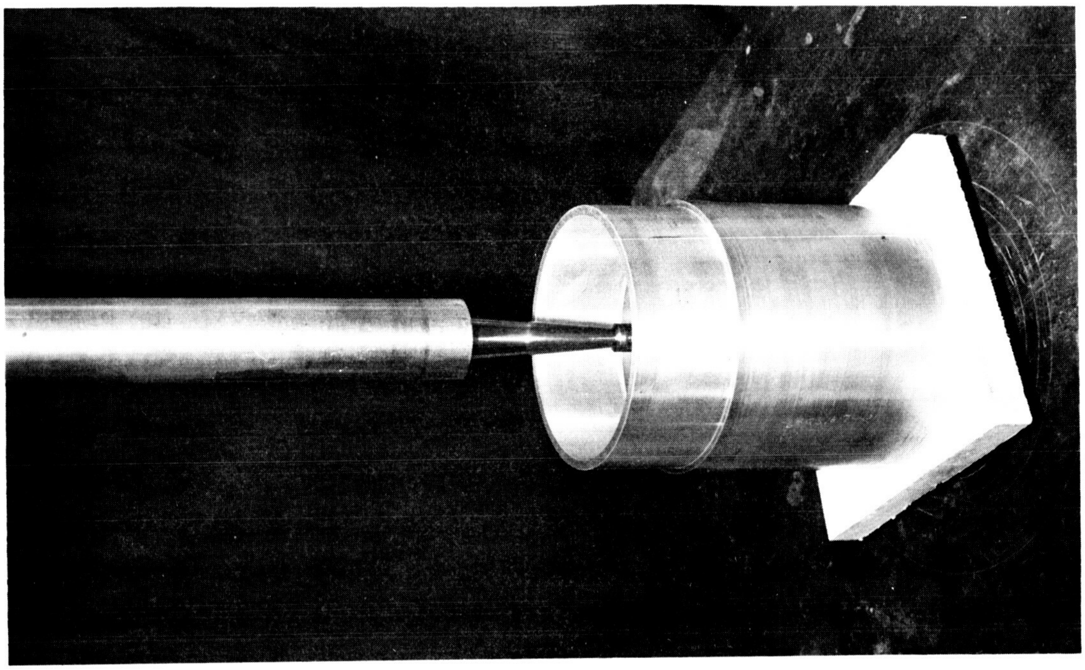

Figure 51. Buckling Rod in Test Machine with Centering Rig Removed

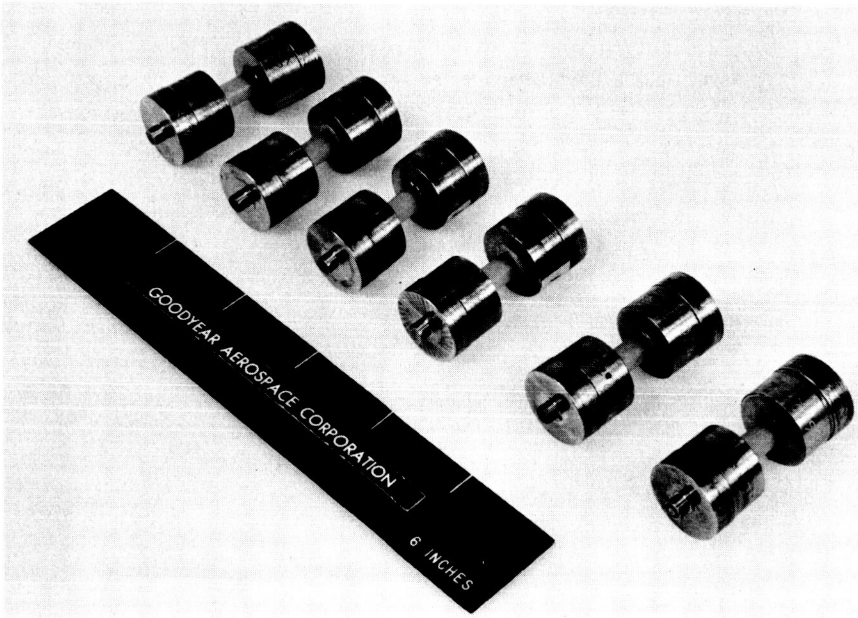

Figure 52. Compression Rod Specimens before Test

Figure 53. Compression Tube Specimens before Test

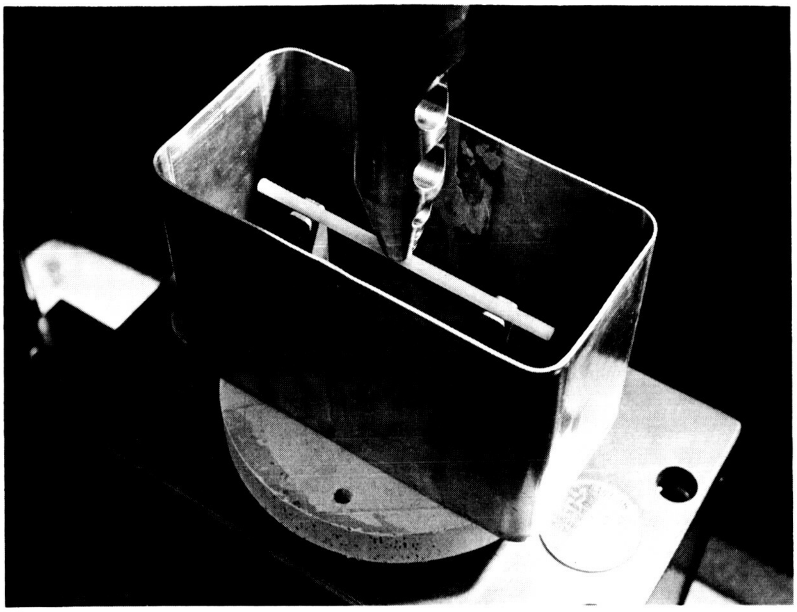

Figure 54. Flexural Rod in Cryostat before Test

Figure 55. Flexural Rod in Cryostat
with Liquid Nitrogen

D. RESULTS

1. General

The purpose of the third task of the program was to determine the ability to achieve in structural shapes the properties previously obtained in the mechanical properties testing program.

The tabulated results of the tests conducted in Task III are given in Table 32. This table includes the test results of the individual specimens, the average result for each group of three tests, and the expected results as determined from the mechanical properties testing program. The values obtained indicate good agreement with the mechanical properties testing data, and show that the mechanical properties values obtained in the previous testing portion of the program are reproducible in actual structural shapes as long as the fabrication process is comparable. The individual tests are discussed in the following paragraphs.

2. Compression

Figure 56 shows a compression tube specimen in the test machine just after specimen failure. In general, all of the compression test results of the filament-wound roving specimens compared favorably with the average values previously obtained in the mechanical properties testing program. The test results for the cloth specimen, however, are below the values obtained in the previous mechanical properties testing. This was to be expected since it was not possible to achieve the compaction in the small diameter cloth tube specimens as it was in the autoclave-cured cloth flat panel specimens. However, if the comparison of results had been based on the amount of reinforcement in the specimen instead of composite thickness, the results would have appeared more favorable. Table 33 shows a comparison of the thickness per layer as achieved on the flat panels

Table 32. Task III Test Results

Test	Configuration	Material	Test Temperature (°K)	Specimen No.	Test Results (psi)	Average Results (psi)	Expected Properties* (psi)
Compression	Tube	BFW	298	CC-2 CC-3 CC-4	65,300 66,300 75,200	68,933	79,225
			77	CC-5 CC-6 CC-7	111,200 93,050 92,900	99,050	99,330
		1543	298	CC-3 CC-4 CC-11	41,900 50,200 50,000	47,367	89,503
			77	CC-6 CC-7 CC-8	84,050 76,100 74,600	78,250	122,448
		1581	298	CC-1 CC-2 CC-3	34,100 32,540 37,820	34,820	62,587
			77	CC-4 CC-5 CC-6	54,450 57,900 54,450	55,600	103,202
	Rod	UFW	298	RC-14-1 RC-14-2 RC-14-3	161,818 140,808 140,530	147,719	151,209
			77	RC-14-4 RC-14-5 RC-15-1	271,487 279,261 280,808	277,185	237,646
Tension	Tube	BFW	298	CT-1 CT-2 CT-3	114,300 103,000 115,900	111,067	127,200
			77	CT-4 CT-5 CT-6	95,200 115,700 93,000	101,300	162,800
		1543	298	CT-1 CT-2 CT-3	138,900 145,000 145,800	143,233	169,316
			77	CT-4 CT-5 CT-6	149,800 191,900 208,200	183,300	232,385
		1581	298	CT-1 CT-2 CT-3	65,800 56,000 78,100	66,633	92,506
			77	CT-4 CT-5 CT-6	100,500 103,000 106,300	103,266	144,543

*Based on mechanical properties testing.

Table 32. Task III Test Results (Continued)

Test	Configuration	Material	Test Temperature (°K)	Specimen No.	Test Results (psi)	Average Results (psi)	Expected Properties* (psi)
Tension	Rod	UFW	298	RT-7-2	330,088		
				RT-7-1	304,800		
				RT-8-2	292,800	309,229	294,928
			77	RT-13-1	301,600		
				RT-6-2	345,372	323,486	330,628
Flexure	Rod	UFW	298	RF-15-3	238,200		
				RF-14-1	274,400		
				RF-16-1	249,200	253,933	223,711
			77	RF-14-2	416,000		
				RF-15-1	423,000		
				RF-15-2	423,000		
				RF-16-2	407,000	417,250	468,554
Buckling	Tube	BFW	298	CB-2	42,550		
				CB-3	47,450		
				CB-4	45,250	45,083	37,600
			77	CB-5	64,800		
				CB-6	62,300		
				CB-7	59,400	62,167	41,550
			temp grad	CB-8	51,450		
				CB-9	47,200	49,325	--
		1543	298	CB-6	38,860		
				CB-7	42,200		
				CB-8	44,900	41,653	45,750
			77	CB-1	45,800		
				CB-2	50,000		
				CB-3	41,450	45,750	48,650
			temp grad	CB-4	44,250		
				CB-11	46,800	45,525	--
		1581	298	CB-1	25,260		
				CB-2	29,760		
				CB-3	32,400	29,140	28,500
			77	CB-4	29,820		
				CB-5	36,580		
				CB-6	33,020	33,140	32,360
			temp grad	CB-8	40,650		
				CB-9	25,160	32,905	--
	Rod	UFW	298	RB-9-1	16,050		
				RB-9-2	27,080		
				RB-9-3	20,140	21,090	9,000
			77	RB-12-1	31,120		
				RB-12-2	32,020		
				RB-12-3	30,420	31,137	9,870
			temp grad	RB-10-1	26,000		
				RB-10-2	32,400	29,200	--

*Based on mechanical properties testing.

Table 33. Determination of Stresses Based on Theoretical Thicknesses

Specimen	Material	Thickness (inches)	Number of Layers	Thickness/ Layer
Flat Panels	1581	0.140	13	0.0108
	1543	0.140	14	0.0100
Compression Tubes				
Actual	1581	0.052	4	0.0130
	1543	0.045	4	0.0112
Theoretical	1581	0.043	4	0.0108
	1543	0.040	4	0.0100
Tension Tubes				
Actual	1581	0.040	3	0.0133
	1543	0.035	3	0.0117
Theoretical	1581	0.032	3	0.0108
	1543	0.030	3	0.0100

Stresses Based on Theoretical Thickness

Material	Tension		Compression	
	$298^{O}K$	$77^{O}K$	$298^{O}K$	$77^{O}K$
1543 Cloth	163, 900 psi	221, 600 psi	57, 900 psi	87, 400 psi
1581 Cloth	82, 600 psi	128, 800 psi	42, 500 psi	68, 100 psi

against the thickness per layer of the cloth tubes. If the thickness of the tubes were based on the number of layers of the tubes and the layer thickness of the flat panels, the theoretical stresses would be as shown in Table 33. These values are still below the expected values; however, this confirms the belief that the presence of voids is a major factor in determining compressive strength of fiberglass laminates as reported in Reference 5.

The axial direction on the cloth tube specimens and the UFW rod specimens corresponds to the parallel direction of the mechanical properties testing, whereas on the BFW tube specimens, the axial direction corresponds to the normal test direction. The BFW tubes before and after testing are shown in Figures 53 and 57. Before and after test photos for the other compression tube specimens are shown in Figures 58 through 61. The UFW compression rods before and after testing are shown in Figures 52 and 62.

3. Tension

Tensile testing of the rods and tubes required that special attention be given to the bond of the metal sleeves to the fiberglass specimens. In both the rod and tube specimens, problems developed in this bond. The original tensile rod specimens had a primer coat of Bondmaster M602 on the steel sleeve before using a 901-B1 adhesive, and although ultimate failures occurred in the room temperature tests, this bond to the steel failed prematurely at the liquid nitrogen temperature. The tests at the liquid nitrogen temperature were rerun, this time using no primer but acid etching the steel sleeve and using an Adiprene and Moca adhesive. Although one specimen failed in this bond at a stress level of 235,000 psi, the other two specimens failed correctly (see Table 32). The UFW tensile rods before testing are shown in Figure 44, and a typical ultimate failure is shown in Figure 63.

Preliminary tests were conducted on tensile tubes using only the internal loading plug as shown in Figure 64. However, tensile testing of this specimen produced a failure within the bond of the plug to the tube rather than a tensile failure of the tube (see Figure 65). By adding the external sleeve bonded to the specimen as shown in Figure 66, a failure within the specimen occurred as shown in Figure 67. The test results for the cloth tubes again appear lower than the expected values because of the lack of compaction possible in these specimens. However, when the comparison is based on the amount of reinforcement instead of composite thickness as in Table 33, the results are equal to the values obtained on the mechanical properties testing program. The photos of the tensile test specimens before and after testing are shown in Figures 68 through 73.

4. Flexure

The results of the filament-wound rods tested in flexure with center-point loading and with a four-inch span are shown in Table 32. No problems were involved in the room temperature or liquid nitrogen temperature testing, and the results of the tests were satisfactory.

5. Compression Buckling

The compression buckling rods and tubes were axially compressed and the specimen lengths were sufficiently long to create a buckling condition. The critical buckling stresses at room temperature and at 77°K for the column buckling specimens versus column length were determined from the following equations:

$$S_{cr} = \frac{n\pi^2 EI}{AL^2} \quad \text{for } S_{cr} \text{ less than } S_u/2 \tag{6}$$

and

$$S_{cr} = S_u \left(1 - \frac{S_u L^2 A}{4n\pi^2 EI}\right) \quad \text{for } S_{cr} \text{ greater than } S_u/2, \tag{7}$$

where S_u represents the ultimate compressive strength of the column material in the axial direction and n is a constant depending on the conditions of restraint of the column ends (see Reference 4). For the both-ends-free condition of our test setup, n = 1.0. The photos of the buckled rod (Figure 74) and the buckled tube (Figure 75) would indicate that a both-ends-free condition does exist. The test results are plotted on the calculated buckling curves of Figures 76 through 78, and whereas the results of the cloth specimen tests are similar to the calculated values, the filament-wound specimen test results are substantially higher than the calculated values.

The buckling of specimens with a temperature gradient along their axes was also performed. The temperatures at three points along rod and tube specimens with one end in liquid nitrogen and the other end open to the room were determined using the test setups as seen in Figures 79 through 81. The thermocouple locations on the specimens are shown in Figure 82. The temperature survey results are presented in Table 34. This temperature gradient along the axis had no adverse structural effect on the test specimens, with the test results in all cases falling between the room temperature and liquid nitrogen temperature results previously obtained.

Before and after test photos of the compression buckling specimens for each material are shown in Figures 83 through 86.

Table 34. Temperature Survey Results

Elapsed Time (minutes)	Thermocouple 1 Temp (^{o}K)	Thermocouple 2 Temp (^{o}K)	Thermocouple 3 Temp^{o}K
Rod - Reinforced Plastic UFW			
0	84	181	292
7	90	181	291
12	90	181	292
15	91	180	293
Tube - Filament-Wound Reinforced Plastic			
0	86	292	297
5	86	294	301
10	86	295	301
22	86	296	301
30	86	296	303
35	86	296	301

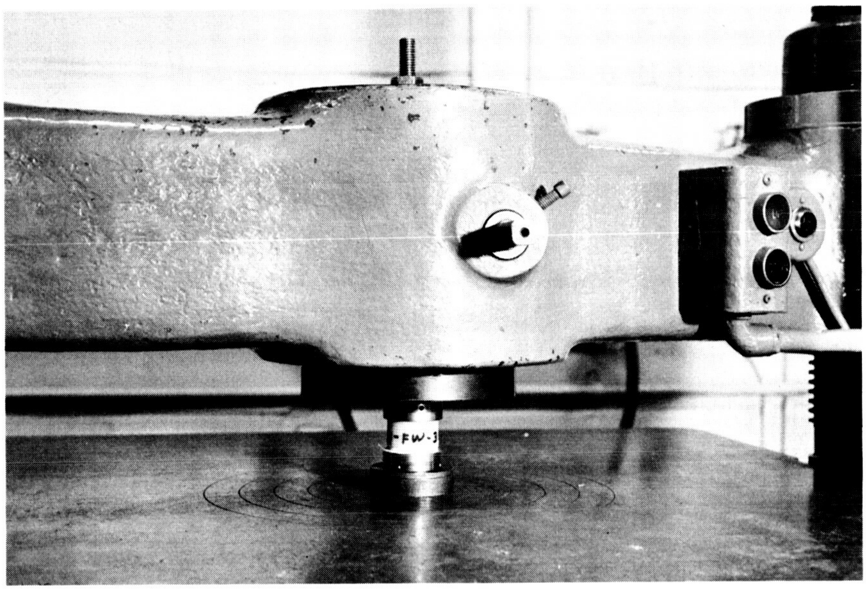

Figure 56. Failed Compression Tube in Test Machine

Figure 57. BFW Compression Tubes after Test

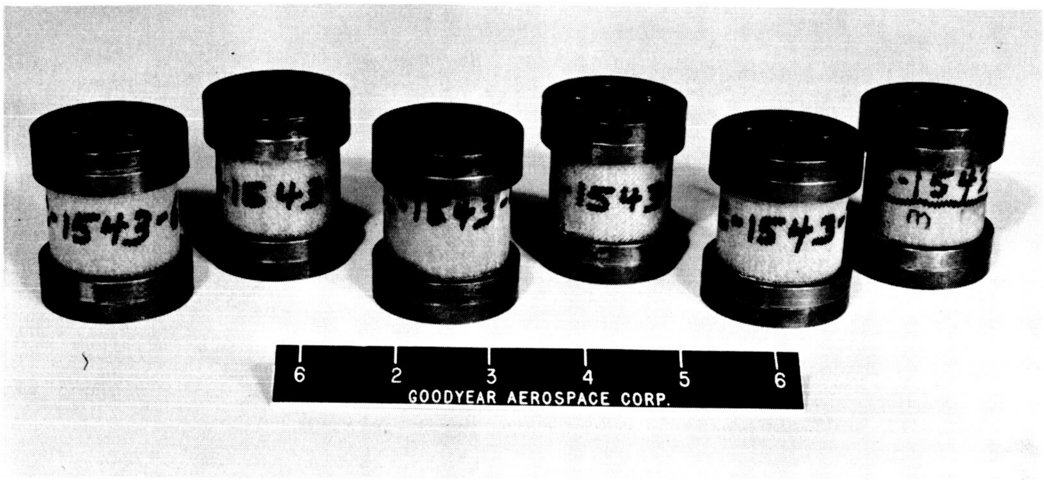

Figure 58. 1543 Cloth Compression Tubes before Test

Figure 59. 1543 Cloth Compression Tubes after Test

Figure 60. 1581 Cloth Compression Tubes before Test

Figure 61. 1581 Cloth Compression Tubes after Test

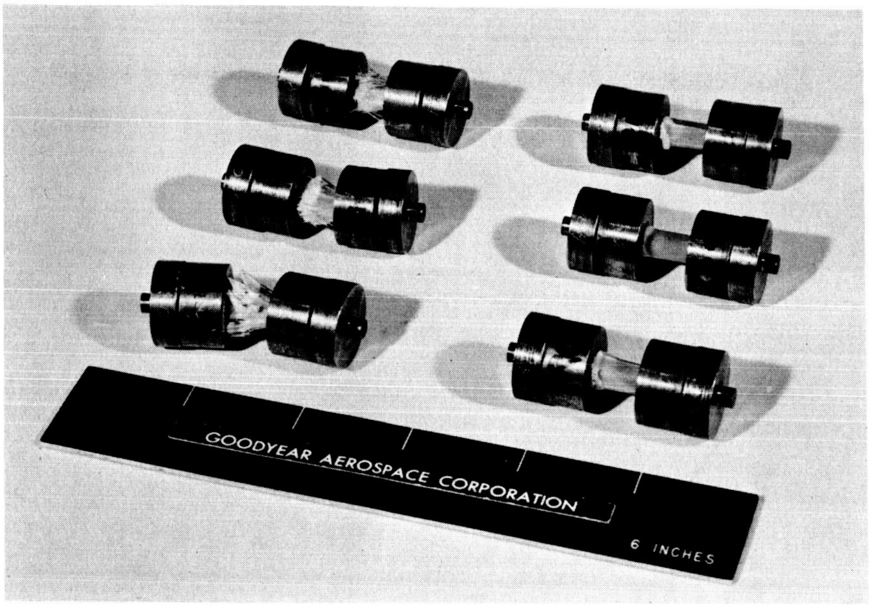

Figure 62. UFW Compression Rods after Test

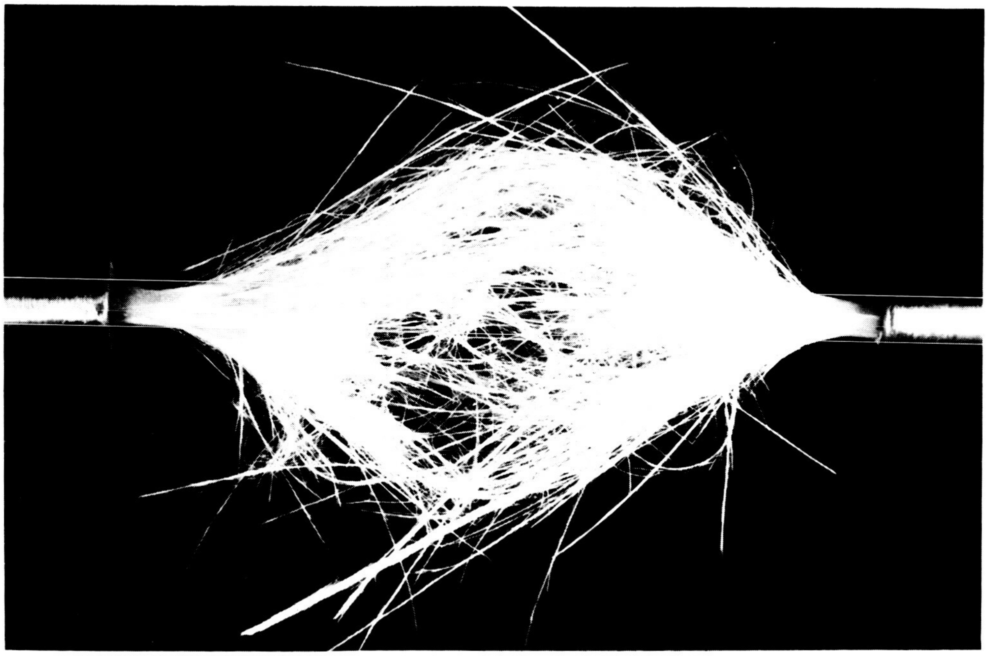

Figure 63. Typical Failure of UFW Tensile Rod

Figure 64. BFW Tensile Tube before Test

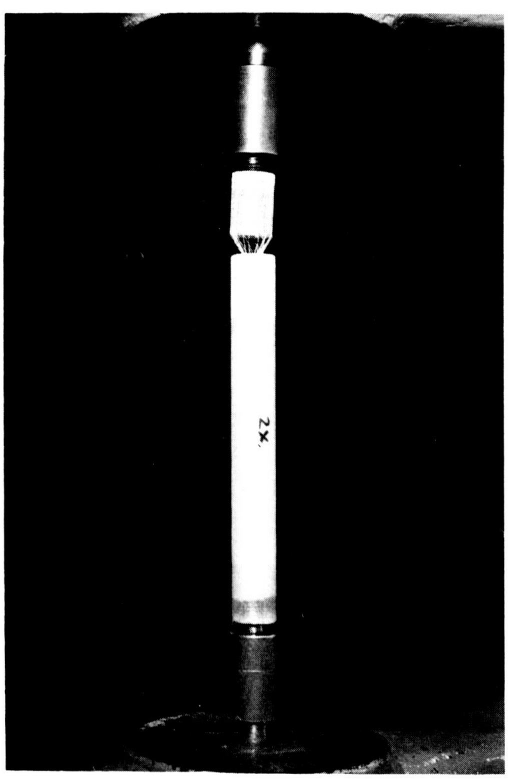

Figure 65. BFW Tensile Tube after End Plug Bond Failure

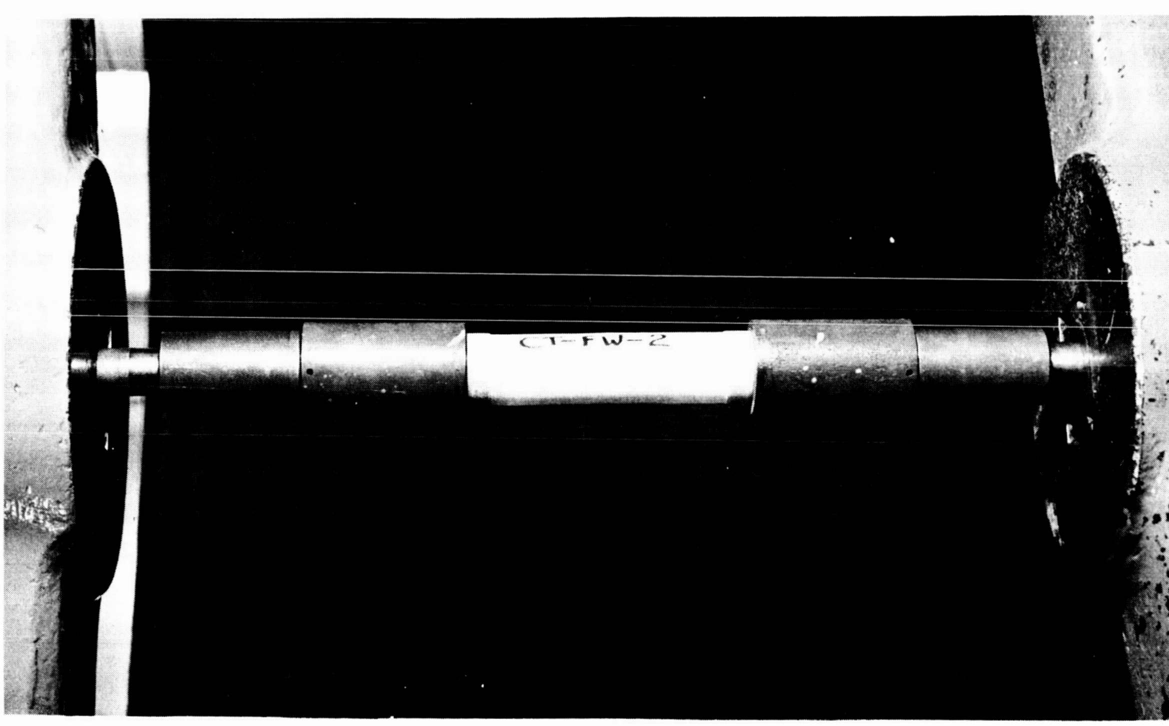

Figure 66. BFW Tensile Tube with External Sleeve in Test Machine

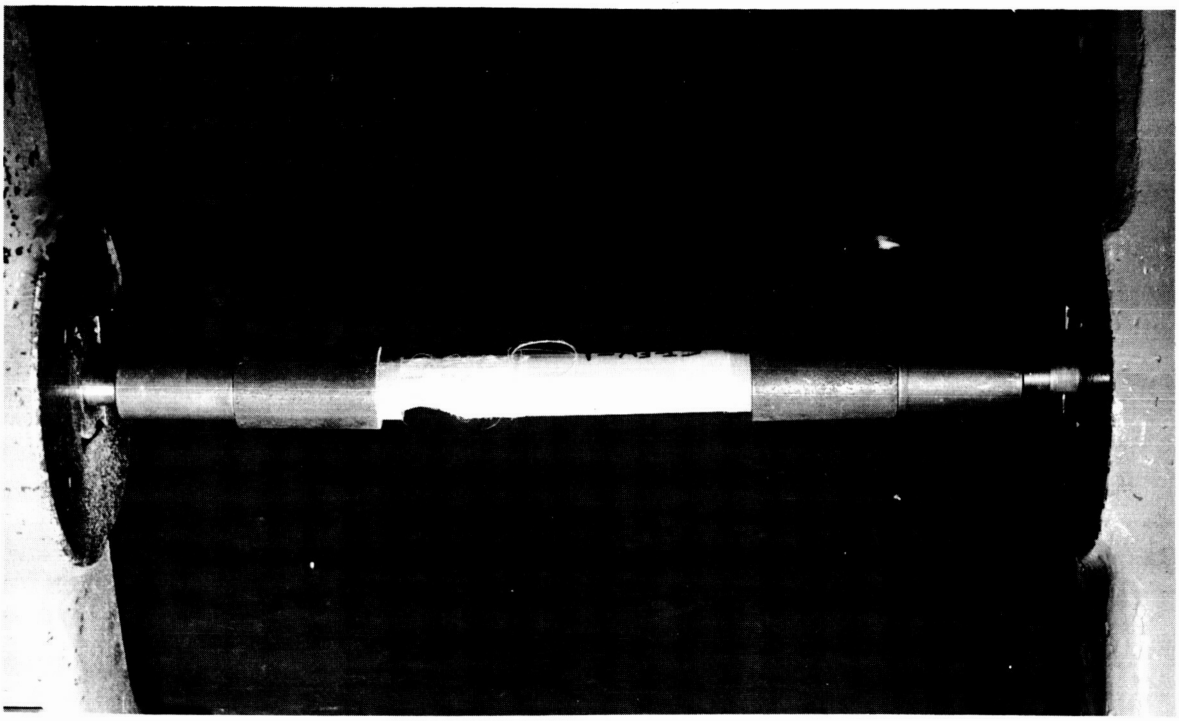

Figure 67. BFW Tensile Tube after Failure

Figure 68. BFW Tensile Tubes before Test

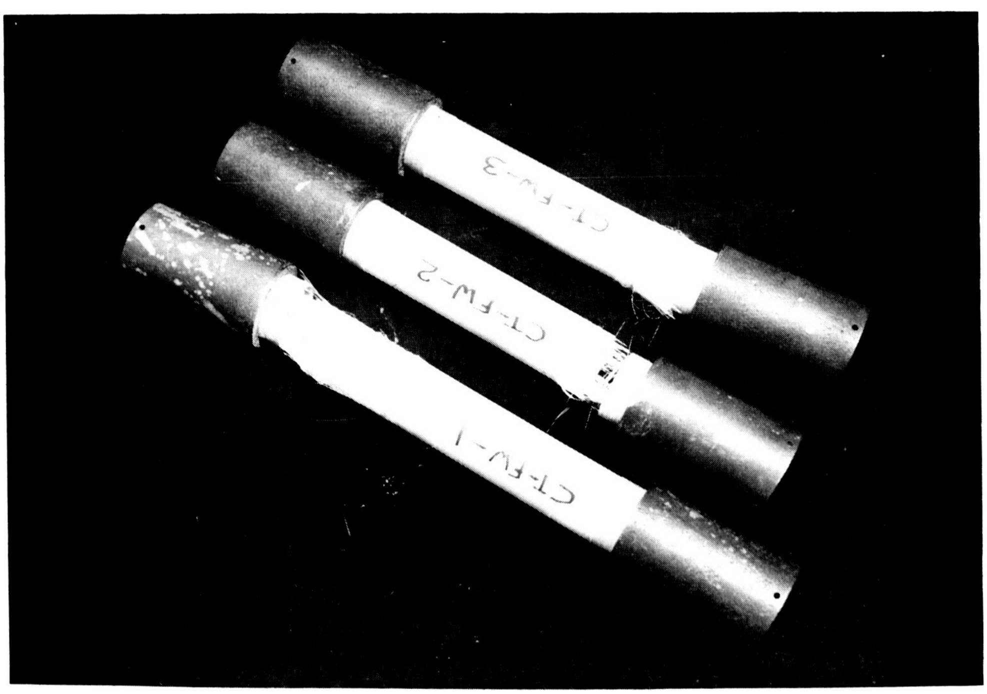

Figure 69. BFW Tensile Tubes after Test

Figure 70. 1543 Cloth Tensile Tube before Test

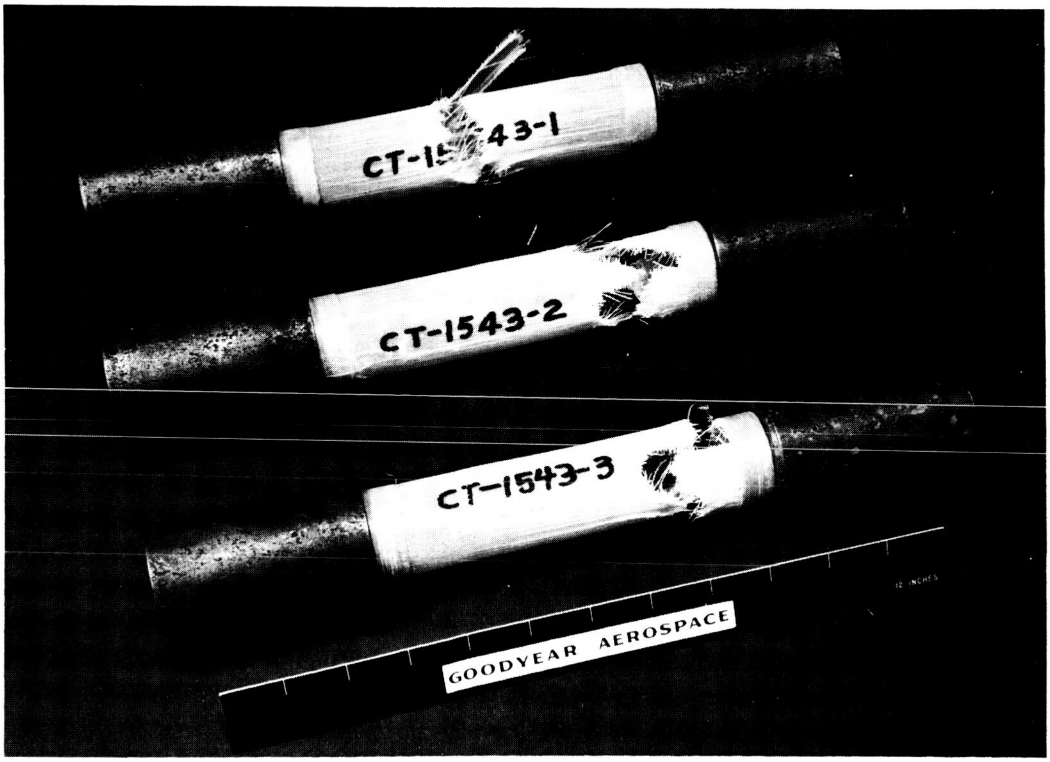

Figure 71. 1543 Cloth Tensile Tubes after Test

Figure 72. 1581 Cloth Tensile Tube before Test

Figure 73. 1581 Cloth Tensile Tube after Test

Figure 74. UFW Rod in Buckled Position

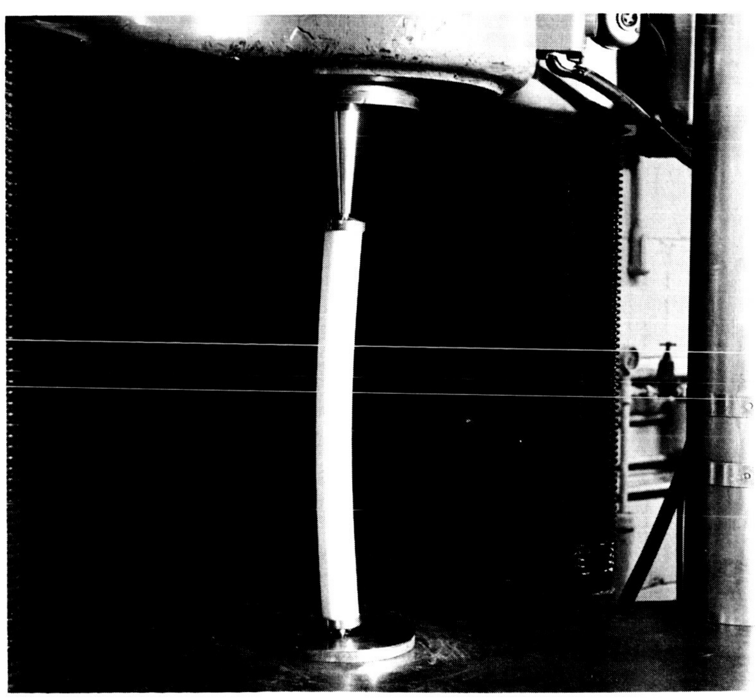

Figure 75. BFW Tube in Buckled Position

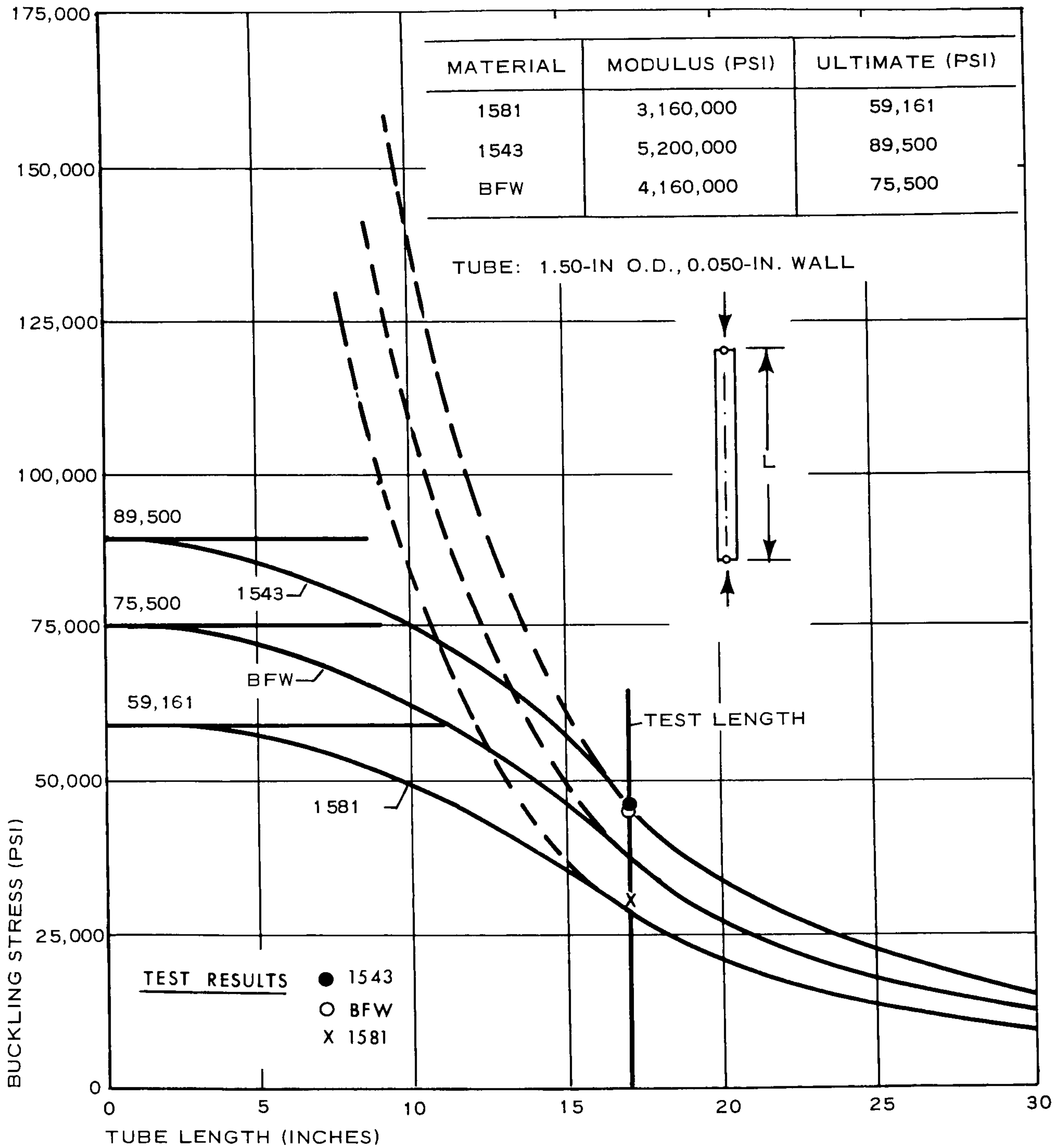

Figure 76. Calculated Buckling Curves (Room Temperature)

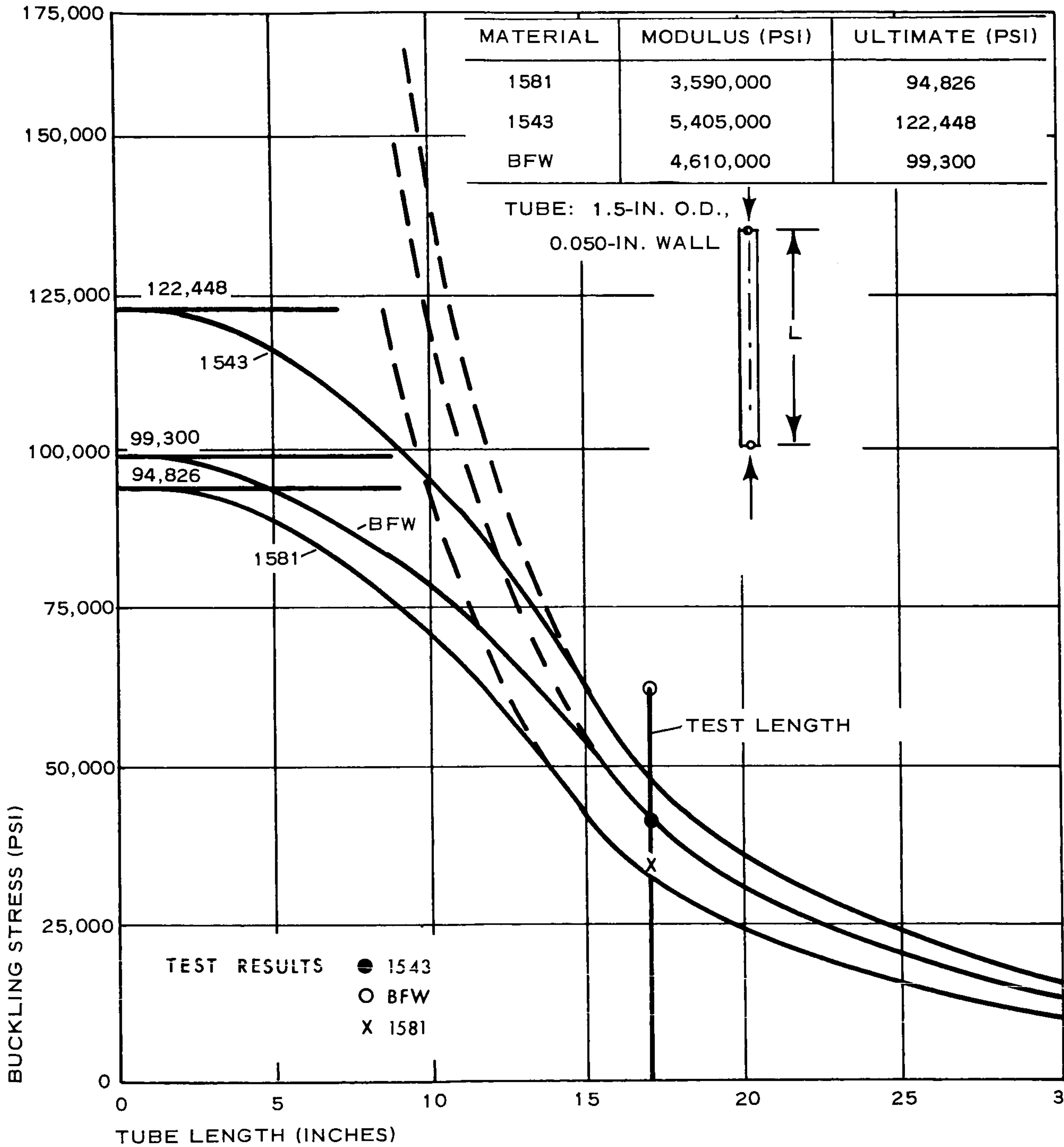

Figure 77. Calculated Buckling Curves (77°K)

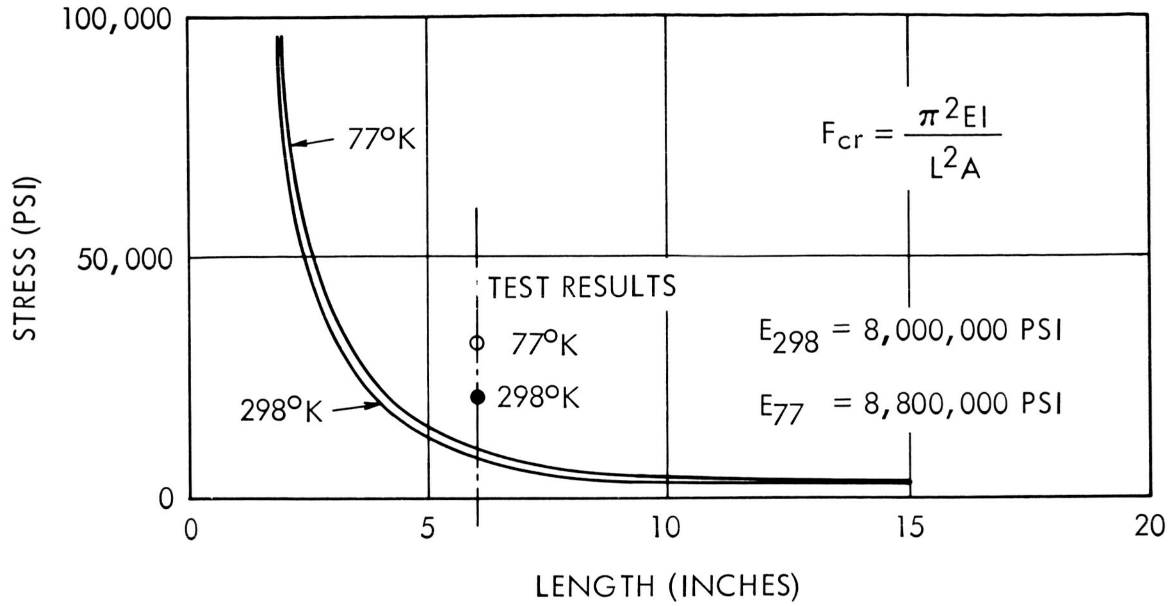

Figure 78. Calculated Rod Buckling Curves

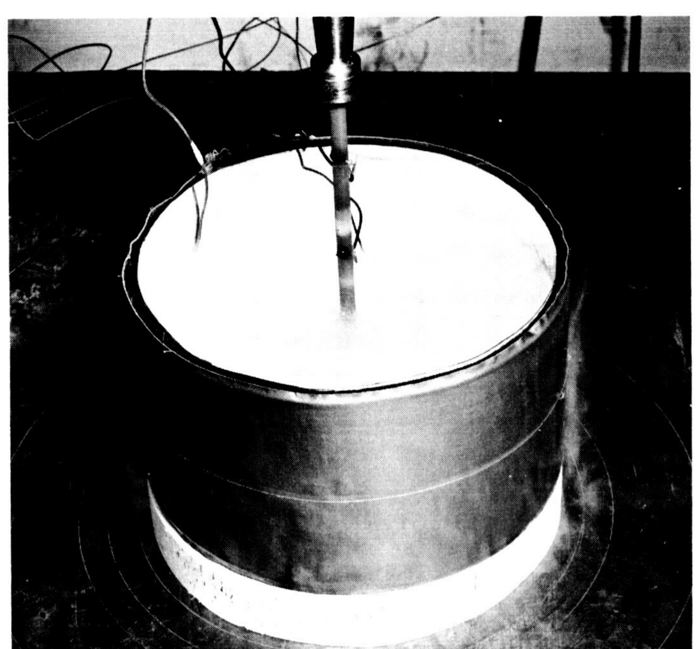

Figure 79. Buckling Rod with One End in Liquid Nitrogen

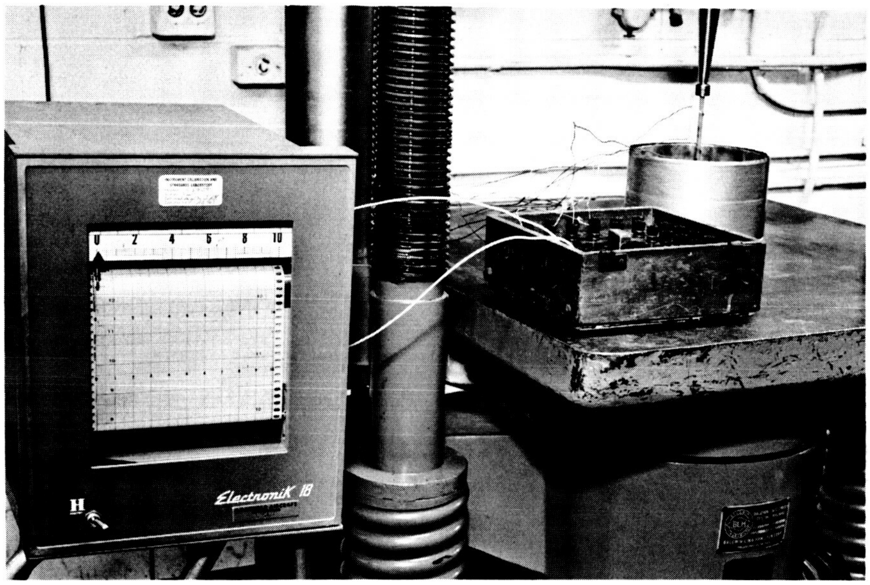

Figure 80. Determining Temperature
Gradient along Rod

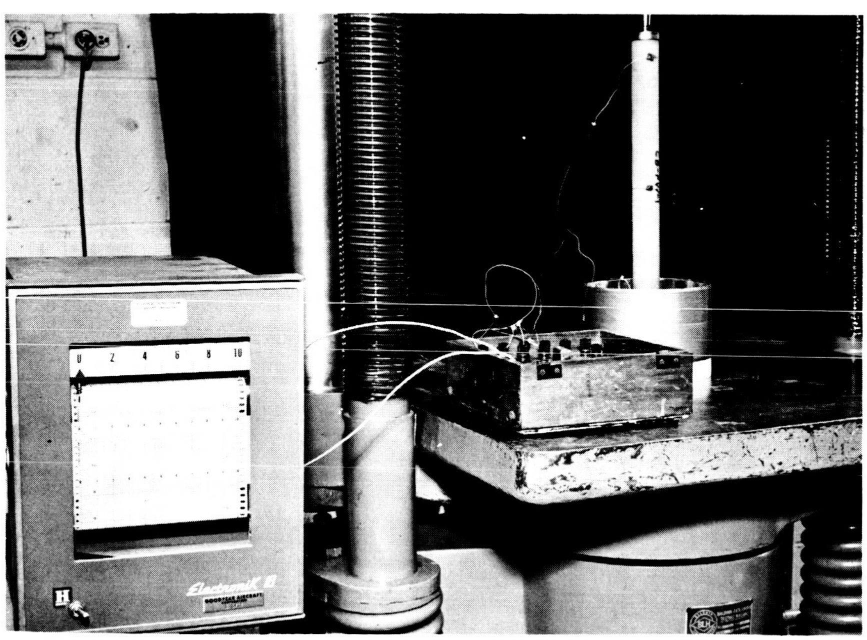

Figure 81. Determining Temperature
Gradient along Tube

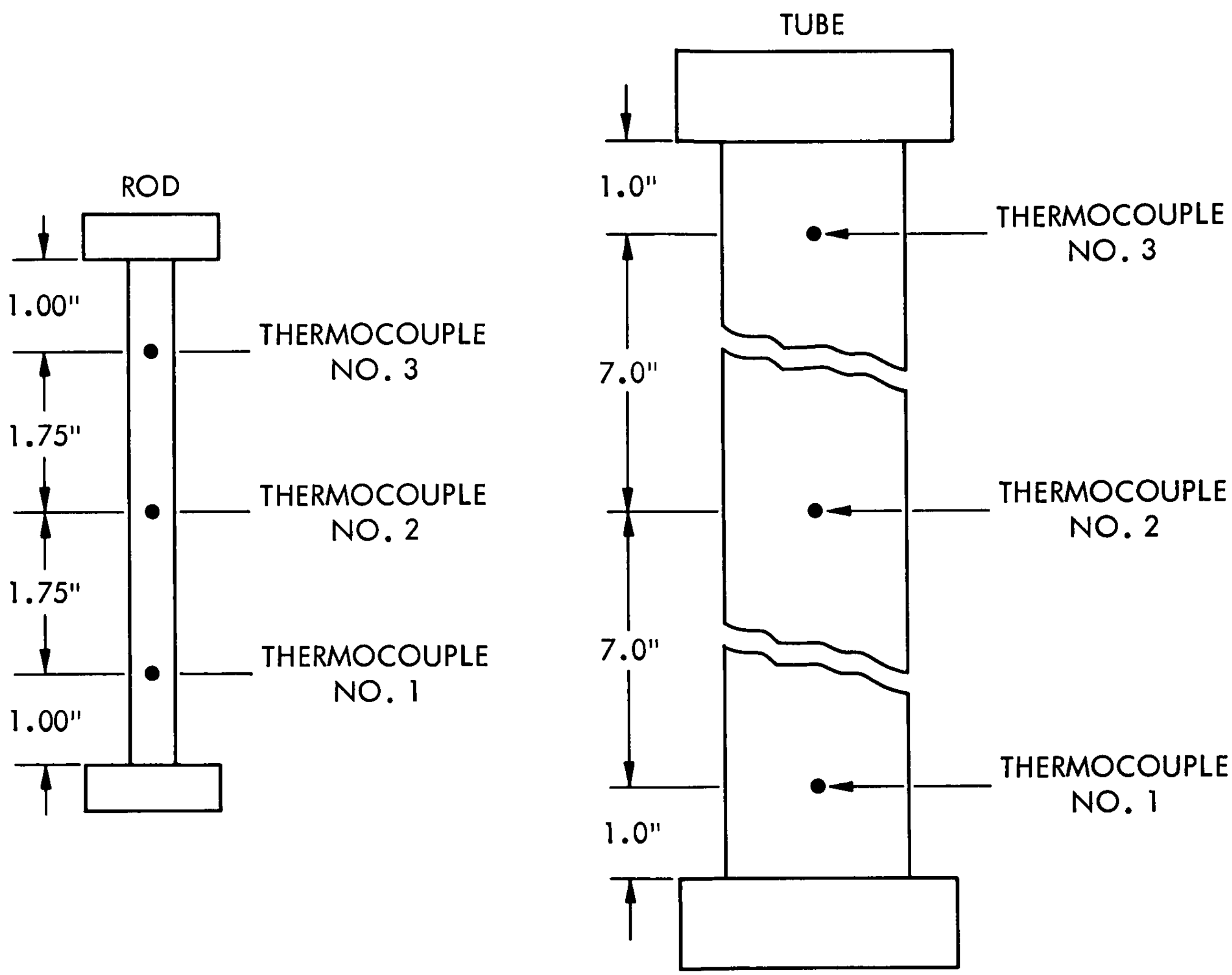

Figure 82. Thermocouple Locations for Temperature Survey for Rod and Tube

Figure 83. Typical Buckling Tube Specimens before Test

Figure 84. BFW Buckled Tubes after Test

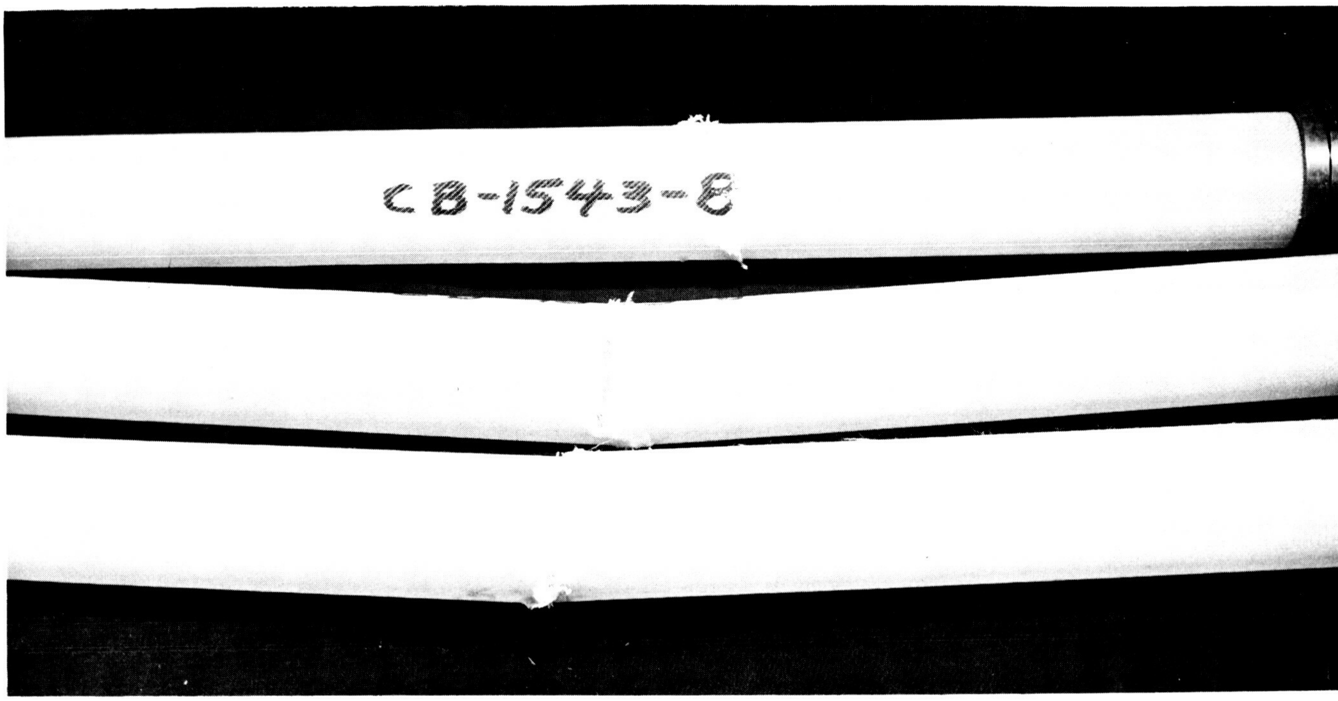

Figure 85. 1543 Cloth Buckled Tube after Test

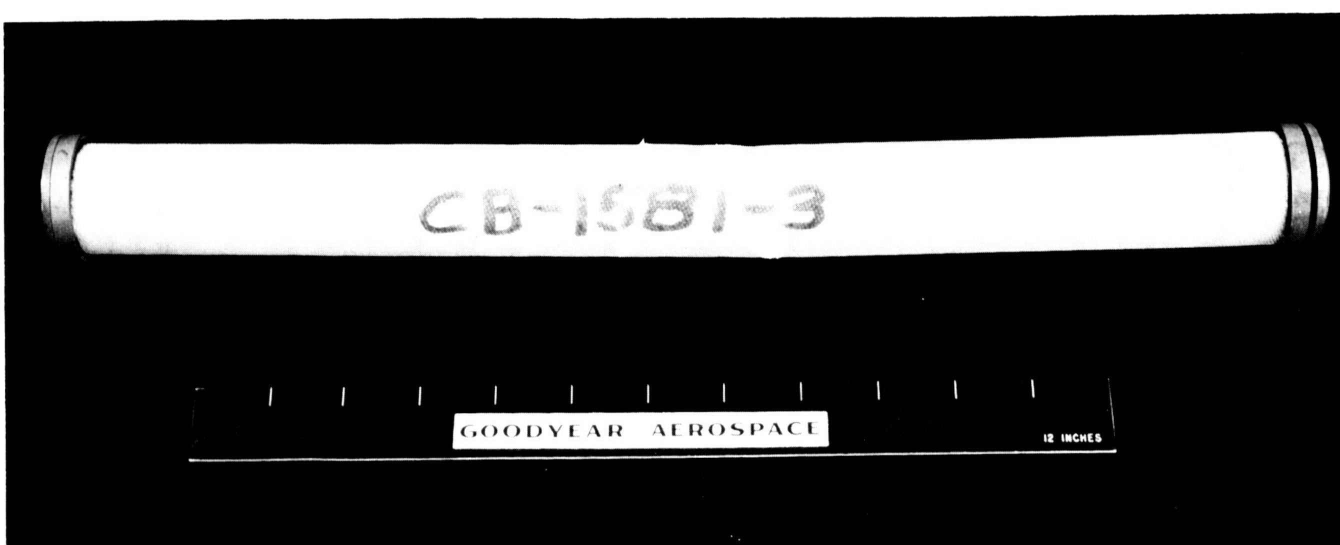

Figure 86. Typical 1581 Cloth Buckled Tube after Test

SECTION V. CONCLUSIONS

As a result of the work performed on this program, significant progress has been made toward the ultimate goal of obtaining a handbook of design data for reinforced plastics at cryogenic temperatures. During the first year's effort, new testing techniques, procedures, and specimen configurations were developed for the purpose of upgrading and improving the validity and direct design utility of the test data. During the second year's effort, a statistical analysis of the test data obtained from these specimens and methods has confirmed the general validity of the test results. Further statistical evaluations have determined the minimum mechanical properties of the S/HTS glass and epoxy resin combination in each of four forms through the room temperature to $20^{o}K$ range that would be exceeded by 95 percent of future specimens with a confidence probability of 95 percent. Furthermore, the model testing has shown that these values apply not only to these test specimens but also to actual structural parts fabricated of these materials.

Throughout the two-year effort, the potential for the use of fiberglass-reinforced plastics for structural applications at cryogenic temperature has continued to grow. The ability to reproduce the small specimen data in the structural models and the determination of no detrimental effects due to weathering have further demonstrated that fiberglass will be the material of the future in cryogenic applications.

SECTION VI. RECOMMENDATIONS

The initial goal of this program is the development of improved test techniques and methods to more realistically determine the engineering potential of reinforced plastics for structural applications at cryogenic temperatures. Although this goal has been generally accomplished, further work is needed in the areas traditionally noted for their wide variance in test values such as shear and bearing to obtain a more usable statistical lower limit value. These test techniques and methods should also be applied to other material combinations that are commercially available and appear promising for cryogenic service. This would help to broaden the base from which the use of reinforced plastics in cryogenic structural applications must grow. Also, provisions should be made for the limited study of any new advancements in composite materials that enter the reinforced-plastics field, so that the advantages offered by these materials can be properly utilized in cryogenic service.

SECTION VII. PROGRAM PLAN AND MAN-HOUR EXPENDITURES

The general program plan for the second phase of the evaluation of structural plastics materials at cryogenic temperatures is shown in Figure 87. This program plan is maintained in each progress report. The original planned approach for the accomplishment of the over-all contract objective is charted. The work accomplished to date and any anticipated changes in the original plan are also depicted.

An accumulative man-hour expenditure chart is presented in Figure 88. Both the estimated and actual man-hours are shown. This chart will be maintained in all succeeding progress reports.

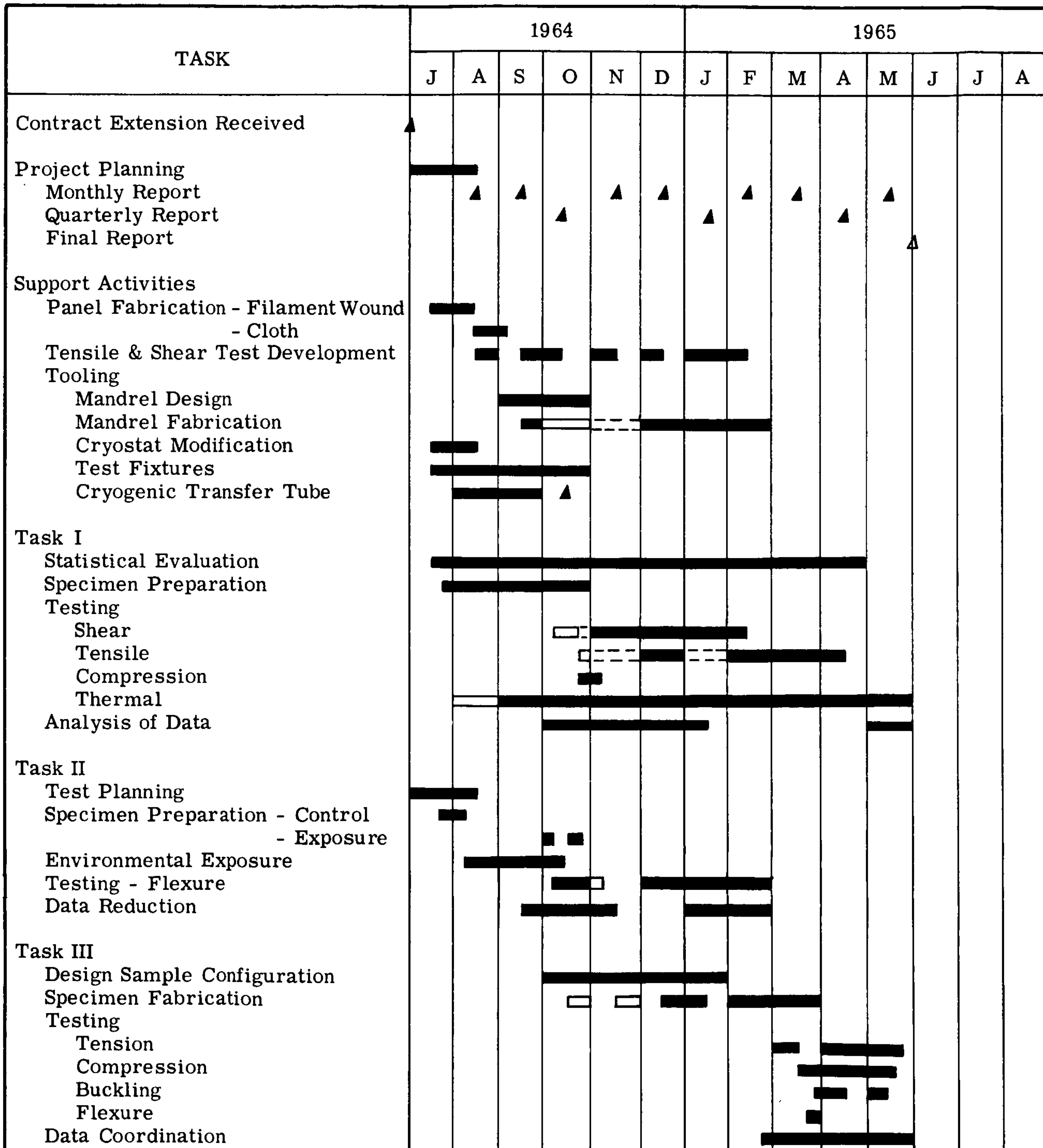

Figure 87. Program Plan (Phase II)

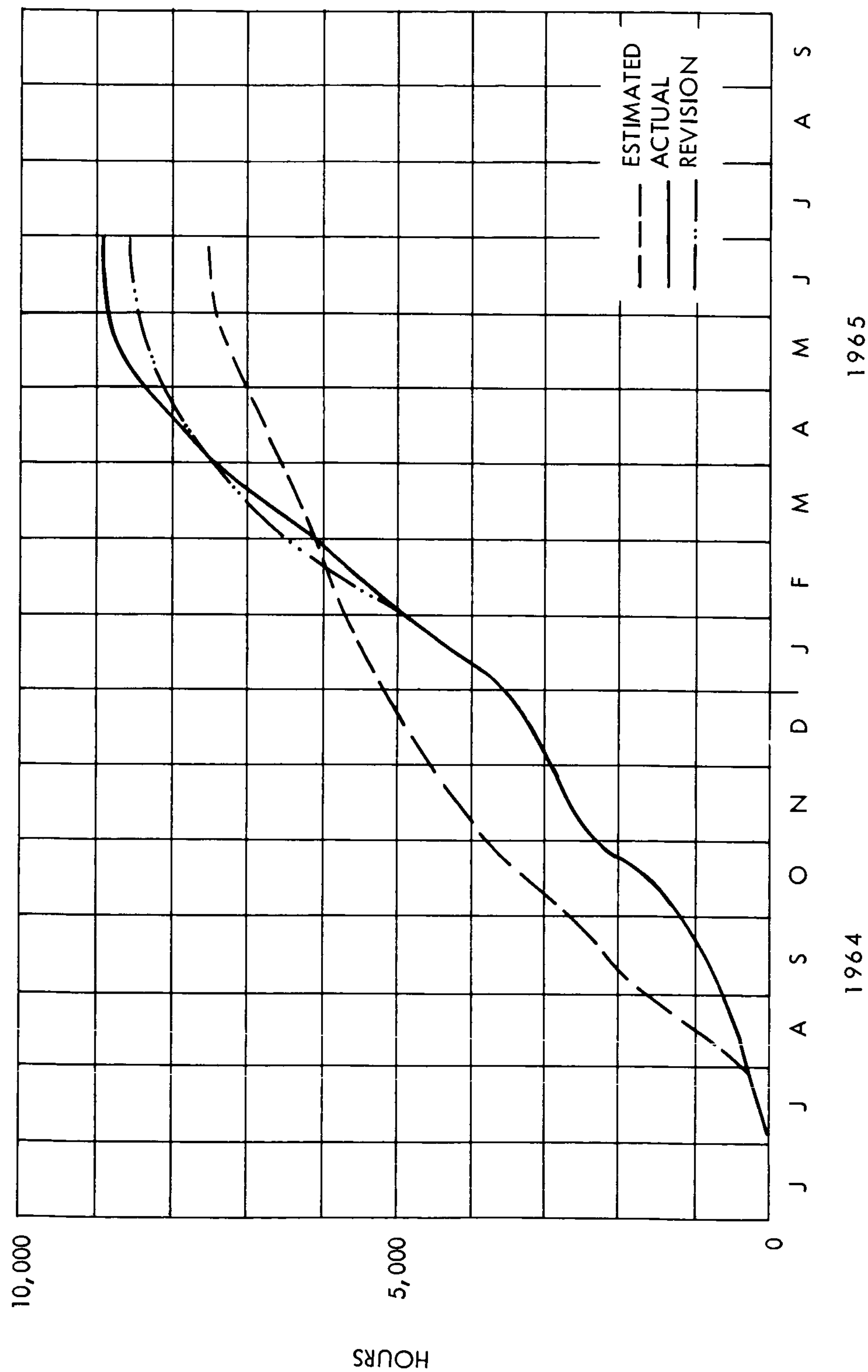

Figure 88. Man-Hour Expenditures (Phase II)

REFERENCES

1. Eisenhart, Hastay, and Wallis, Techniques of Statistical Analysis, McGraw-Hill, Chapter I.

2. Hald, A., Statistical Theory with Engineering Applications, J. Wiley, pp 303-316, p 541.

3. Natrella, M. G., Experimental Statistics, Handbook 91, National Bureau of Standards, Superintendent of Documents.

4. Ravenhall, R., Designing for Stiffness and Buckling in Filament Wound Fiberglass Structures, Hercules Powder Co.

5. Fried, N., The Response of Orthogonal Filament-Wound Materials to Compressive Stress, Paper Presented at 1965 SPI Reinforced Plastics Division Conference in Chicago, 2 February 1965.

APPENDIX A. COMPUTER PROGRAM - STATISTICAL EVALUATION

1. Regression Tolerance Limits

Statistical methods are applied to data from a small number of samples to infer large population properties. Correctly inferred properties may be safely used as design values when related to statistical tolerance limits.

This appendix documents the IBM 1410 FORTRAN IV Program employed on this contract to derive the statistical evaluation results discussed in Section II of this report.

2. Data Input Description

The required data for solution of the problems specified by engineering is contained on data input cards. The format of these cards is shown in Figure 89. The type of data required for each of these cards is described in the following paragraphs. A sample input data run is shown in Figure 90.

a. Cards 1 through 3. A table of $K_{(1-\%)}$ or $K_{(1-C)}$ versus % or C is read first. This table consists of three cards. The present values for % or C are 0.50, 0.75, 0.85, 0.90, 0.95, and 0.99. The corresponding $K_{(1-\%)}$ or $K_{(1-C)}$ values were obtained from "Tables of Probability Functions", Volume II, U.S. Department of Commerce, National Bureau of Standards, Second Edition, 1948.

b. Card 4. A header card that may contain any header that the user desires (columns 1 to 80).

c. Card 5. A control card that tells the program which Z_i's are to be selected for a run. For generality, a maximum of 35 Z_i's is allowed. The form of these Z_i's is described in Table 35. In this card the first 35 columns are used for

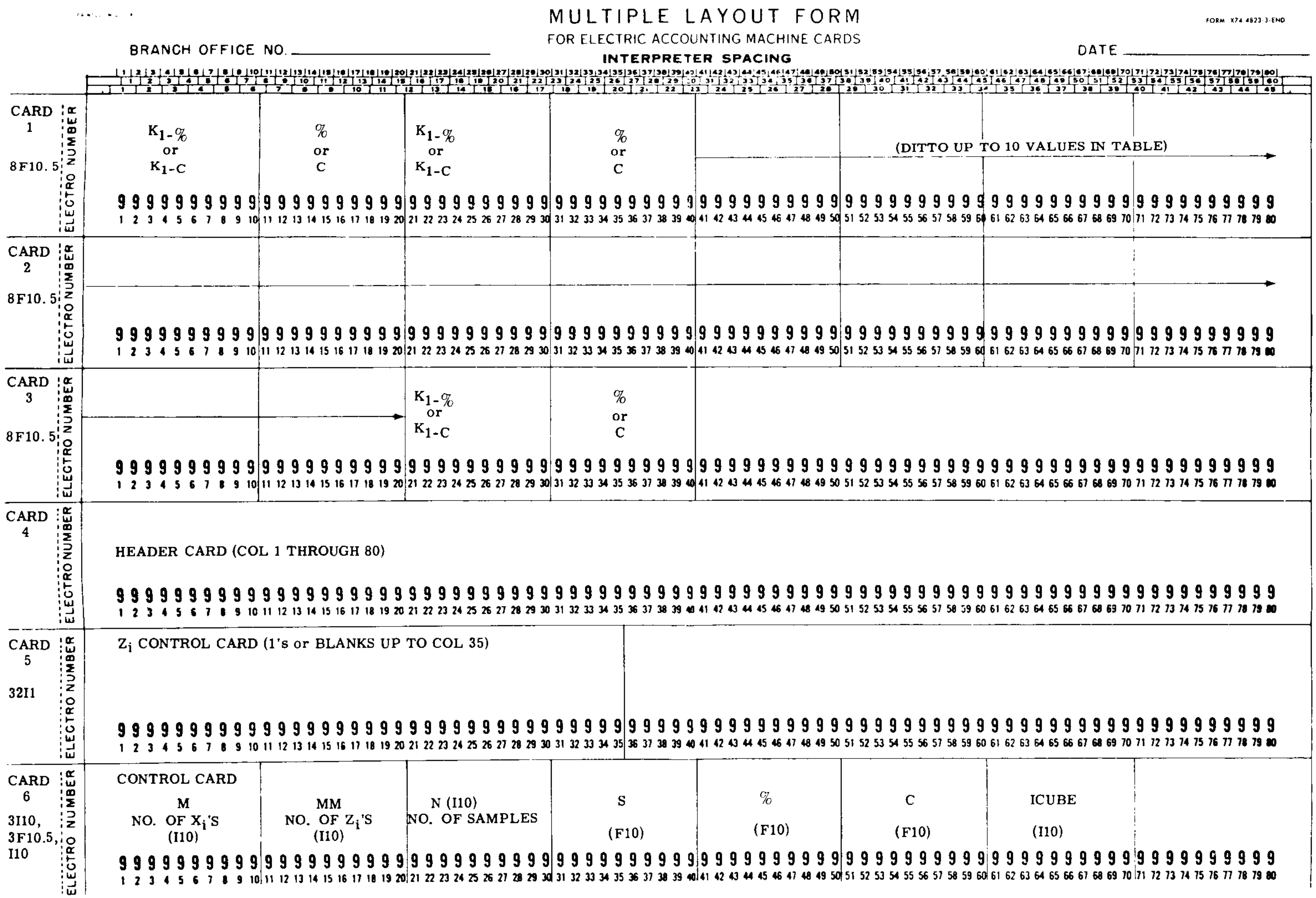

Figure 89. Data Input Sample Format (Sheet 1)

MULTIPLE LAYOUT FORM
FOR ELECTRIC ACCOUNTING MACHINE CARDS
INTERPRETER SPACING

BRANCH OFFICE NO. ____________ DATE ____________

FORM X24 4923-3 END

Card	Cols. 1–10	Cols. 11–20	Cols. 21–30	Cols. 31–40	Cols. 41–50	Cols. 51–60	Cols. 61–70	Cols. 71–80
CARD 7 VARIABLE NO. OF C CARDS	F12.5 or E12.5 (cols. 1–12)							
CARD 8 $\bar{Z}$'S (VARIABLE NO. OF THESE CARDS)	$\bar{z}_1$	$\bar{z}_2$	$\bar{z}_3$	$\bar{z}_4$	$\bar{z}_5$	ETC	ETC	
CARD 9	a_0	a_1	a_2	a_3	a_4	a_5	a_{11}	a_{22}
CARD 10	a_{33}	a_{44}	a_{55}	a_{12}	a_{13}	a_{14}	a_{15}	a_{23}
CARD 11	a_{24}	a_{25}	a_{34}	a_{35}	a_{45}	a_{111}	a_{222}	a_{333}
CARD 12	a_{444}	a_{555}	a_{123}	a_{124}	a_{125}	a_{134}	a_{135}	a_{145}

Figure 89. Data Input Sample Format (Sheet 2)

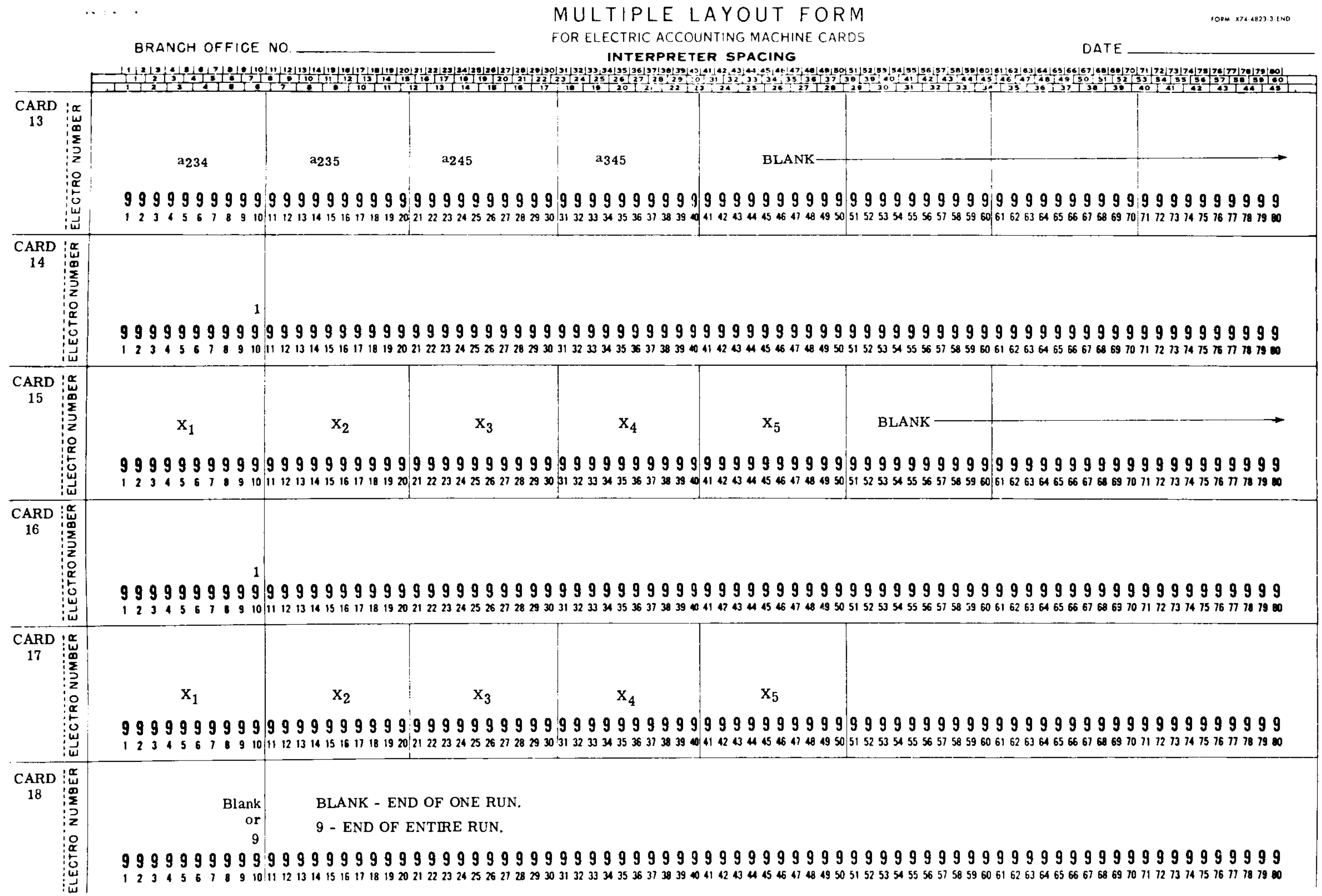

Figure 89. Data Input Sample Format (Sheet 3)

$K_{1-\%}$	%	$K_{1-\%}$	%	$K_{1-\%}$	%	$K_{1-\%}$	%	
0.	.5	.6745	.75	.84163	.8	1.03647	.85	TABLE OF % VS $K_{1-\%}$
1.28157	.90	1.64486	.95	2.3264	.99	2.3264	.99	OR C VS K_{1-C}
2.3264	.99	2.3264	.99					

BFW COMPRESSIVE STRENGTH - HEADER CARD

11 11 1 - CONTROL CARD THAT TELLS X_i'S TO BE USED

2(No. of X_i's)5(No. of Z_i's)481.40707E&4.95(%) .95(C) ICUBE

No. of Samples S

3.75982E-5 C_{11}
2.49495E-4 C_{22}
3.38614E-10 C_{33}

2.79428E-8 C_{44}
1.29210E-9 C_{55}
6.45400E-6 C_{12}

-1.07813E-7 C_{13}
-7.24377E-13 C_{14}
-4.36076E-8 C_{15}

1.67671E-13 C_{23}
-2.40054E-6 C_{24}
-1.91231E-7 C_{25}

1.89236E-15 C_{34}
-2.23136E-15 C_{35}
3.61048E-15 C_{45}

1.48000E&23.37500E&13.34855E&42.53125E&34.99500E&3 $\bar{Z}$'S

1.2368E&5 2.3379E&2 -3.1809E&3 -1.0723 3.1781E&1
3.0151E-1 5 a_i CARDS

1 CONTROL TO READ X_i CARD
298. X_1 0. X_2
1
298. X_1 45. X_2
1
298. 90.
1
197. 0.
1
197. 45.
1
197. 90.
1
77. 0.
1
77. 45.
1
77. 90.
1
20. 0.
1
20. 45.
1
20. 90.
9 (SIGNALS END OF RUN)

Figure 90. Sample Input Data Run

Table 35. Z_i Values

Z_i	Corresponding a Coefficient	Z_i	Corresponding a Coefficient
	a_0 (constant term)	$Z_{18} = X_3X_4$	a_{34}
$Z_1 = X_1$	a_1	$Z_{19} = X_3X_5$	a_{35}
$Z_2 = X_2$	a_2	$Z_{20} = X_4X_5$	a_{45}
$Z_3 = X_3$	a_3	$Z_{21} = X_1^3$	a_{111}
$Z_4 = X_4$	a_4	$Z_{22} = X_2^3$	a_{222}
$Z_5 = X_5$	a_5	$Z_{23} = X_3^3$	a_{333}
$Z_6 = X_2^2$	a_{11}	$Z_{24} = X_4^3$	a_{444}
$Z_7 = X_1^2$	a_{22}	$Z_{25} = X_5^3$	a_{555}
$Z_8 = X_3^2$	a_{33}	$Z_{26} = X_1X_2X_3$	a_{123}
$Z_9 = X_4^2$	a_{44}	$Z_{27} = X_1X_2X_4$	a_{124}
$Z_{10} = X_5^2$	a_{55}	$Z_{28} = X_1X_2X_5$	a_{125}
$Z_{11} = X_1X_2$	a_{12}	$Z_{29} = X_1X_3X_4$	a_{134}
$Z_{12} = X_1X_3$	a_{13}	$Z_{30} = X_1X_3X_5$	a_{135}
$Z_{13} = X_1X_4$	a_{14}	$Z_{31} = X_1X_4X_5$	a_{145}
$Z_{14} = X_1X_5$	a_{15}	$Z_{32} = X_2X_3X_4$	a_{234}
$Z_{15} = X_2X_3$	a_{23}	$Z_{33} = X_2X_3X_5$	a_{235}
$Z_{16} = X_2X_4$	a_{24}	$Z_{34} = X_2X_4X_5$	a_{245}
$Z_{17} = X_2X_5$	a_{25}	$Z_{35} = X_3X_4X_5$	a_{345}

control of Z_1 through Z_{35}. If a Z_i is to be used, the column corresponding to that Z_i will have a 1 in it. Z_i's that are not used remain blank. Example: If Z_1, Z_2, Z_6, Z_7, Z_{11} are to be used, columns 1, 2, 6, 7, and 11 of this card will contain 1's; all other columns will be blank.

d. Card 6. A control card that contains the following:

M - the number of X_i's
MM - the number of Z_i's
N - the number of samples
S
PERCNT - the % of population (must be limited to the values referenced in paragraph a.)
CC - confidence level (must be limited to the values referenced in paragraph a.)
ICUBE - blank for quadradic, 1 for cubic.

e. Card 7. C_{ii} (i = 1, MM); C_{ij} (i = 1, MM-1, j = 1, MM) - coefficients by S_y equation (one per card).

f. Card 8. $\bar{Z}_i$ (i = 1, MM) average Z_i's (eight per card).

g. Cards 9 through 13. a_i (i = 1, 36) coefficients of y equation (eight per card) in the following order: a_0, a_1, a_2, a_3, a_4, a_5, a_{11}, a_{22}, a_{33}, a_{44}, a_{55}, a_{12}, a_{13}, a_{14}, a_{15}, a_{23}, a_{24}, a_{25}, a_{34}, a_{35}, a_{45}, a_{111}, a_{222}, a_{333}, a_{444}, a_{555}, a_{123}, a_{124}, a_{125}, a_{134}, a_{135}, a_{145}, a_{234}, a_{245}, a_{345}. (Blanks must be left for missing a's; total number of cards must be five).

h. Cards 14 and 16. A card with a 1 in column 10. This is a control card to allow stacking of several sets of values for X_i. It signals the program that an X_i card is next.

i. Cards 15 and 17. X_i - Any number of X_i cards may be stacked, separated by the card described in the preceding paragraph. (one card, i = 1, 5.)

j. Card 18. A blank card at the end of all X_i cards; this signals the end of a run and tells the program the next card to be read is the header card for a new run. Cards 2 through 17 are repeated, then another blank, etc. Any number of runs may be stacked in this manner. Card 18 can also be a card with a 9 in column 10. This card signals the end of all runs. It is placed immediately after the last set of data. No blank is required in front of this card; it essentially takes the place of the blank on the last run.

3. FORTRAN Program Listing

The program listing is given in Table 36. A summary of equations for the calculation of tolerance limits is as follows:

$$y = a_0 + a_1 Z_1 + a_2 Z_2 + a_{11} Z_3 + a_{22} Z_4 + a_{12} Z_5 + \ldots\ldots + a_{345} Z_{35}. \tag{8}$$

$$S_y = s \left[1/n + \sum_{i=1}^{MM} C_{ii} (Z_i - \overline{Z}_i)^2 + 2 \sum_{i=1}^{MM-1} \sum_{j=i+1}^{MM} C_{ij} (Z_i - \overline{Z}_i)(Z_i - \overline{Z}_j) \right]^{1/2} . \tag{9}$$

$$1 - \% = \frac{1}{\sqrt{2\pi}} \int_{K_{1-\%}}^{\infty} e^{-x^2/2} \, dx \text{ and } 1 - C = \frac{1}{\sqrt{2\pi}} \int_{K_{1-C}}^{\infty} e^{-x^2/2} \, dx. \tag{10}$$

From table obtain $K_{1-\%}$, K_{1-C}.

$$K_{C,\%} = \frac{K_{1-\%} + \sqrt{K_{1-\%}^2 - ab}}{a} . \tag{11}$$

Table 36. FORTRAN Program Listing

```
      REALKCPER
      DIMENSIONX%5□,Z%35□,ZBAR%35□,A%36□,C%35,35□
      DIMENSIONXX%10□,YY%10□
      DIMENSIONDUM%8□,NZ%35□
00100 FORMAT%3I10,3F10.5,I10□
00101 FORMAT%8F10.5□
00102 FORMAT%1X,5E15.8□
00104 FORMAT%8A10□
00105 FORMAT%F12.5□
00106 FORMAT%1H1,8A10/□
00107 FORMAT%1X,1HX,I1,2X,F10.5□
00108 FORMAT%1X,1HY,2X,E15.8,5X,4HK SY,2X,E15.8,2X,5HY-KSY,2X,E15.8□
00109 FORMAT%5X,8HAT LEAST,F6.1,52H% WILL EXCEED Y-KSY WITH A CONFIDENCE PROBABILITY OF ,F6.1,1H%/□
00110 FORMAT%35I1□
      DO960I#1,35
00960 Z%I□#0.
      READ%1,101□%XX%I□,YY%I□,I#1,10□
00300 READ%1,104□DUM
      WRITE%3,106□DUM
      READ%1,110□NZ
      READ%1,100□M,MM,N,S,PERCNT,CC,ICUBE
      EN#N
      CPRNT#100.*CC
      PPRNT#100.*PERCNT
      WRITE%3,109□PPRNT,CPRNT
      MM1#MM-1
      DO311I#1,MM
00311 READ%1,105□C%I,I□
      DO310I#1,MM1
      JJ#I&1
      DO310J#JJ,MM
00310 READ%1,105□C%I,J□
      READ%1,101□%ZBAR%I□,I#1,MM□
      IM1#MM&1
      READ%1,101□%A%I□,I#1,36□
00301 READ%1,100□ISWTCH
      IF%ISWTCH.EQ.9□GOTO999
      IF%ISWTCH.EQ.0□GOTO300
      READ%1,101□%X%I□,I#1,5□
C     CALCULATE Z TABLE
      DO900I#1,5
00900 Z%I□#X%I□
      DO901I#6,10
      J#I-5
00901 Z%I□#X%J□**2
      I#11
      DO902J#1,4
      JJ#J&1
      DO902K#JJ,5
      Z%I□#X%J□*X%K□
00902 I#I&1
      IF%ICUBE.EQ.0□GOTO200
```

Table 36. FORTRAN Program Listing (Continued)

```
      DO903I#21,25
      J#I-20
00903 Z%I□#X%J□**3
      I#26
      DO904J#1,3
      JJ#J&1
      DO904K#JJ,4
      KK#K&1
      DO904L#KK,5
      Z%I□#X%J□*X%K□*X%L□
00904 I#I&1
0020C SUM#0
      DO6I#1,35
00006 SUM#A%I&1□*Z%I□&SUM
      Y#A%1□&SUM
      II#1
      DO950I#1,35
      IF%NZ%I□.EQ.0□GOTO950
      Z%II□#Z%I□
      II#II&1
0095C CONTINUE
      SUM2#0.
      SUM3#0
      DO7I#1,MM
00007 SUM2#C%I,I□*%Z%I□-ZBAR%I□□**2&SUM2
      DO8I#1,MM1
      JJ#I&1
      DO8J#JJ,MM
00008 SUM3#C%I,J□*%Z%I□-ZBAR%I□□*%Z%J□-ZBAR%J□□&SUM3
      SY#S*SQRT%1./EN&SUM2&2.*SUM3□
      DO202I#1,10
      IF%PERCNT.EQ.YY%I□□GOTO201
00202 CONTINUE
      PAUSE111
00201 P#XX%I□
      DO203I#1,10
      IF%CC.EQ.YY%I□□GOTO204
00203 CONTINUE
      PAUSE111
00204 CL#XX%I□
      AA#1.-%%CL**2□/%2.*%EN-1.□□□
      BB#P**2-CL**2/EN
      KCPER#%P&SQRT%P**2-AA*BB□□/AA
      FIN#KCPER*SY
      DO306K#1,M
00306 WRITE%3,107□K,X%K□
      YKCY#Y-FIN
      WRITE%3,108□Y,FIN,YKCY
      GOTO301
00999 CALLEXITD
      END
```

where

$$a = 1 - \frac{K^2_{1-C}}{2(n-1)},$$

$$b = K^2_{1-\%} - \frac{K^2_{1-C}}{n}.$$

$$K_{C,\%}\, S_y. \tag{12}$$

4. Data Output Description

The program prints a line containing the values of % and C for identifying purposes. A header line is printed for each run (i = 1, M). Finally Y, $K_{C,\%}$ and S_y are printed as shown in the sample data output run (Figure 91).

```
BFW       COMPRESSIVE STRENGTH

     AT LEAST  95.0% WILL EXCEED Y-KSY WITH A CONFIDENCE PROBABILITY OF  90.0%

X1    298.00000
X2      0.00000
Y    0.98124891E 05      K SY    0.10137073E 05    Y-KSY    0.87987818E 05
X1    298.00000
X2     45.00000
Y    0.23384165E 05      K SY    0.10587569E 05    Y-KSY    0.12796596E 05
X1    298.00000
X2     90.00000
Y    0.77356489E 05      K SY    0.13398056E 05    Y-KSY    0.63958433E 05
X1    197.00000
X2      0.00000
Y    0.12812174E 06      K SY    0.80689002E 04    Y-KSY    0.12005284E 06
X1    197.00000
X2     45.00000
Y    0.52010650E 05      K SY    0.97219312E 04    Y-KSY    0.42288719E 05
X1    197.00000
X2     90.00000
Y    0.10461261E 06      K SY    0.10085152E 05    Y-KSY    0.94527460E 05
X1     77.00000
X2      0.00000
Y    0.13532416E 06      K SY    0.71224420E 04    Y-KSY    0.12820172E 06
X1     77.00000
X2     45.00000
Y    0.57584920E 05      K SY    0.88034782E 04    Y-KSY    0.48781442E 05
X1     77.00000
X2     90.00000
Y    0.10855873E 06      K SY    0.96231338E 04    Y-KSY    0.98935594E 05
X1     20.00000
X2      0.00000
Y    0.12792688E 06      K SY    0.93766144E 04    Y-KSY    0.11855027E 06
X1     20.00000
X2     45.00000
Y    0.49414264E 05      K SY    0.10166866E 05    Y-KSY    0.39247398E 05
X1     20.00000
X2     90.00000
Y    0.99614698E 05      K SY    0.12347170E 05    Y-KSY    0.87267528E 05
```

Figure 91. Sample Output Data Run

DISTRIBUTION LIST

Mr. J. T. Schell, M-P & VE-MR
George C. Marshall Space Flight Center
National Aeronautics and Space Administration
Huntsville, Alabama
(14 Copies)

Mr. James Barber, Code 9510
Apollo Propulsion Office
Lewis Research Center
National Aeronautics and Space Administration
Cleveland, Ohio
(Immediate Distribution)

Mr. Robert Hickel, Code 2323
Head, Structure Protection Section
Lewis Research Center
National Aeronautics and Space Administration
Cleveland, Ohio
(Immediate Distribution)

General Dynamics/Astronautics
Post Office Box 1128
San Diego 12, California
Attn: Library and Information Services (128-00)
Quarterly Reports Only
(Immediate Distribution)

Plastics Technical Evaluation Center
Picatinny Arsenal
Dover, New Jersey
(Distribution 60 Days from Issue)

Mr. R.C. Tomashot
Air Force Materials Laboratory (MAC)
Materials Development Branch
Advanced Filaments and Composites Division
United States Air Force
Wright-Patterson Air Force Base, Ohio 45433

Mr. R. Hoener
Air Force Flight Dynamics Laboratory
Research and Technology Division
Air Force Systems Command
United States Air Force
Wright-Patterson Air Force Base, Ohio 45433
(Distribution 60 Days from Issue)